MEKELLE UNIVERSITY

COLLEGE OF NATURAL AND COMPUTATIONAL SCIENCES

FACULTY OF MINING AND GEOSCIENCES

POST GRADUATE PROGRAM IN STRUCTURAL GEOLOGY

MSc. Thesis on:

GEOLOGICAL, GEOCHEMICAL AND STRUCTURAL ANALYSIS OF THE PRECAMBRIAN ROCKS OF ADI NEBRI'ED AREA, TIGRAY, NORTHERN ETHIOPIA.

By:

Azeb Nigus Weldu

This thesis is submitted to Faculty of Mining and Geosciences in Partial Fulfillment of the Requirement for the Master of Science (MSc.) Degree in Structural Geology.

Main advisor: Prof. Miruts Hagos

Co-advisor: Dr. Kassa Amare

March 2026

Mekelle, Ethiopia

Declaration of Originality

This is to announce that this thesis work is entitled **"GEOLOGICAL, GEOCHEMICAL AND STRUCTURAL ANALYSIS OF THE PRECAMBRIAN ROCKS OF ADI NEBRI'ED AREA, TIGRAY, NORTHERN ETHIOPIA"**. This thesis is submitted in partial fulfillment of the requirement for the Master of Science (MSc.) Degree in Structural Geology to the Faculty of Mining and Geosciences, Mekelle University, has been done by Mrs. AZEB NIGUS WELDU with the I.D No: CNCS/PGR/021/09 under the supervision of **Prof. Miruts Hagos** and **Dr. Kassa Amare** is an authentic work carried out during 2018-2021 academic year. In addition, I announce this thesis work has not been presented, submitted, or published to any institution/organization and it is well referenced and acknowledged.

I hereby declare this is my original work as part of the Master of Science program in Structural Geology.

Name of student candidate: **Azeb Nigus Weldu**

Signature with date: _____ 01/05/2026

This thesis has been submitted for examination with my approval as an **advisor/co-advisor**.

Name of the main advisor: **Prof. Miruts Hagos**

Signature: _____ 30/04/2026

Name of the co-advisor**: Dr. Kassa Amare**

Signature: _____ 30/04/2026

Place: Mekelle University, Mekelle, Ethiopia

Date of submission: 07/05/2026

Geological, Geochemical and Structural Analysis of the Precambrian Rocks of Adi Nebri'ed Area 2026

Approval Sheet

We, the undersigned, member of the board of examiners of the final open defense by "AZEB NIGUS WELDU" have read and evaluated her thesis entitled **"GEOLOGICAL, GEOCHEMICAL AND STRUCTURAL ANALYSIS OF THE PRECAMBRIAN ROCKS OF ADI-NEBRI'ED AREA, TIGRAY, NORTHERN ETHIOPIA"** evaluated the candidate. This is therefore to certify that, the thesis has been accepted in partial fulfillment of the requirements for the Master Science (MSc.) in Structural Geology.

SUBMITTED BY:

Azeb Nigus Weldu	CNCS/PGR/021/09		01/05/2026
Student's Name	ID No.	Signature	Date

APPROVED BY:

1. Prof. Miruts Hagos Main advisor's Name	Signature	30/04/2026 Date
2. Dr. Kassa Amare Co-Advisor's Name	Signature	30/04/2026 Date
3. Dr. Fethangest W/mariam School Head	Signature	07/05/2026 Date
4. Dr. Kassa Amare Chairperson	Signature	30/04/2026 Date
5. Konka Bheemalingeswara (Prof.) Internal Examiner	Signature	28/04/2026 Date
6. Mr. Fiseha Adhanom External Examiner	Signature	29/04/2026 Date

MSc. Thesis in Structural Geology By: Azeb Nigus II

Acknowledgment

I sincerely appreciate **Adigrat University** giving me the chance to begin my postgraduate studies at Mekelle University. I also want to express my gratitude to the **Mekelle University,** Faculty of Mining and Geosciences for providing me with unwavering support during the entire research work.

I would like to express my profound appreciation to my advisers, **Prof. Miruts Hagos** and, **Dr. Kassa Amare** for their unwavering support, follow-up, wise counsel, constructive criticism and recommendations, encouragement, discussion, and boundless assistance at various points in time. They also possesses extensive knowledge and have insightful technical discussions.

Friends and coworkers provided me with a great deal of support while I worked on the research. My family is the one I am most grateful for their unwavering strength and support.

Last but not least, the people of Adi-Nebri'ed village have been extremely helpful to me in my research work. I am grateful for all of their thoughtful and enduring assistance during the fieldwork.

Table of Contents

Contents **Pages**

List of Figures

List of Tables

List of Acronyms

AAB	Augaro-Adobha Belt	MORB	Mid-Ocean Ridge Basalts
A.m.s.l	Above Mean Sea Level	Ms	Muscovite
ALS	Australian Laboratory Science	MV	Metavolcanic
ANB	Asmara-Nakfa Belt	MVC	Metavolcanoclastic
ANS	Arabian Nubian Shield	N=	Number of Measurements
Bt	Biotite	N-MORB	Normal Mid-Ocean Ridge Basalt
Cal	Calcite	Ol	Olivine
Chl	Chlorite	Opq	Opaque
D1	Deformational Event 1	Px	Pyroxene
D2	Deformational Event 2	Plg	Plagioclase
D3	Deformational Event 3	PAO	Pan African Orogen
DTB	Da'ero Tekli Belt	PPL	Plane Polarized Light
EAO	East African Orogeny	PPM	Parts Per Million
E.G	East Gondwana	Qtz	Quartz
Ep	Epidote	REE	Rare Earth Element
Fig.	Figure	RS#	Rock sample Number
GCDkit Tool	Geochemical Data Kit Tool	S_0	Primary Bedding
GPS	Global Positioning System	S_1	Secondary Foliation
HREEs	Heavy Rare Earth Elements	S_2	Crenulation Cleavage
JS	Joint set	Ser	Sericite
LILE	Large Ion Lithophile Elements	W. G	West Gondwana
LOI	Loss of Ignition	WPB	Within Plate Basalt
MB	Mozambique Belt	Wt	Weight
ME- ICP06	Multi Element Inductively Coupled Plasma 06	XPL	Cross Polarizer Light
ME-MS81	Multi Element Mass Spectrometry 81	ZB	Zager Belt

Abstract

The Adi Nebri'ed structural domain is located at the northern tip of Ethiopia, bordering with Eritrea and form the southern part of Arabian Nubian Shield. It is covered by widely distributed low-grade metavolcano-sedimentary Neoproterozoic basement rocks, syn-to late-tectonic granitoids that belong to the Tsaliet and Tambien Groups of the northern Ethiopian stratigraphy.. The geotectonic and litho-stratigraphy of the metamorphic terrain in northern Ethiopia has been examined, frequently on a review-type. However, this area is exceptionally important, because it links the Nakfa Terrain in Eritrea and the Nubian Terrain in Eastern Sudan. It is also a major tectonic domain in Tigray, separating the Shiraro and Adi-Hageray blocks from West with that of the Chilla and Adwa blocks from East. The aim of the present research is to study geology, geochemical characteristics; and to constrain the geological structures and their deformation phases of study area; and to understand the tectonic history of the region. To achieve the aim of this study, review of previous work and searching maps of northern Ethiopia, and Eritrea were the prior works before the field campaign. Then, fieldwork follows to identify and describe the lithologic units, shear fabrics, structural measurement and mapping. 14 representative rock samples were taken for petrographic and geochemical analyses. Rock thin sections were prepared at the Geological Survey of Ethiopia for petrographic investigations and studied using petrological Leica Microscope. Furthermore, major, minor and trace elements data was generated using X-ray Fluorescence Spectrophotometer (XRF) and Inductively Coupled Plasma Mass Spectrometry (ICP-MS) in the Geochemical Laboratories of the Australian Laboratory Sciences.

Findings of this study indicate that Adi Nebri'ed is southern extension of Nakfa Terrain where it comprises of low-grade rocks. The geologic studies indicate that both foliated and non-foliated rocks are prevalent in the study area. These include phyllitic, graphitic- talc schist, micaceous slate, ferruginous sandstone, metalimestone, metavolcaniclastic and metavolcanic rocks displaying well-developed slaty cleavage, recrystallized fabrics, porphyroblastic,porphyroclast and xenoblast textures. The studied rocks demonstrate well-defined index mineral assemblages that record their metamorphic development and grade. These assemblages comprise minerals such as chlorite and biotite occurring in different combinations according to the degree of metamorphism. Chlorite-dominated assemblages typically indicate low-grade conditions, whereas the appearance of biotite signifies progression

to medium-grade metamorphism Furthermore, the Adi Nebri'ed mafic and ultra- mafic rocks are present in appreciable qualitities and show significant strike continuation even outside the study area, perhaps as far to southwest of Eritrea, and western Ethiopia. A number of primary (bedding) and secondary structures like normal, inferred, and thrust faults, NE to SW striking foliations and shear zones, joints, quartz veins, and dykes are present in the study area. These structures share the same trend with the regional structural extensions of Northern Ethiopia and Eritrea.

Geologically, these rocks represent volcano-sedimentary sequences that have undergone regional metamorphism and deformation during the Pan-African Orogeny. Geochemically, metavolcanic rocks typically show tholeiitic to calc-alkaline affinities, suggesting formation in island arc to back-arc tectonic settings, while metasedimentary units reflect mixed provenance and depositional environments. Structurally, the rocks exhibit well-developed foliations, folds, and shear zones, with multiple phases of deformation (D_1, D_2, and D_3) recorded through features such as slaty cleavage, and crenulation cleavage. The deformation history indicates progressive tectonic evolution, where early compressional events formed regional foliations and folds, followed by later transpressional to shear-related deformation. These structural and deformational features are consistent with regional N–S to NE–SW shortening recognized across the northern Ethiopian and Eritrean basement. Overall, the integration of geological, geochemical, and structural evidence demonstrates that these rocks share a common tectono-metamorphic evolution with the Arabian–Nubian Shield, reflecting arc accretion, crustal thickening, and subsequent deformation during the Pan-African orogenic cycle.

Keywords: Neoproterozoic, Northern Ethiopia, Adi Nebri'ed, Metavolcanics, Metasediments, Tectonic setting.

1. GENERAL INTRODUCTION

1.1 Introduction

The East African Orogen (EAO) is one of Earth's great deformation belts, stretching ~6000 km N-S along the eastern flank of Africa. Evolution of the EAO reflects a Neoproterozoic Cambrian Wilson Cycle that began with the breakup of Rodinia (870 - 800 Ma) and led to the final amalgamation of Gondwana in Cambrian time. The EAO was even longer before rifting truncated it in the north and opening of the Southern Ocean removed ~2000 km of the orogeny in Antarctica (Stern et al., 2004).

The Arabian Nubian Shield represents the northern part of EAO which formed by collision between East and West Gondwana at the end of a Wilson cycle. Geochemical and isotopic signatures indicate that these rocks are dominantly mantle-derived juvenile crust (Stern, 1994, 2008). The shield is dominated by supracrustal metavolcanics including volcaniclastics and immature sediments mostly metamorphosed in the green schist facies, variously deformed and intruded by granites, gabbros, and dikes. It extends from Jordan and Israel in the north, through to Ethiopia and Sudan in the south (Teklay et al., 1998; Stern, 2008). In Ethiopia, the ANS merges with the Mozambique Belt which is the southern half of the EAO and which accommodated the most intense collision between East and West Gondwana fragments (Stern, 1994).

Within the Pan-African domains, Orogenic belts of the Arabian Nubian Shield (ANS) and the Mozambique Belt (MB) are believed to be more prominent in outcrop in Ethiopia than in any other country of the Horn of Africa (Kazmin et al., 1978). However, the rocks belonging to these orogenic belts are only exposed in a few areas, which have not been affected by Cenozoic volcanism and rifting, and where the Phanerozoic cover rocks have been eroded away (Tefera et al., 1996).

The deformation of the ANS is linked to continental collision in the Mozambique Belt to the south infers a Wilson Cycle, beginning with the breakup of the supercontinent Rodinia, ending with the formation of a new supercontinent, and lasting most of Neoproterozoic time (Stern, 1994, 2008). The basement in northeast Africa and Arabia is referred to as Arabian Nubian Shield predominantly juvenile continental crust formed by differentiation of mantle melts largely without reworking of preexisting continental crust (Stern, 1994, 2008). Eritrea and

northern Ethiopia is clearly underlain by juvenile Neoproterozoic crust and on this basis should be considered part of the Arabian–Nubian shield (Kazmin et al., 1978).

The Northern Ethiopia metamorphic terrain consists of a series of thick, inhomogeneous volcano-sedimentary assemblages that belong to the ANS of the Pan-African Orogen (900-500 Ma) (Asrat et al., 2004). These are the events that formed the East African Orogen (EAO) (Stern, 2008), as East and West Gondwanaland collided to form the supercontinent 'Greater Gondwanaland' or 'Pannotia' and led to the dramatic climatic and biological changes marking the transition to Phanerozoic time. The well-exposed structure and stratigraphy of Neoproterozoic sequences of the EAO in Ethiopia and Eritrea provide an opportunity for studying two aspects of the evolution of the orogen: the mechanism of orogenic collapse following collision as indicated by the exhumation of the rocks of the high pressure-high temperature Gedem Domain (Beyth et al., 2003). This suggestion is supported by the lithologic characteristic of the Mozambique Belt and its extension to the north, the Arabian-Nubian Shield (ANS).

The stratigraphy of the Late Neoproterozoic low-grade metasediments of Tambien Group and metavolcanics of Tsaliet Group of north Ethiopia was described by Kazmin et al. (1978); and Avigad et al. (2007). Furthermore, as summarized by Tadesse et al., (1999) previous studies have indicated that the Precambrian geology of northern Ethiopia belongs to a well-defined tectonostratigraphic framework. The Tsaliet Group and the Tambien Group with minor but locally important and younger stratigraphic formations; namely the Didikama Formation, the Shiraro Formation and Matheows Formation in younging stratigraphic sequence.

1.2 Description of the study area

1.2.1 Location and Accessibility

The study area is located in Adi Nebri'ed, Seyemti Adyabo wereda, about 42 kilometers Northwest of Shire town, which is the zone of Northwestern Tigray regional state, Northern Ethiopia. It is located in the country's far north, near the border of Ethiopia and Eritrea. Geographically, the study area is bounded between 1590000 - 1598000 m N latitude and 408000 - 423000m E longitude (Fig. 1.1). The area coverage of study is approximately 72 Km^2.

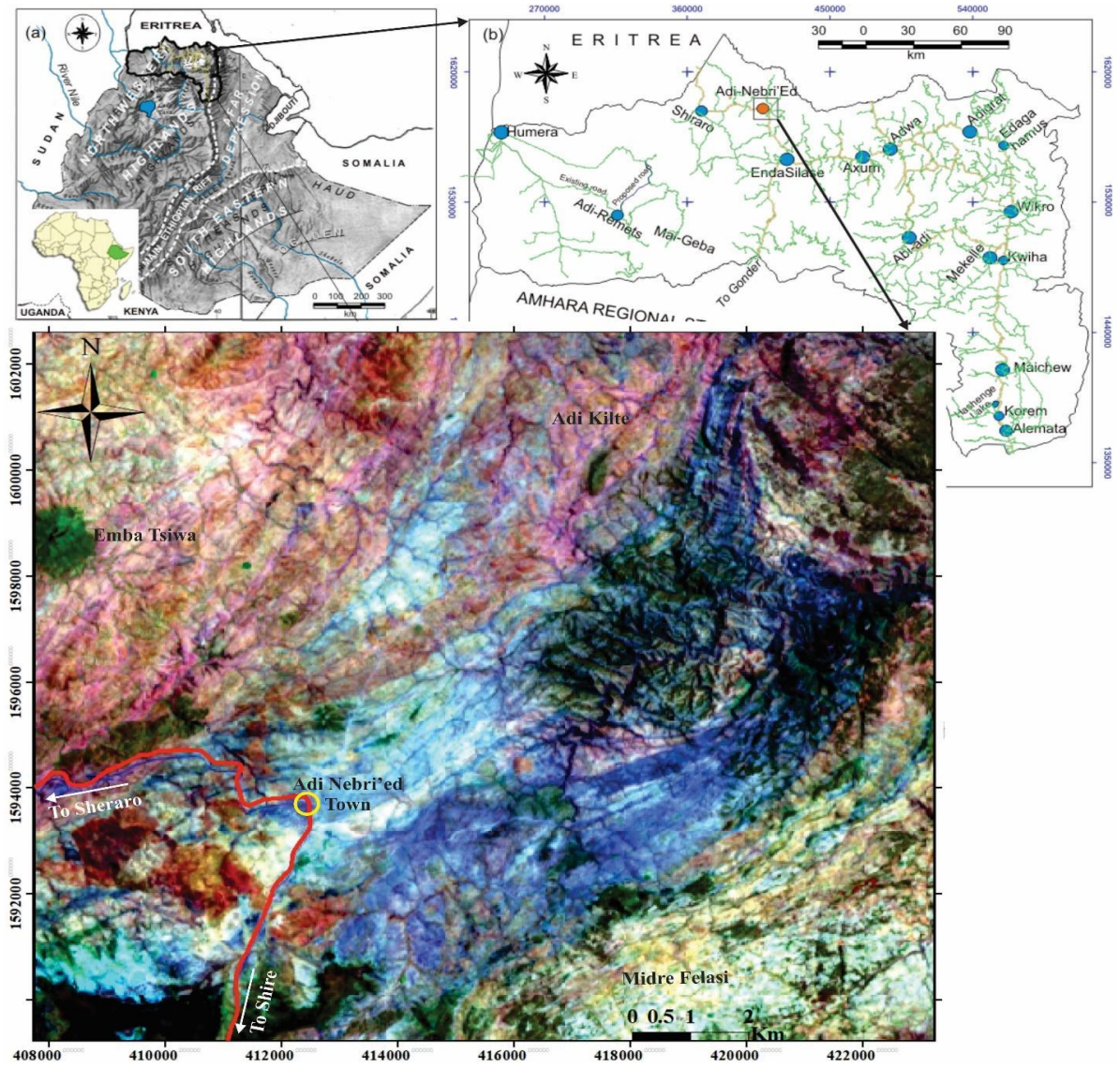

Figure 1.1: Location and accessibility map of the study area with reference to Ethiopia (a) and Tigray (b). Projected Coordinate System: Adindan_UTM_Zone_37N. Projection: Transverse Mercator.

The study area is well accessed from Mekelle, the capital city of Tigray regional state through asphalted roads via Adigrat-Adwa-Aksum-Shire or Abi Adi-Adwa-Aksum-Shire, and the road is crossing through Adi-Nebri'ed to Shiraro - Humera. Generally, the accessibility was quite easy especially in the flat land of the area mainly at the center of the area surveyed. The presences of the road network in the area were useful for the mapping purposes. However, near the boundary sides mainly Northeast, East, and Southeast parts of the area posed a little challenge because of they were mountainous and hills with no more trails for travel.

1.2.2 Physiography and Drainage pattern

The Ethiopian landmass consists of a large, high elevated plateau bisected by the Rift Valley into the northwestern and the southeastern highlands, each with associated lowlands. The contrast in relief is remarkable as land elevation ranges between −116 m of Dalol in the Afar depression to the peak of Mt. Ras Dashen at 4,533 m a.s.l. in the Simen Mountains, which is situated within the Simien National Park (a UNESCO World Heritage site) (Billi, 2015; Fazzini et al., 2015).

The physiographic condition of the Adi Nebri'Ed area is determined by taking into account a relatively vast area of the surrounding environment. Thus, ridges, hills, and flat terrain are among the topographic features that define the study area and its environs. Adi Nebri'ed is found at an elevation of about 1900 m.a.s.l, which is top flat area, whereas the northern, northeastern, and northwest surroundings have varying topography, with an elevation ranging from 900 – 2300 m.a.s.l (Fig. 1.2 A). However, the study area specifically have an elevation ranging from 1480 – 1900 m.a.s.l. The lower elevated portion is located along the route towards the Adi Hageray direction, while the higher elevated area is thought to be around the Midre Felasi villages (Fig. 1.2 B). The study area's hills and plateaus are made up mostly of metavolcanic rock units, whereas the flat areas are mostly made up of metasedimentary rock units.The ridges typically go north to south and feature a number of saddles and steep slopes.

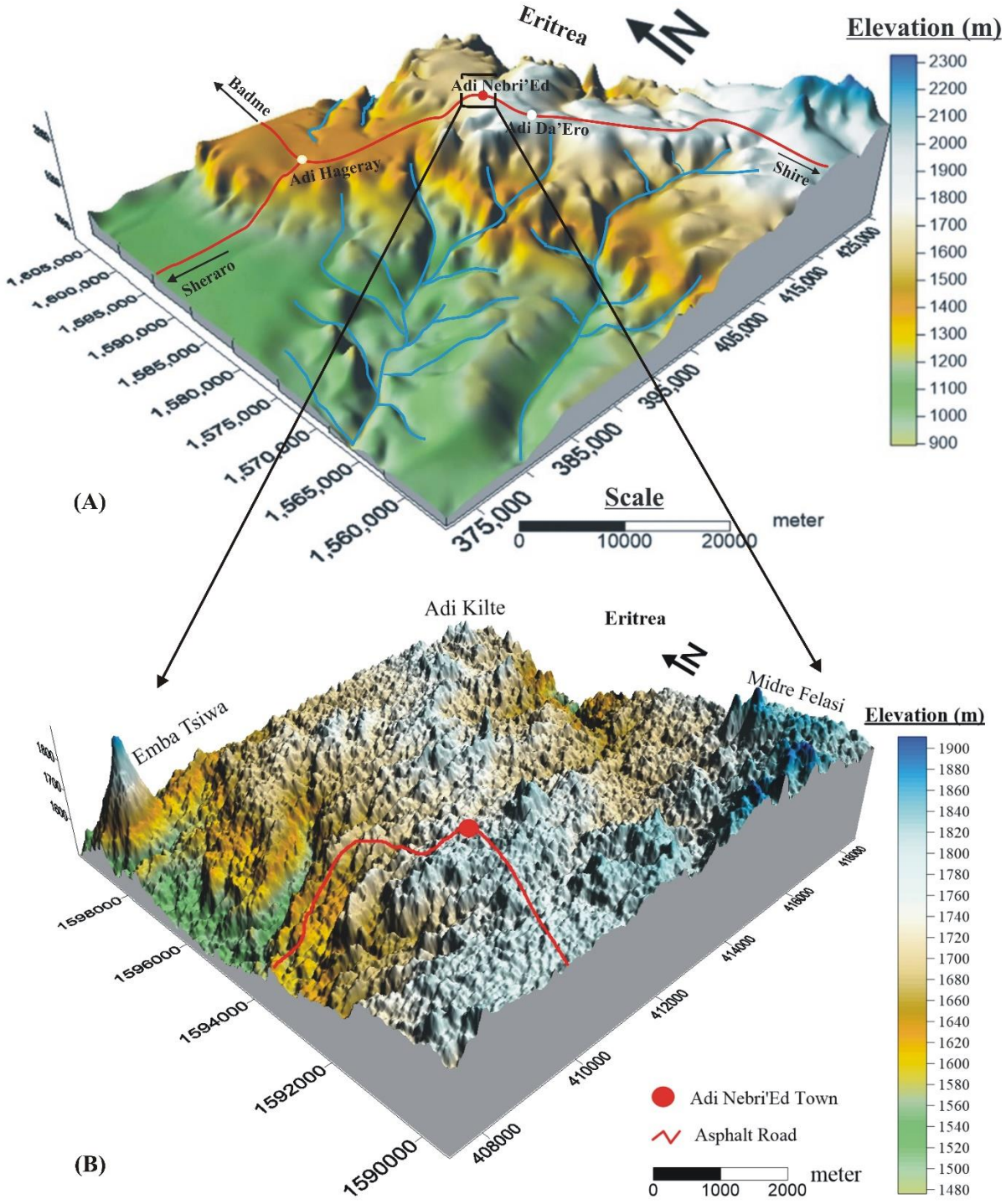

Figure 1.2: The physiographic features of the study area (B) and its vicinities (A). The image is extracted from the Digital elevation model of Ethiopia (resolution of 30x30 meters) using Global Mapper and later processed by Surfer-10.

The streams and rivers in the studied area shape the drainage patterns, which are influenced by the topography, geological formations, gradient, and/or geomorphology of the region. The

study area is drained by a number of small, erratic rivers. These rivers have their source in the highlands nearby, which are dense where there are steeper slopes and scarce where there are relatively flat slopes. While the mild slopes and plain areas typically have long streams in places where the soils are deep and permeable, the majority of the steep well-drained sections typically have multiple minor tributaries. The study area typically features a dendritic drainage pattern, which is defined as "pertaining to a tree" (Fig. 1.3).

Sections north of Adi Nebri'ed area flows to the main Mereb River, which marks the border between Ethiopia and Eritrea, while sections south of study area flows to the Tekeze River. The drainage pattern of the stream shows fluctuations in water flow density as a result of seasonal variations.

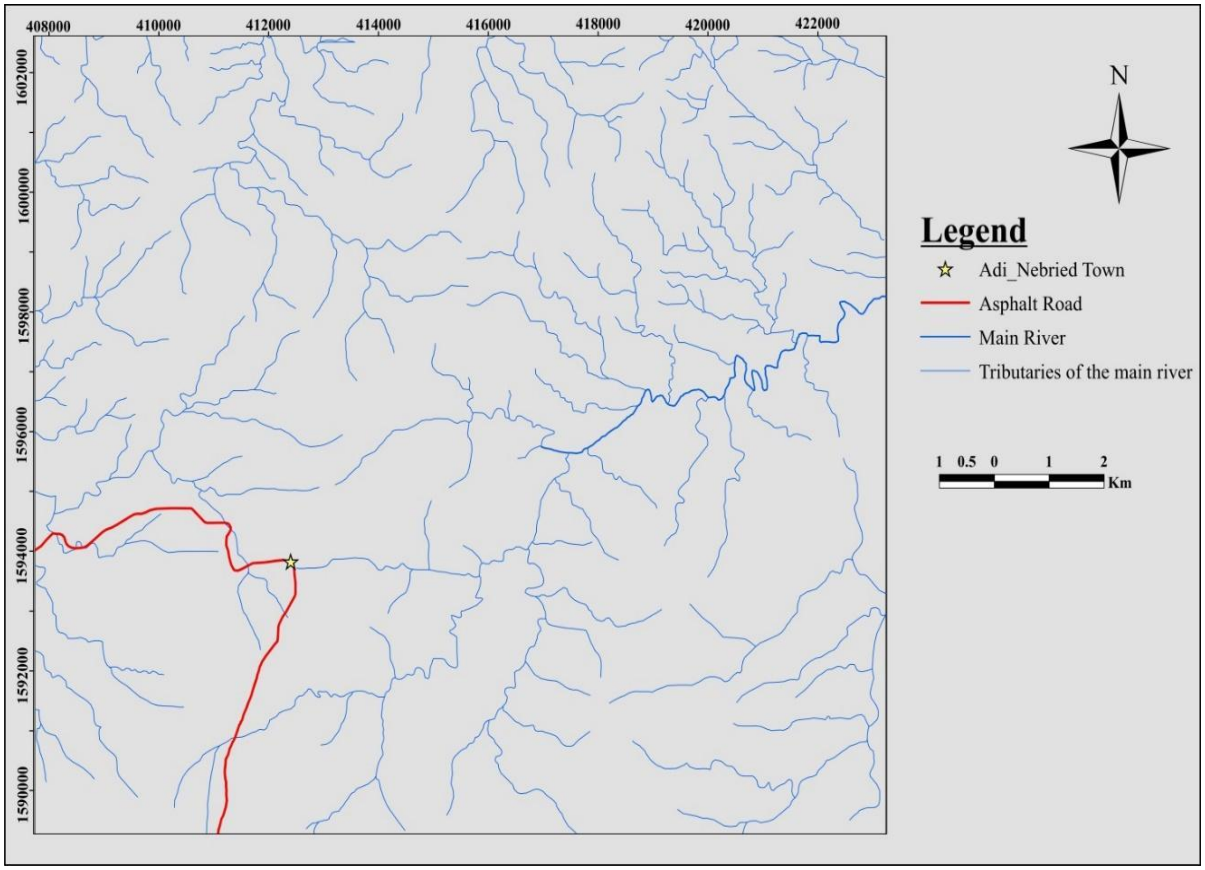

Figure 1.3: Drainage map of the study area showing dendritic type patterns. Prepared from watershed analysis of Digital elevation model of Ethiopia (resolution of 30x30 meters).

1.3 Climate and Vegetation Cover

The area experiences both a humid, and hot environment. The main rainy season begins in the middle of June and lasts until the middle of September, with sporadic rainfall in March. Since the study area location is close to Shire Town, 2008 to 2015 climate data from that town was used to analyze the climate condition of the area. According to climate statistics, the average annual rainfall in the area ranges from 600 to 800 mm. Similarly, the temperature can get as high as 36 degrees Celsius in the dry season, while it can be as low as 20^0C in the wet season (Fig. 1.4).

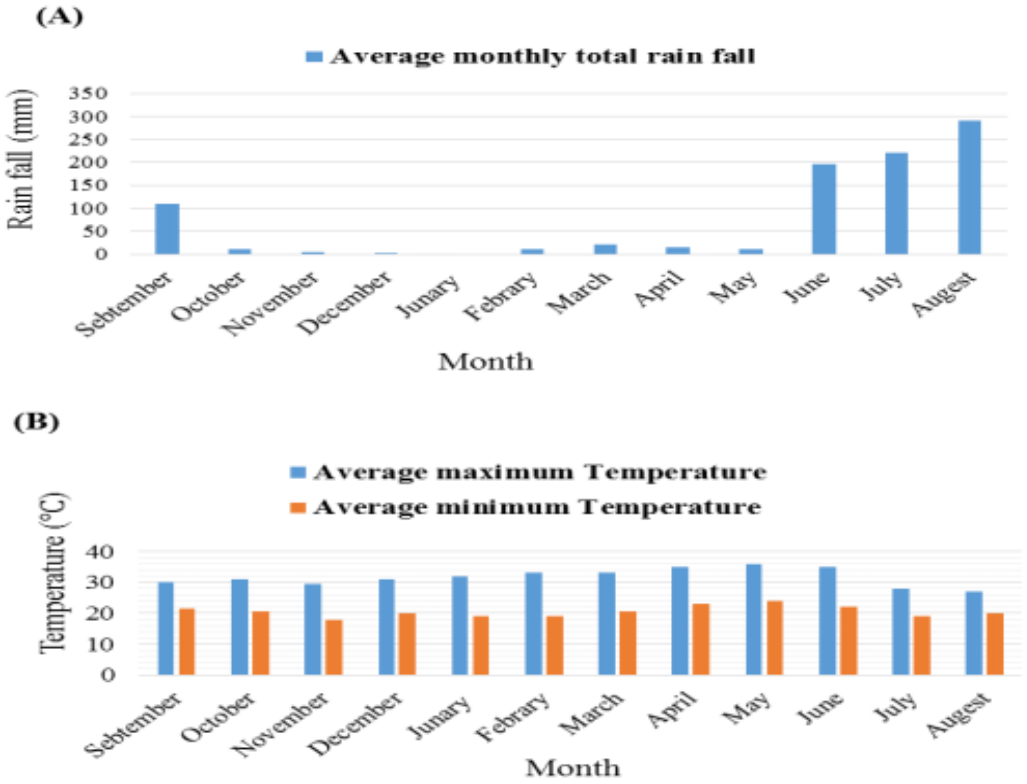

Figure 1.4: Histogram showing A) Average monthly rainfall and B) Minimum and maximum temperatures of the study area (NMAT, 2019).

A limited vegetation cover distinguishes the study area. Thorny bushes, shrubs, and deciduous trees cover the area, which is relatively vegetated in the North, East, Northeast, southwestern corners. Additionally, there have been several scattered trees in the areas of sporadic and permanent river valleys.

1.4 Problem statement

Although the geotectonic setting and lithostratigraphy of the metamorphic terrains in northern Ethiopia have been extensively studied, most of the existing works are largely review-based and lack detailed. This region is of considerable geological significance, as it serves as a crucial link between the Nakfa Terrain of Eritrea and the Nubian Terrain of eastern Sudan. Moreover, it represents an important tectonic domain within Tigray, connecting the northern Ethiopian blocks with the Eritrean terrains. Previous studies have recognized widespread occurrences of low-grade Neoproterozoic basement rocks, including metavolcanic, metavolcaniclastic, metasedimentary, and intrusive units with diverse compositions. Nevertheless, a clear gap remains in the comprehensive correlation, integration, and tectono-stratigraphic linkage of these units within the broader African framework.

Therefore, this study presents the history of local deformation supported by field observations, petrographic and structural analyses, and geochemical characterization of the basement rocks (i.e., metavolcanic, metavolcaniclastic, metasedimentary, and intrusive rocks), which will contribute to a wider understanding and future research on geological studies, mineral exploration and exploitation, and understanding the tectonic setting of the region.

1.5 Objectives of the study

1.5.1. General objective

The general objective of this study is to constrain the lithologic units, geological structures and their deformation phases, and to understand the tectonic domain of the area.

1.5.2 Specific objectives

Within the framework of the above general objective, this study aims to achieve the following specific objectives:

- To prepare a detailed geological and structural map of the study area at a scale of 1:50,000.
- To identify, describe, measure, and analyze geological structures at both macro- and micro-scales, and to correlate them with regional structural frameworks.

- To conduct petrographic analysis of representative rock samples from each lithological unit in order to determine their mineralogical composition and textural characteristics.
- To establish the sequence of deformation phases (D_1, D_2, etc.) and evaluate the relationships between lithology and metamorphism through detailed analysis of metamorphic microstructures using thin sections.
- To perform geochemical analysis of selected rock samples to constrain the tectonic setting and infer the origin and evolution of the Precambrian basement rocks in the study area.

1.6 Significance of the study

As stated in the statement of problem, the study area is exceptionally important, because it is an extension of the Nakfa Terrain in the north (Eritrea) and Nubian Terrain in the East Sudan. It is also a major tectonic domain in Tigray, Northern Ethiopia, separating the Shiraro and Adi-Hageray blocks from West with that of the Chilla and Adwa blocks from East. Therefore, the geological petrographical, and geochemical, data may supplement the local structural and geological data which in turn significantly aid in understanding the tectonic history of the region.

In general, the current study's findings and results will be beneficial for:

- The experts who are working in the investigation and exploration of minerals and natural resources,
- For academic institutions (especially those who are interested in related works that provide relevant information in the country and elsewhere) with similar geological and structural setup.

2. METHODOLOGY

2.1 Introduction

The methods used in this investigation were formulated based on the goals that were established. Thus, in order to achieve the previously described objectives, the following methods were employed. Prior to the field campaign, office preparation was done. This included review of previous work and gathering of available maps in order to have an overview about the geology and geological structures in the area and its surrounding zones; aerial photos/satellite images examination and interpretation using appropriate techniques, requesting field material and equipment from Mekelle University store and other pre-field preparation works has been accomplished.

2.2 Review of previous works

The Precambrian terrain of northern Ethiopia and Eritrea is predominantly composed of a low-grade, metavolcano-sedimentary assemblage (Beyth, 1978; Tadesse et al., 1999; Alene et al., 2006) and has long been regarded as the southern part of the Arabian-Nubian Shield. The studies on northern part of the Arabian-Nubian Shield (in Saudi Arabia, Egypt and Sudan) show that it has developed by Wilson-type plate tectonic processes involving repeated arc accretion and terrain amalgamation during Pan-African Orogeny (Beyth, 1978).

In contrast to the above-mentioned Precambrian terrains, the Precambrian basement terrain of northern Ethiopia is one of the least studied parts of NE Africa. Therefore, structural, geochemical and petrographic details from the study area and their integration with field observations will help to improve the knowledge of geological evolution of the region. The basement rocks of Ethiopia have long been considered part of the Arabian– Nubian Shield (Kazmin et al., 1978; Tadesse et al., 1999; Barbeyet al., 2003).

The structure of the basement complex is defined by NE-trending folds with NW-dipping bedding and foliation on the plateau, and SE-dipping structure in the Ethiopian escarpment area (Beyth et al., 2003). The tectonic structures recorded by the Tsaliet and Tambien Group rocks are related to the collisional stress that resulted in the amalgamation of the ANS. Generally, two phases of deformation (D1 and D2) are recognized (Alene et al., 2006). Deformation D1 is caused by N-S compression and resulted in tight minor folds with a wavelength of several

mm to dm, elongation lineation and pervasive regional foliation. D2 deformation resulted from E-W directed compression at the waning stage of the collision between East and West Gondwana and yielded long wave length (about 8 km), upright, open parallel folds without a significant cleavage, thrust, and strike slip faulting (Alene et al., 2006). Geological, structural, and geochemical correlations were established with previous regional studies, which provide essential structural, petrographic, and geochemical data that support and enhance the findings of the present study.

2.3 Fieldwork

During the identification of lithologic units, structural mapping and sampling, traverses were designed across the structures or shear fabrics and denser observation points were taken where the exposure of the rocks are clear and abundant. Accordingly, seven traverse lines were selected that potentially targeting to cover the lithological units, structures and/or shear zones. Observation points were made depending the change on the lithology and/or structural complexity.

In the field, different rock formations and their relationship to the other formations were observed. At each location, rock outcrops were carefully examined and properly located by GARMIN global positioning system (GPS) on the base map for further digitization using ArcGIS. Descriptions of lithostratigraphy in relation to documentation, measurement, and recording of all structural data have been undertaken.

Description of all the lithological variation in color, texture, mineral composition, kind and degree of weathering, color of fresh surface, and fabric have been done. Quartz veins that possibly occur in the sequence of metamorphic rocks with their aerial extent, attitude and contact relationship were also examined and noted for further analysis. More than thirty (30) samples were collected, but about fourteen (14) representative rock samples are randomly selected for geochemical analysis and nine (9) for petrographic analysis.

2.4 Data analysis

The data collected in the field were analyzed and compiled using various techniques. They include analyzing, synthesizing, and interpreting the data. After the fieldwork the following tasks were undertaken.

2.4.1 Petrographic Analysis

Rock thin sections were prepared by cutting each sample into approximately 300 g hand-specimen–sized blocks (dimension suitable for standard billet preparation) using a rock cutter, after which the samples were coded and sent to the Geological Survey of Ethiopia, Addis Ababa, Ethiopia, for thin section preparation. The prepared thin sections were subsequently studied and analyzed using a petrological Leica microscope at the Faculity of Mining and Geoscineces, Mekelle University, Ethiopia. All images were observed and photomicrographs captured under cross-polarized light (XPL), with a standard scale of 200 µm applied to ensure consistent thin-section resolution and accurate mineralogical interpretation.

2.4.2 Structural analysis

Geological structures like folds, foliation, lineation, faults, and joints were recorded for properly during the fieldwork. GPS was used to gather and locate the field data, and ArcGIS software used to create a detailed geological map and structural at a scale of 1:50,000 that displays the orientation of significant geological structures and lithological units. Each structural component linked to each phase of deformation is examined separately using Stereonet, which is also used to show structural and geometric correlations. The Stereonet has been contoured and plotted with the poles of these planes to provide a general orientation of the foliations, folding, quartz veins, dykes, shear zones, and fractures.

2.4.3 Geochemical analysis

Geochemical analysis of selected rock samples determines their elemental composition to infer origin, formation conditions, and geological history through laboratory preparation and analysis.14 rock samples made into fine powder to ensure homogeneity in the milling chamber at Mekelle University, and weighed 200 gm each, packed and sent to the Geochemical Laboratories of Australian Laboratory Sciences (ALS), Nifas Silk sub-city branch, Addis Ababa, Ethiopia. The major, minor and trace elements concentrations were generated using X-ray Fluorescence Spectrophotometer (XRF) and Inductively Coupled Plasma Mass Spectrometry (ICP-MS) in the ALS Geochemical Laboratory. The geochemical data are then processed using GCDkit software package to produce different geochemical diagrams. The accuracy and analytical procedure for both major and trace elements are available on the ALS official website (alsglobal.com).

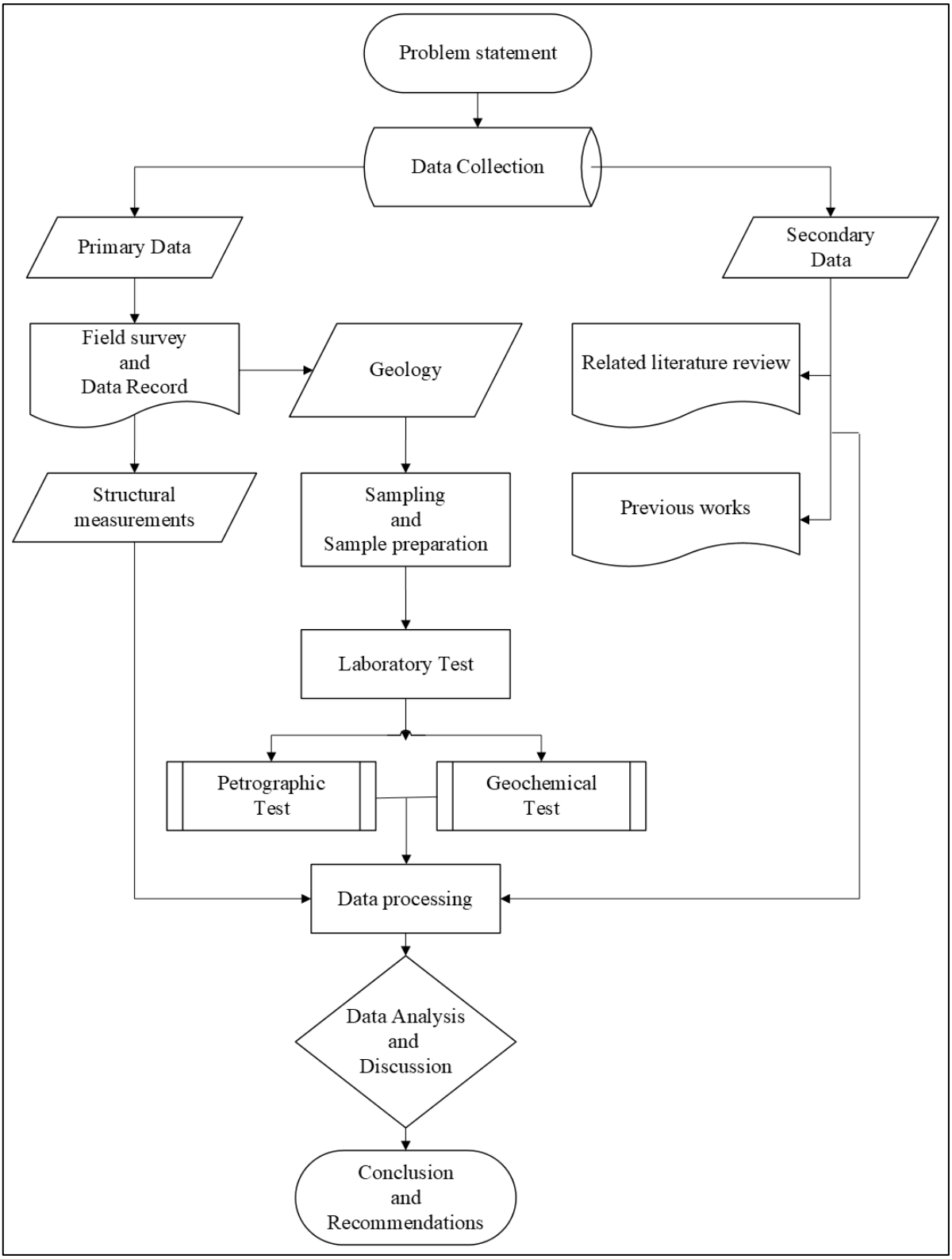

Figure 2.1: Summarized flow chart of the methodological approach

3. GEOLOGY

3. 1. REGIONAL GEOLOGICAL SETTING

3.1.1 Geodynamic Evolution of the East African Orogen

The East African Orogen (EAO) is one of Earth's largest collision zones, where East and West Gondwana collided to form the supercontinent 'Greater Gondwana' or 'Pannotia' at the end of Neoproterozoic time (Stern, 2002, 2005). The EAO is also one of the largest collision zones on Earth, spanning over 6000 kilometers. (i) Rodinia rifting and break-up at approximately 900 - 850 Ma; (ii) seafloor spreading, arc and back-arc basin formation, and terrain accretion from 870 - 690 Ma; (iii) continent-continent collision from 630 - 600 Ma; and (iv) additional crustal shortening, orogenic collapse, and extension that resulted in the break-up of Gondwana between 600 and 540 Ma (Stern, 1994, 2006) (Fig. 3.1).

The ophiolites, granulites, and structures of the EAO are fossil fragments of a Neoproterozoic Wilson cycle, representing the opening and closing of an ocean basin that lay between the older crustal blocks of East and West Gondwanaland .Even if the understanding of the style and timing of collision between East and West Gondwanaland to form the East African Orogen is incomplete, the general outline of this important event in Earth history is slowly emerging (Stern, 1994).

The Neoproterozoic rocks formed during a supercontinent cycle (Nance et al., 2014) bracketed by the 900 - 720 Ma break-up of Rodinia (Li et al., 2008) and the ~650 - 530 Ma multiphase assembly of Gondwana concurrent with East African Orogeny (Collins and Piskarevsky, 2005; Meert and Liberman, 2008) (Fig. 3.1 and 3.2).

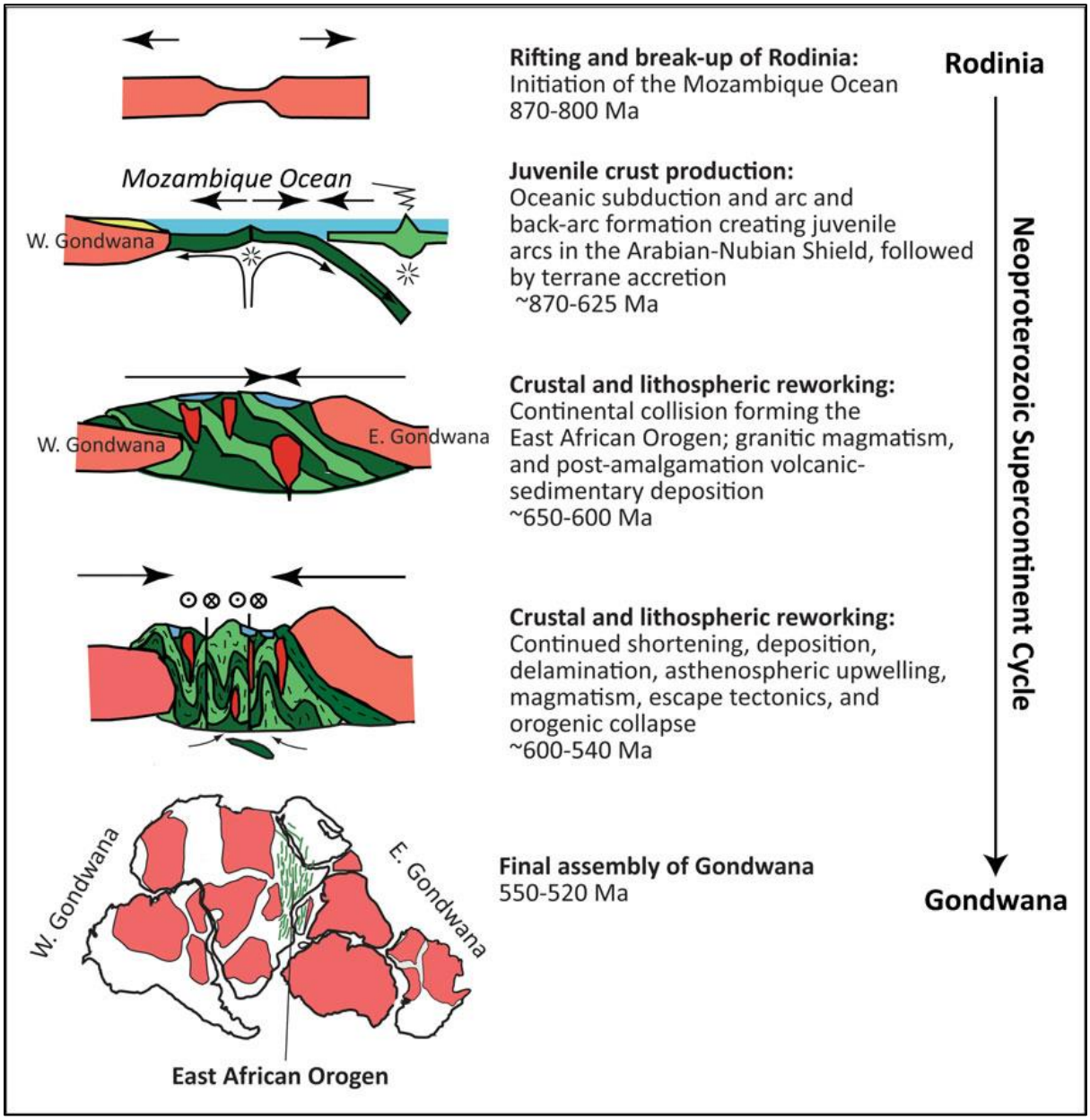

Figure 3.1: Schematic illustration of tectonic events in the Arabian–Nubian Shield associated with the Rodinia Gondwana supercontinent cycle (after Stern and Johnson 2010; Johnson, 2021).

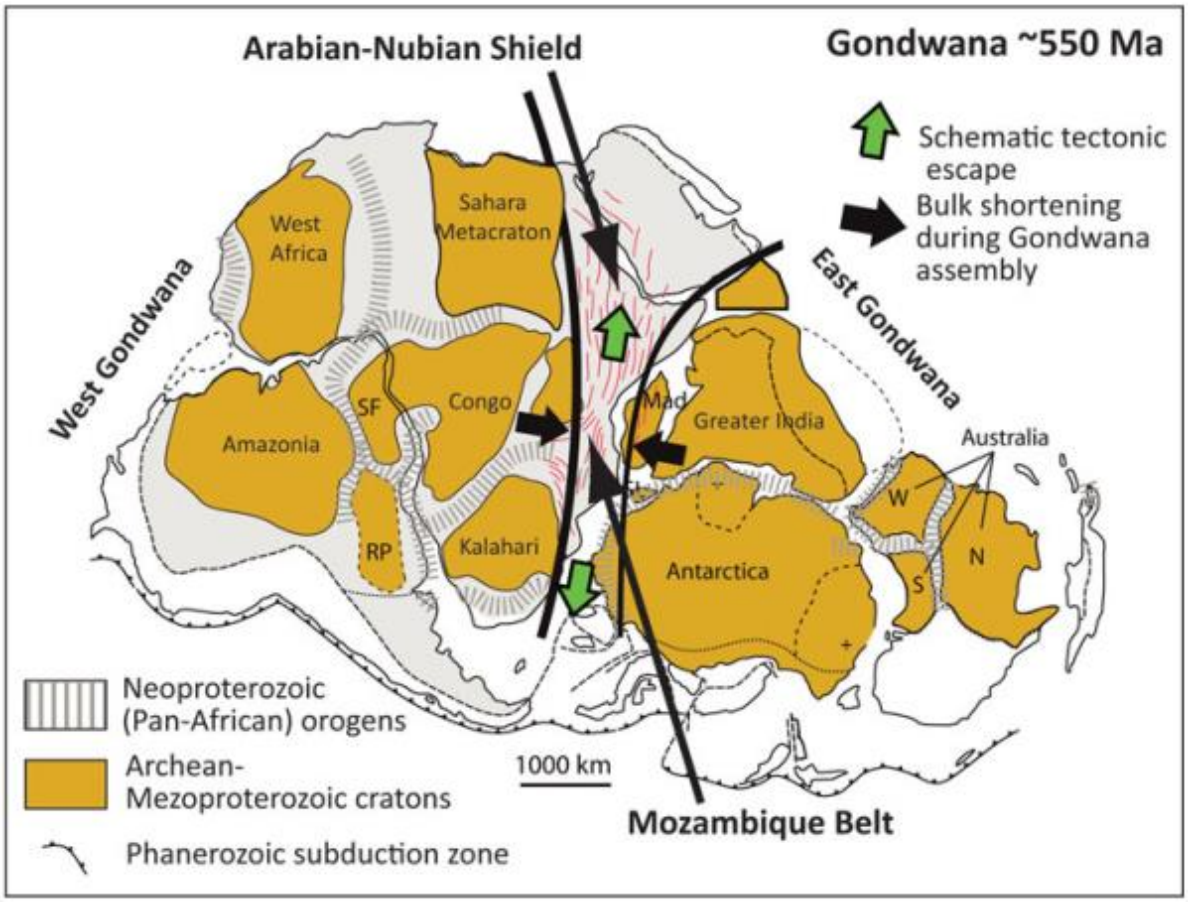

Figure 3.2: Schematic maps showing Gondwana after assembly of its constituent cratonic blocks at about 550 Ma illustrating the axial location of the East African Orogen (after Gray et al., 2008; Johnson, 2021).

3.1.2 The Arabian Nubian Shield

The Arabian Nubian Shield (ANS) underlies parts of the African and Arabian Plates (Fig. 3.3), and the Nubian Shield is being further subdivided by the East African Rift System so that the eastern portion of the Nubian Shield is in the nascent Somalia Plate (Johnson, 2021; Hamimi et al., 2021). It consists of Neoproterozoic rocks ranging in age from ~980 - 535 Ma and Archean Paleoproterozoic structural enclaves. The ANS came into being because of plate tectonics the shifting and rearrangement of crustal blocks in the Earth's crust over time and is being modified and broken up because of current plate tectonics. The ANS rocks formed in the Mozambique Ocean (Dalziel, 1991), an ocean basin between the Saharan, Congo–Tanzania, and Indian cratons created by Rodinia break-up (Hamimi et al., 2021).

According to Johnson (2021), the correlation of basement structures in Egypt and Sudan with equivalent geologic features in Saudi Arabia is clear proof that the Arabian and Nubian Shields were contiguous prior to Red Sea rifting at ~25 Ma although the degree of proximity of the African and Arabian Plates prior to Red Sea rifting is strongly debated (Bosworth, 2015). This author also stated that, correlation of basement structures across the Gulf of Aden is not as well established, but there is general consensus that pre-Neoproterozoic crust in northern Somalia and northeastern Ethiopia broadly correlates with pre-Neoproterozoic crust in Yemen and Oman.

According to Abdelsalam and Stern (1996), and Tadesse et al. (1999), the Arabian Nubian Shield (ANS) is mostly composed of sutured low-grade assemblages of Neoproterozoic volcanic, volcano sedimentary and sedimentary units, intrusive, and contains several ophiolites, which are remains of oceanic crust. The high-grade rocks were also derived from continental crust recycled during the East African Orogen, greenschist to lower amphibolite metamorphosed volcano-sedimentary terranes including calc-alkaline basaltic and andestic lavas, tuffs, pyroclastics, and rhyolites, which are intruded by various pre-, syn-, and post-tectonic granitoids and occurring between the western and eastern terrain (Abdelsalam and Stern, 1996), recognized two deformation belts in the ANS:

1) Related to arc-arc and arc-continent collision, which are both associated with sutures. The arc-arc deformation belts are manifested by the occurrence of E-W and N-S verging ophiolities in the northern and southern parts of the ANS respectively. The E-W verging ophiolities are steepened by upright folds, whereas those of N-S vergence are deformed by up-right folds and strike slip faults related to oblique collision of the terrains at about 800 - 700 Ma. The arc-continent deformation belts are related to the collision of East and West Gondwana.
2) Post-accretionary structures (~650 - 550 Ma) resulted from continuous shortening of the ANS and developed NW trending strike slip faults and shear zones during the waning stages of ANS formation. According to (Avigad et al., 2007). Northern Ethiopia (Tigray) and much of Eritrea and Ethiopia plateaus expose ANS-type green-schist facies volcano-sedimentary sequences.

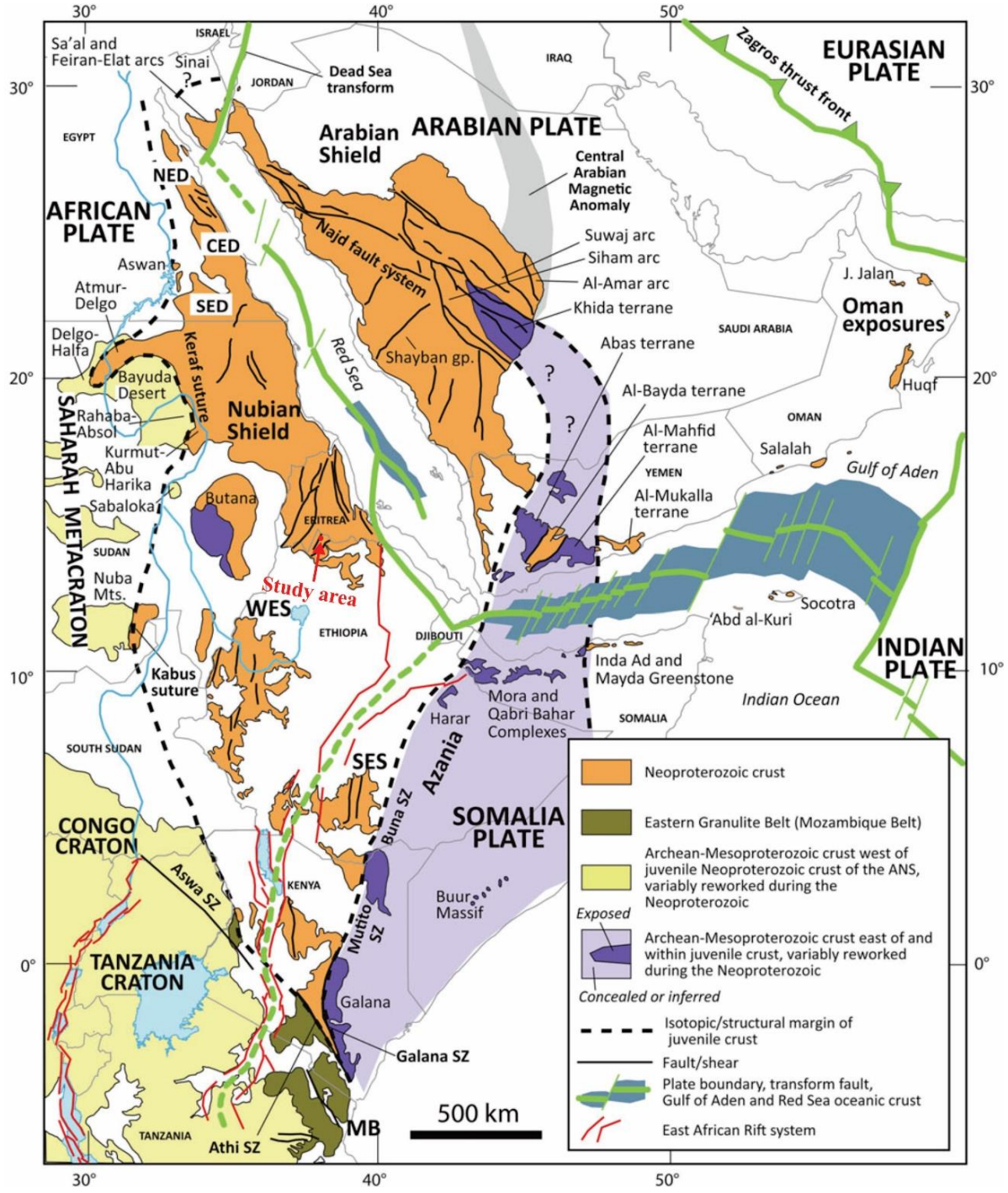

Figure 3.3: Map of Northeast Africa and the Arabian Peninsula showing the distribution of juvenile Neoproterozoic crust and adjacent regions of Archean Mesoproterozoic crust (after Fritz et al., 2013) and Cenozoic plate boundaries, Red Sea-Gulf of Aden spreading centers, and the East African Rift system (after Johnson, 2021). CED = Central Eastern Desert; NED = North Eastern Desert; SED = South Eastern Desert; SES = South Ethiopian shield; WES = West Ethiopian shield.

3.1.3 Mozambique Belt

The Mozambique Belt (MB) was first named by Holmes (1951), who recognized a structural discontinuity between the Tanzanian Craton and gneisses to the east, which were found to have an age of 1300 Ma. It is the southern part of the East African Orogeny and essentially consists of medium to high-grade gneisses and voluminous granitoids and it extends south from the Arabian-Nubian Shield into southern Ethiopia, Kenya and Somalia via Tanzania to Malawi and Mozambique and includes Madagascar (Stern and Kroner, 2005). There is no overall model for the evolution of the MB although most workers agree that it resulted from collision between East and West Gondwana. Compared to the strong deformation and metamorphism experienced during collision in the Mozambique belt, the ANS was considerably less affected by the collision. The Mozambique Belt exposes higher temperature and pressure suites with abundant amphibolite and granulite-facies metamorphic rocks and gneiss terrains (Avigad et al., 2007).

3.1.4 Neoproterozoic geologic setting of Eritrea

The Neoproterozoic juvenile crust of Eritrea consists of a high-grade gneiss domain and a low-grade volcanosedimentary domain (Ghebreab et al., 2005, 2009; Andersson et al., 2006). The high-grade domain represents deep crustal rocks characterized by low-angle fabrics and structures, whereas the low-grade domain represents steeply dipping upper crustal rocks. The gneiss domain structurally underlies and bounds the volcano-sedimentary domain both to the east and to the west. Syn-, late- and post-tectonic intrusive rocks are scattered between the Augaro-Adobha Belt and Asmara-Nakfa Belt, and also occur locally within the belts as elliptical or circular rigid bodies, locally as much as 10 km in diameter (Filjak et al., 1959; Mohr, 1979; Drury and Berhe, 1993; Drury and de Souza Filho, 1998).

A discontinuous N–S-trending belt of high-grade rocks and synto late-tectonic granitoid rocks occurs in central Eritrea within the low-grade domain (Ghebreab, 1996; Drury and de Souza Filho, 1998). This tectonic unit forms part of the Arag terrain of Drury and de Souza Filho (1998) and extends from Sudan to northern Ethiopia, and has been attributed by Ghebreab et al. (2005) to hot rocks with low densities and viscosities that were tectonically extruded along shear zones probably during the late Neoproterozoic vertical collapse before they were embrittled.

Four or perhaps five large terrains that are structurally and lithologically distinct constitute the Neoproterozoic of Eritrea (Drury and de Souza-Filho, 1998). From west to east, these are the Barka, Hager, Adobha Abiy and Nakfa Terrains (Fig. 3.4). De Souza Filho (1995) further subdivided the Hager Terrain into the Shemegui and Hager Terrains. The Nakfa terrain supracrustal rocks are greenschist facies metamorphic rocks with dominantly steep fabrics, which are exposed in the central Eritrea plateau and along the Red Sea escarpment (Ghebreab, 1999; Woldehaimanot, 2000). These authors also stated that the main lithological units in the Barka Terrain are gneisses, amphibolites, marbles, politic schists and orthoquarzites metamorphosed at mid-to upper amphibolite-facies. The Shemegui Terrain is dominated by chlorite schist, Fe-Mn cherts, marbles, pillowed metabasalts, metagabbros and serpentinites. It is separated from the Barka Terrain by a major sinstral strike-slip shear system, the Barka Shear Zone (suture). The Hager Terrain comprises of mafic and felsic metavolcanics, pre-tectonic intrusives (diorites, tonalities, granodiorites, gabbros and pyroxenites) and various schists. The Adobha Abiy Terrain consists of quartzo-feldspathic sandstones, conglomerates, graphitic and chloritic schist, and marbles.

The Precambrian rocks in the Augaro area (Western Eritrea) are part of the Nakfa terrain of Drury and de Souza-Filho (1998), which is characterized by well preserved green-schist facies supracrustal rocks of dominantly sedimentary origin with subordinate volcanic rocks (Teklay et al., 2003). These supracrustal assemblages are intruded by pre- or syn-tectonic intrusive rocks of gabbroic to granitic composition which, in turn, are intruded by late- to post tectonic granites.

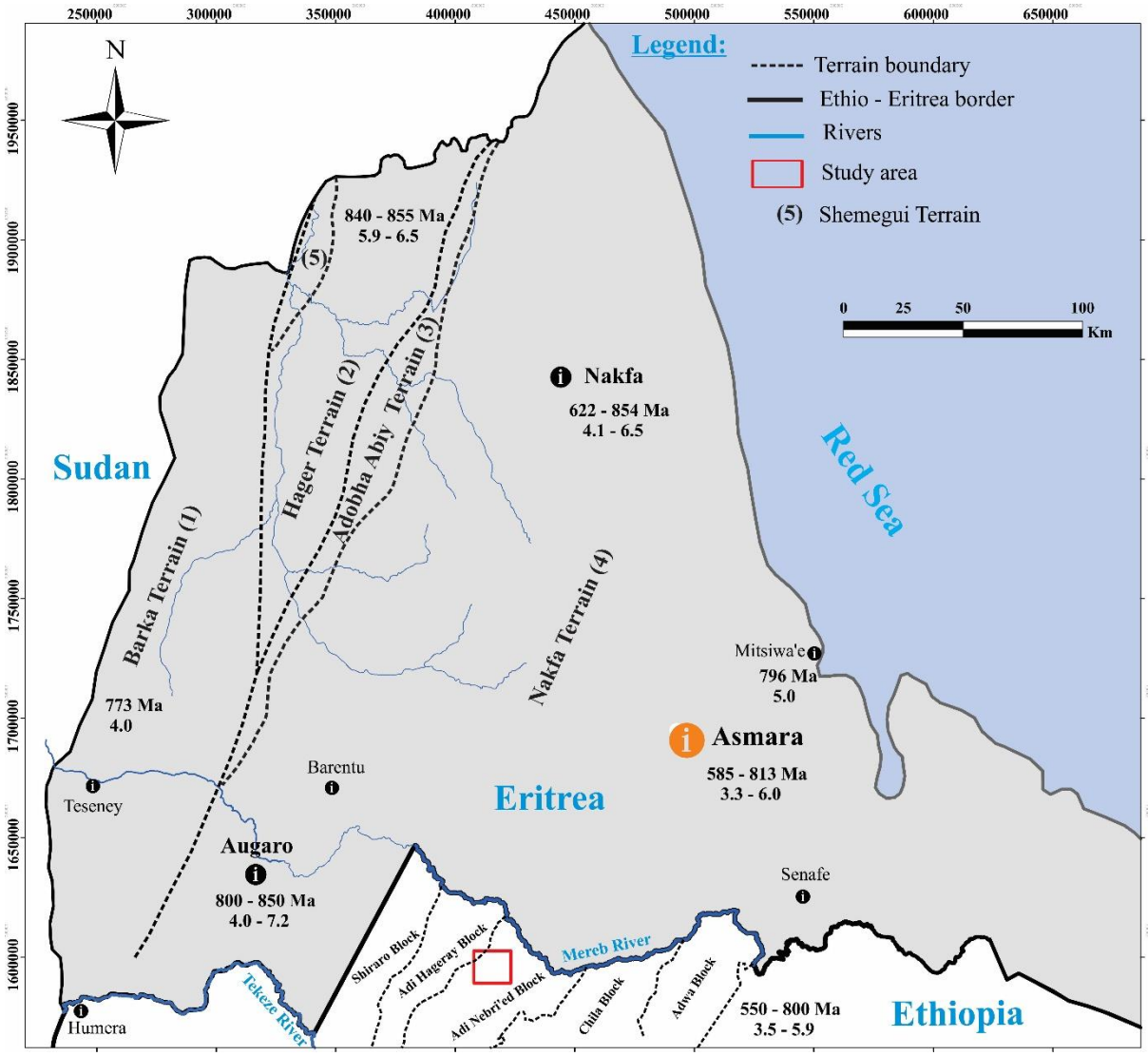

Figure 3.4: Terrane classification of Eritrean Neoproterozoic rocks (after Drury et al., 1994). The volcano-sedimentary blocks, ages and initial epsilon Nd values for northern Ethiopia are from Tadesse (1996) and Tadesse et al. (2000) (Modified after Tadesse et al., 1999; Woldehaimanot, 2000; Teklay et al., 2003; Ghebreab et al., 2009).

3.1.5 Geology of the Ethiopian basement rocks

The basement rocks of Ethiopia are exposed in north, south, southwest, western, and eastern parts of the country which are grouped into three major groups by Kazmin et al. (1978) based on lithologic and structural mapping: Lower Complex (Archean), Middle Complex (Lower –Middle Proterozoic) and Upper Complex (Upper Proterozoic). In similar way, the Precambrian rocks of Ethiopian have been studied by various scholars [Beyth (1971, 1972); Kazmin (1971, 1975); Kazmin et al. (1978); Garland (1980); Berhe (1990); Tefera et al. (1996); Woldhaimanot (1995); Tadesse (1996); Tadesse et al. (1997, 1999, 2000); Tadesse

(1998); Alene and Barker (1993, 1997); Alene (1998); Alene et al. (2000a, 2000b, 2006) and Asrat et al. (2001, 2003, 2004); Tadesse & Allen (2005); Avigad et al. (2007)] to mention only a few.

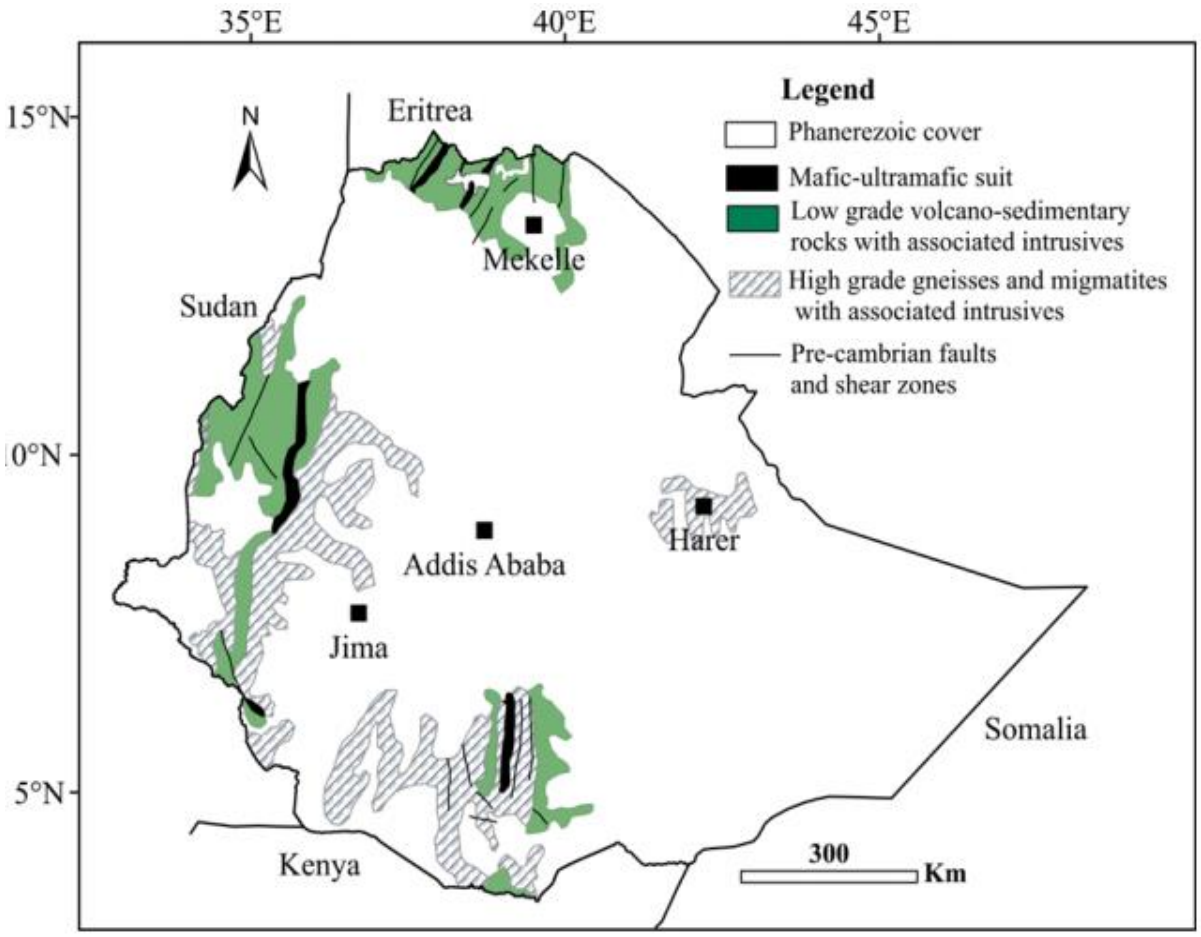

Figure 3.5: A map showing the distribution of low-grade volcano-sedimentary sequences of the ANS and high-grade gneisses and migmatites of the Mozambique belt in Ethiopia (after Tefera et al., 1996).

This subdivision has recently been revised in light of geochronological and isotopic data, as well as two different lithotectonic terrain classifications that exhibit contrasting lithological association, internal structures, and grade of metamorphism (Teklay et al., 1998; Yibas et al., 2003; Stern et al., 2004): (1) the granite-gneiss terrain, which includes the Lower and Middle Complex of the old classification (Kazmin, 1971); and (2) the ophiolitic fold and thrust belts, which are composed of low-grade, mafic–ultramafic and sedimentary assemblages that comprise all the rocks of the Upper Complex (Kazmin, 1971, 1975). According to Asrat et al. (2001), the Gneisic-migmatitic landscape is divided by a large number of Ophiolitic sutures. Two major sequences are recognized in the northern Ethiopian basement (Dow et al., 1971;

Beyth, 1978). The Tsaliet Group, an older mainly metavolcanic/metavolcanoclastic sequence and the Tambien Group, a younger metasedimentary slate and carbonate succession (Beyth, 1978). These classifications are discussed in detail below on the Tigray basement rocks.

3.1.6 Geology of Tigray basement rocks

The basement rocks of northern Ethiopia belong to the southern part of the Arabian-Nubian Shield, which constitutes predominantly low-grade metavolcano-sedimentary assemblages of island arc and ophiolite low-grade metavolcanic, metavolcanclastic and metasedimentary rocks intruded by syn-to late-tectonic granitoids (Ayele and Gangadharan, 2016). This terrain is dominantly characterized by steeply dipping and extensively folded, low-grade metamorphic rocks intruded by various granitic and mafic intrusions (Beyth, 1972; Tadesse, 1998; Tadesse et al., 2000) broadly subdivided the basement rocks of the ANS in the Tigray region into two groups based on stratigraphical relationships: (1) the Tsaliet Group, and (2) the Tambien Group. From the two groups the oldest being the Tsaliet Group also mentiones as meta-volcanic/meta-volcanoclastic unit, followed by phyllite, slate, and carbonate, which fall under the Tambien Group, and the syn- to post-tectonic plutonic units, granite to granodioritic composition (Pearce, 1995; Tadesse et al., 1999, 2000; Asrat et al., 2001; Alene et al., 2006).

Beyth (1971) described the boundary between the two sequences as 'probably unconformable. However, Alene et al. (2006) has described a gradational contact between the Tsaliet Group and basal part of the Tambien Group, although higher units of the Tambien Group overlap the Tsaliet Group indicating tilting of deposites located on the present inliers during Tambien Group deposition. Both sequences have been subjected to two major phases of folding because of N–S and E–W regional compression, respectively (Alene et al., 2000; Alene et al., 2006). D1 folded bedding and produced tight minor folds (wavelength of mm to dm), elongation lineation and pervasive regional foliation. D2 caused long wavelength (up to 8 km), upright, open parallel folds without producing a significant cleavage. D2 is considered to be due to E–W directed shortening associated with the end-phase collision between East and West Gondwanaland, and correlates with post-accretion structures described elsewhere in the ANS (Abdelsalam and Stern, 1996; Beyth et al., 2003).

A) Tsaliet Group

The Tsaliet group is well constrained in the Tigray region and covers most of the area occupied by basement rocks. The Tsaliet Group are unconformably overlain by the Tambien Group

metasediments, but the lower boundary is not exposed (Beyth, 1972). This group consists of calc-alkaline, island arc related metavolcano-sedimentary rocks including metavolcanic and metavolcaniclastic rocks, sericite-chlorite schist, slate, grey wacke, impure marble, calcareous siltstone, well bedded, intermediate to acidic welded tuffs, lappili tuff, agglomerates (Beyth, 1972; Alene et al., 1998, 2000, 2006; Tadesse et al., 1999; Beyth et al., 2003). Mineral assemblages in the Tsaliet metavolcanics indicate that peak regional metamorphism at pumpellyite–actinolite to lower green schist facies.

B) Tambien Group

According to Miller et al. (2009, 2011), the Tambien Group is exposed throughout portions of Northern Ethiopia (Tigray Province) and Eritrea (NNE extensions from Bizen domain and Adobha Abiy terrain of Beyth et al. (2003) and De Souza Filho and Drury (1998)), in green-schist-grade terrains comprising the southern portion of the Arabian–Nubian Shield (ANS). It may be equivalent to similar carbonate-rich units in NE Sudan (Bailateb Group; Stern et al., 1994), SW Saudi Arabia (Hali Group; Greenwood et al., 1976), and possibly western Yemen (inferred from its Red Sea conjugate position).

Tambien Group is mainly exposed in a series of synclinal inliers overlying the Tsaliet Group with gradational contact from west to east Mai kenetal, Tsedia, Chehmit, and Negash (Garland, 1980; Alene et al., 2006). The Tambien Group of northern Ethiopia consists of ~5km thick mixed carbonate siliciclastic succession. According to Beyth (1972), two major sequences in this group have been distinguished: Mai kenetal facies, which is composed of four formation (Werii slate, Assem limestone, Tsedia slate and Mai Kenetal limestone), and Negash facies composed of slate, quartzitic dolomite and limestone.

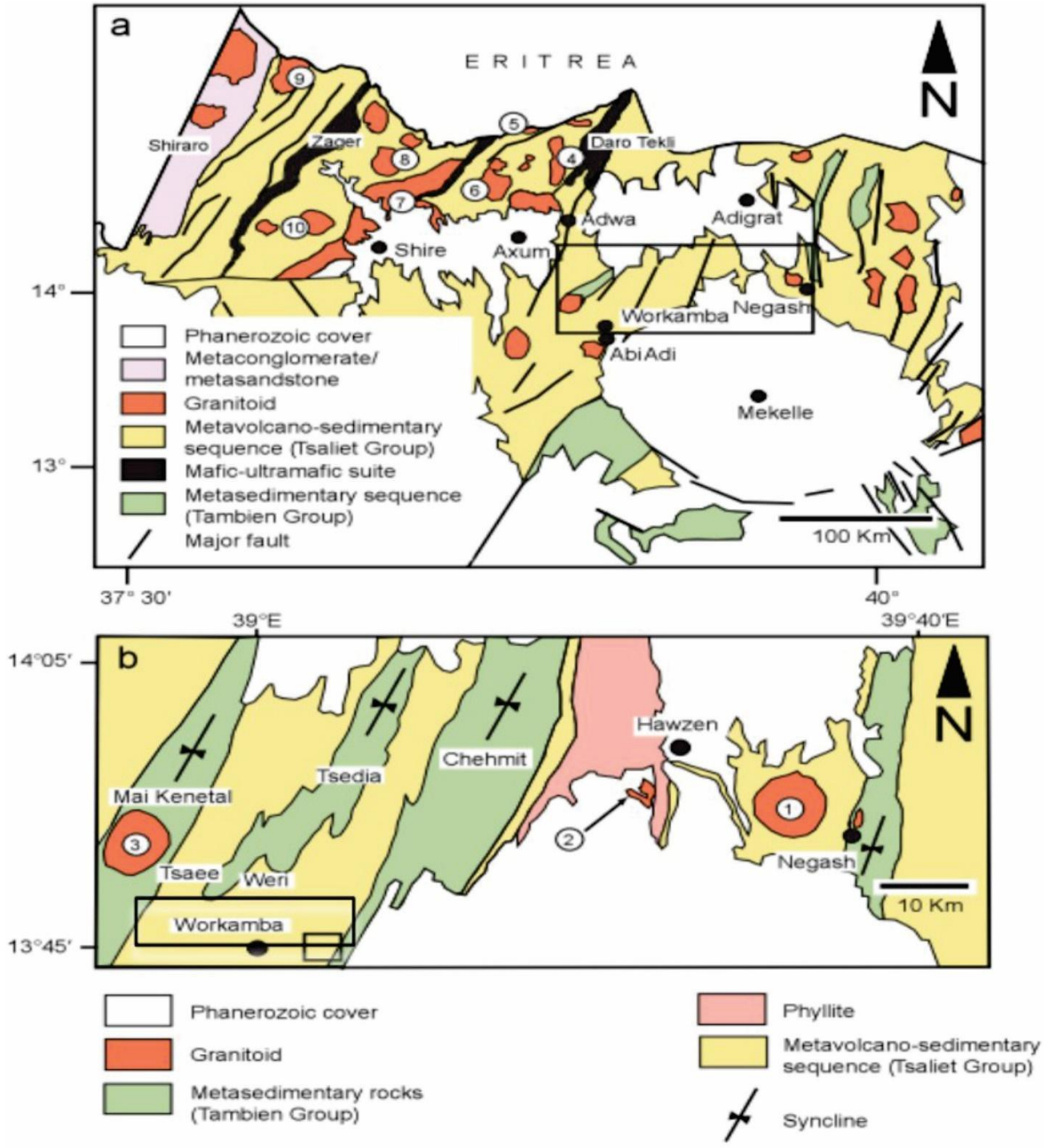

Figure 3.6: (a) Distribution of the Tsaliet and Tambien groups in the Tigray region, northern Ethiopia. The inset great rectangle shows the region near the study area where the Tambien Group is exposed; (b) Close-up of the area between Workamba and Negash. The Tambien Group occurs in four synclinoria inliers (modified from Tadesse et al., 2000; Asrat et al., 2001; Alene et al., 2006). The location of the study area is indicated. The circles with number represent the location of dated granitoids in the region, which are both syn- and post-tectonic in origin (1 = Negash, 2 = Hawzen, 3 = Mai Kenetal, 4 = Rama, 5 = Mereb, 6 = Chila, 7 = Shire, 8 = Deset, 9 = Azeho, and 10 = Sibta granitoids).

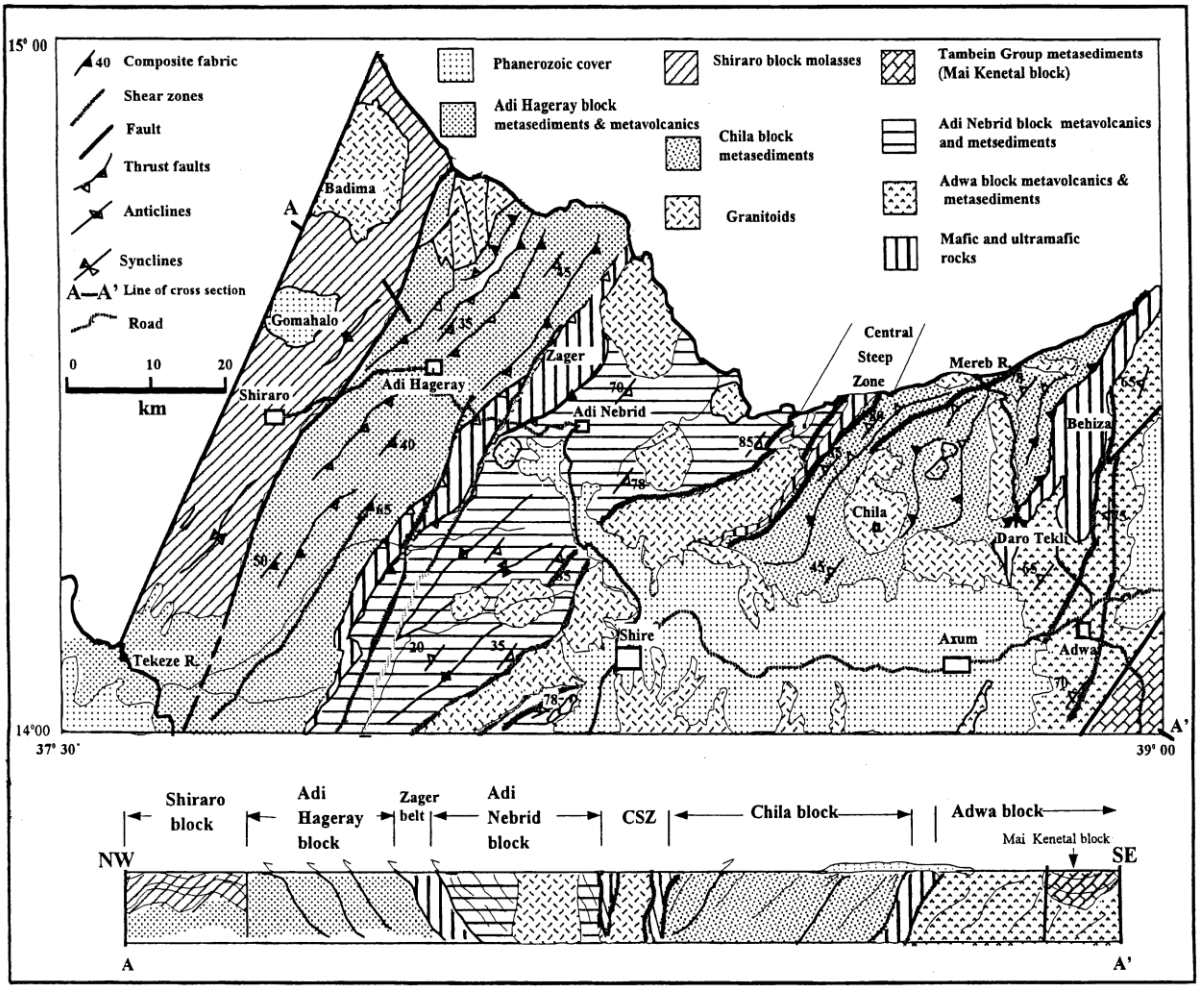

Figure 3.7: Simplified Geological map and NW-SE cross-section of Axum area (Tadesse, 1997, 1999), showing the distribution of the different tectonostratigraphic blocks, mafic-ultramafic belts, and the associated major deformational structures.

3.1.7 Regional Tectonic Setting

As indicated above, the basement rocks Tigray/ northern Ethiopia is part of the Arabian Nubian Shield and represents predominantly juvenile continental crust that was formed differentiation of mantle largely without reworking of pre-existing continental crust (Stern, 1994, 2000; Johnson and Woldehaimanot, 2003). The major structural feature in the northern Ethiopia is the north-northeast – south-southwest striking and variably dipping (i.e., southeast and northwest) composite foliation. The tectonic structures imprinted in the Tsaliet and Tambien groups are related to the collisional stress that resulted in the amalgamation of the ANS in Tigray and rocks have experienced different phases of deformations. Two phases of deformation (D1 and D2) are recognized by Alene et al. (2006). Accordingly, deformation D_1

is caused by N-S compression and resulted in tight minor folds with a wavelength of several mm to dm, elongation lineation and pervasive regional foliation. Whereas, D2 deformation resulted from E-W directed compression at the waning stage of the collision between East and West Gondwana and yielded long wave length (about 8 km), upright, open parallel folds without a significant cleavage, thrust, and strike slip faulting. Major NE SW oriented synclinoria such as the Mai Kenetal, Tsedia, Chehmit and Negash, which folded the Tambien Group are present in central Tigray (Beyth, 1972; Alene et al., 2006).

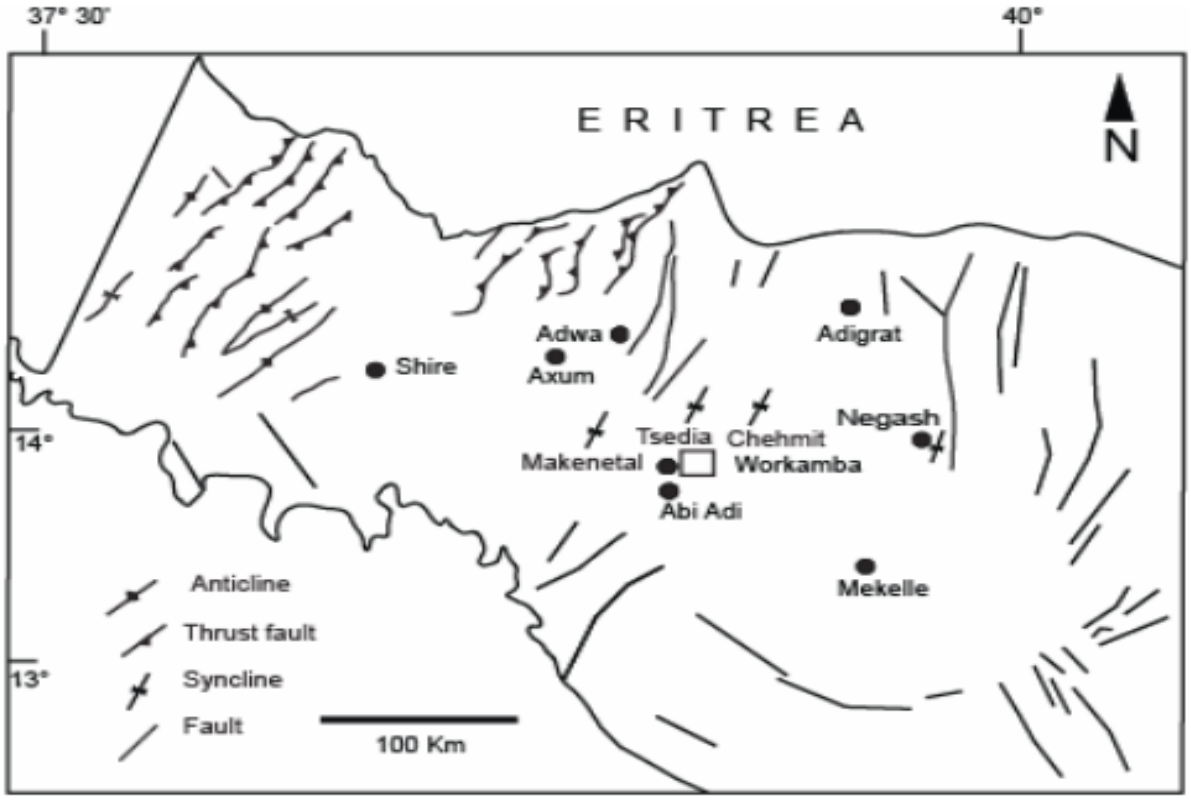

Figure 3.8: Distribution of major tectonic structures in Tigray (Tadesse, et al., 1996, 1999; Asrat, et al., 2001).

3.1.8 Tectonostratigraphic setting

Fault translations of uncertain extent accompanied closure of the Mozambique Ocean and the ensuing Gondwanan collisional orogeny, as indicated by contrasting tectonostratigraphic basement terrains of the southern ANS. According to Tadesse (1996, 1997) and Tadesse et al. (1999), Northern Ethiopia is divided into six blocks tectonically interleaved with two mafic ultramafic ophiolitic belts. The six tectonic bounded tectonostratigraphic blocks include; from west to east: the Shiraro, Adi Hageray, Adi Nebri'ed, Chila, Adwa and Mai Kenetal

tectonostratigraphic blocks. Mai Kenetal block in the east are dominated by weakly metamorphosed and deformed, post-accretionary clastic and carbonate deposits.

Tectonic boundaries and structures within the intervening blocks trend N to NNE, and E- or W-verging thrusts display significant oblique slip (Tadesse, 1997). The age of the ophiolites is not known but in Axum area the ophiolitic belt is penetrated by syntectonic granitoid dated to 0.75 - 0.79 Ga (Tadesse et al., 2000) implying arc terrains were sutured.

A second orogeny took place after Tambien Group deposition, producing folding, thrusting and brittle–ductile lateral displacements (Tadesse, 1996) and probably reflects major squeezing and tightening of the EAO during final collision. The structure of the Neoproterozoic complex is dominated by upright, NNE-trending, tight folds and layering that often dips steeply (Fig. 3.9). As indicated by the orientation of bound in necks, stretching lineations and microfractures, approximately E–W shortening was accompanied by nearly N-S horizontal extension. The exposed Tsaliet-Tambien sequence was metamorphosed to greenschist facies. The Shiraro sequence also displays low-grade metamorphism and faint ductile deformation. Stretched pebbles are elongated SW–NE, and fold axes measured at two localities trend 45º.

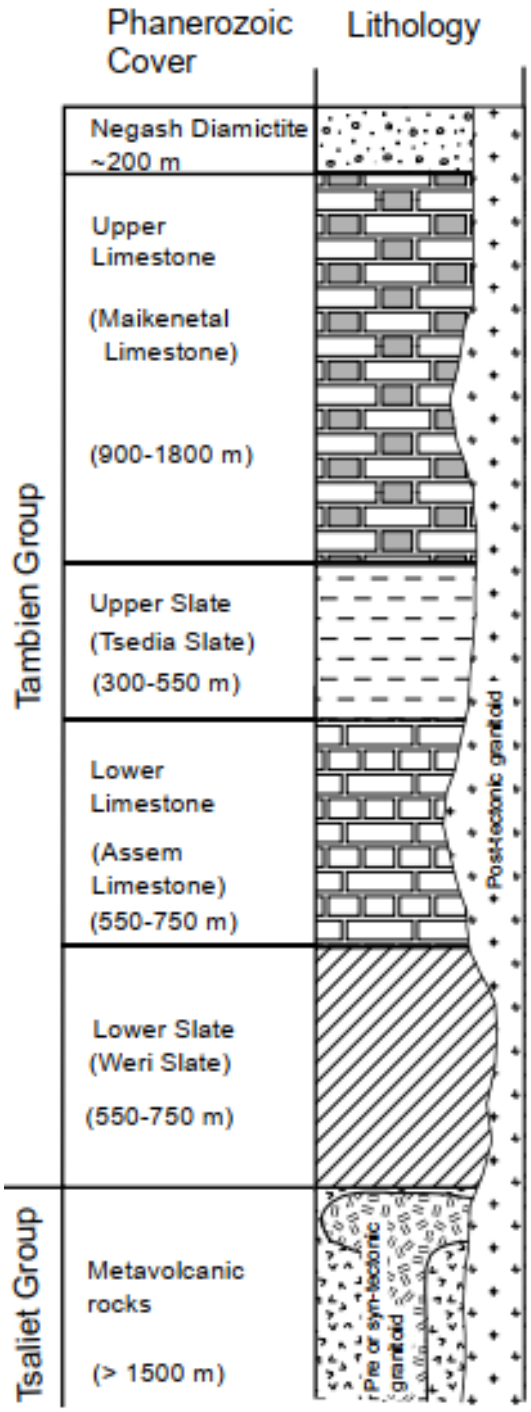

Figure 3.9: Stratigraphic sections of Tigray basement rocks showing relationship between the Tsaliet and Tambien group rocks. The pre- or syn-tectonic granitoids intruded the Tsaliet Group at about ~800 - 735 Ma, whereas the post-tectonic granitoids intruded both the Tambien and Tsaliet groups as well as the diamictites between ~620 and ~520Ma (after Beyth, 1972; Alene et al., 2006; Avigad et al., 2007).

3.1.9 Adi Nebri'ed Block

The Adi-Nebri'ed has located within the Adi Nebri'ed stratigraphic block, which in turn has located within the Nakfa tectonostratigraphic sequence of the Eritrean basement. According to Tadesse et al. (1999), the Adi Nebri'ed block has lithologically comprised of thick southeast dipping basic to intermediate metavolcanics, pyroclastic rocks and immature volcanoclastic sediments. The volcanoclastic rocks of the Adi Nebri'ed block are intruded by a series of post and pre-tectonic granites, dykes, and basic/ultrabasic intrusive and quartz veins. This block is comprised of a thick sequence of felsic to mafic metavolcanics, pyroclastic rocks, and associated immature volcaniclastic sediments. The entire sequence is affected by prominent widely spaced shear zones that strike NE-SW with a sinistral strike-slip fault (Tadesse, 1997). The succession is intruded by syn- to post–tectonic composite granitoids. The block is separated by thrusting related dip-slip dextral shearing with northwest vergence of the Zager mafic and ultramafic rocks in the western side and demarcated by the Meda Kemtse belt of ultramafic mélange in the east. The rocks of the Adi Nebri'ed block are intruded by syn- to post-tectonic composite granitoid. Furthermore, Tadesse et al. (1999) demonstrated that the geochemistry of metavolcanics of this block shows, the predominance of low alkalies especially low K even in felsic magmas, iron-enriched tholeiitic magma series, and primitive trace element contents having similarities to primitive intra-oceanic island arc geochemical signatures of Asir Terrane in the Central Arabian Shield. The Adi Nebri'ed block exhibits a range of structural deformations along its strike. The block can be roughly classified into Asgede and Terer domains based on these significant changes in deformational style (Tadesse, 1997).

3.2 GEOLOGY AND PETROGRAPHY OF ADI-NEBRI'ED AREA

Precambrian rocks of the Tsaliet and Tambien Groups underlie the study area. The Tsaliet Group is predominantly composed of metavolcanic and metavolcaniclastic rocks, including lithologies such as talc schist and micaceous slate. Overlying these units, the Tambien Group comprises mainly metasedimentary rocks, including phyllitic and graphitic schist, meta-limestone, and ferruginous sandstone. These basement rocks are intruded by post-tectonic granites and are unconformably overlain by Tertiary volcanic rocks. The presence of faults, shear zones, and well-developed foliation patterns indicates intense regional deformation and metamorphism associated with Precambrian tectonic evolution.

During the field survey, the color, texture, mineralogy, degree of weathering, metamorphism or alteration, and orientation of structural features were used to describe the lithologic units. The textural and mineralogical characteristics of the rocks discovered during the field investigation, assisted by petrographic and geochemical analysis also used to determine the name of each lithological units.

The area is composed of metasedimentary, metavolcaniclastic and metavolcanic units, which includes large quantities of foliated and non-foliated rocks. The metasedimentary units include micaceous slate, meta-limestone, ferruginous sandstone, and phyllite. The metavolcaniclastic rocks are fine to coarse-grained, primary volcanic (porphyritic) metamorphosed basic to intermediate-acidic volcanic rocks.

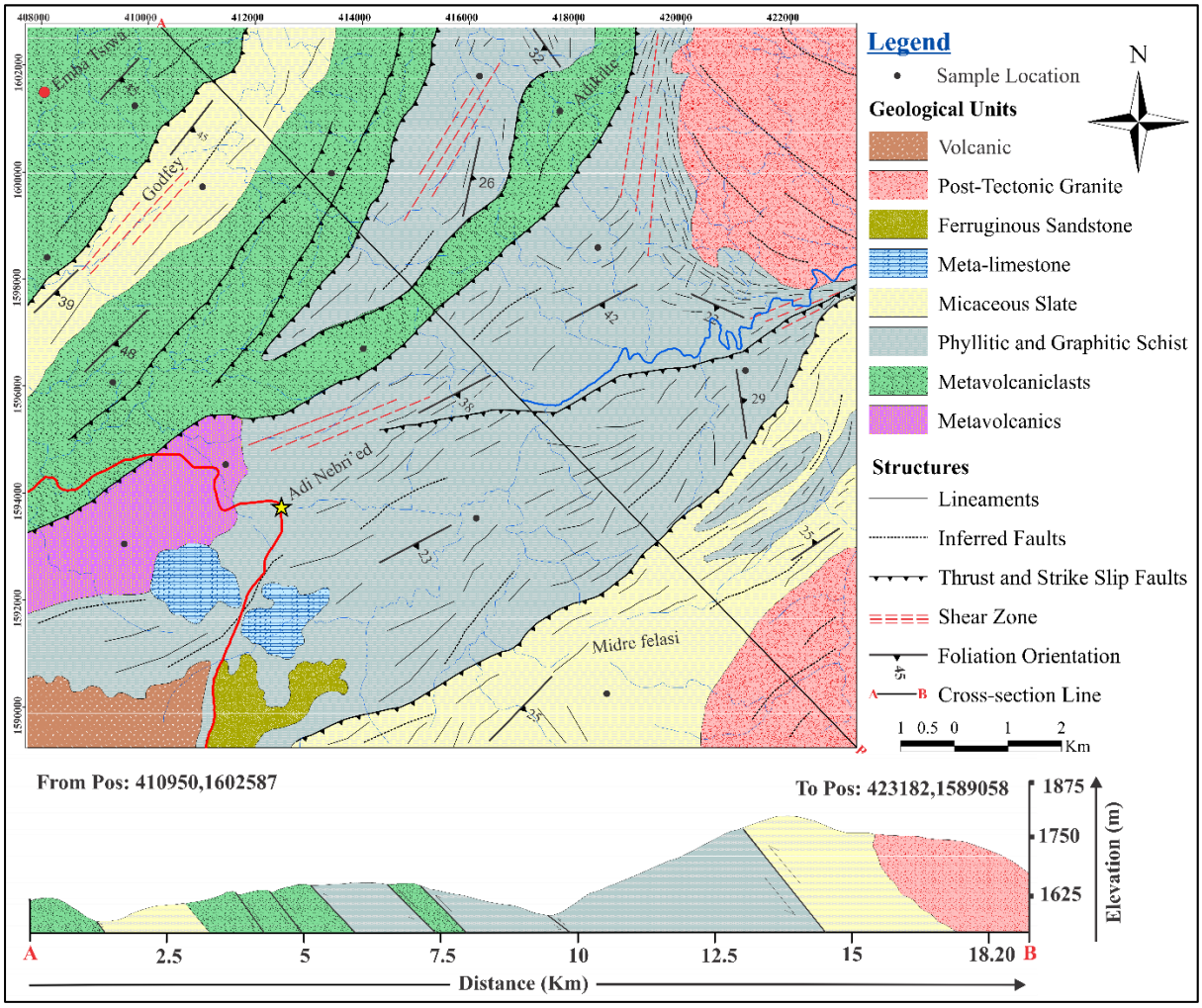

Figure 3.10: (A) Geological map of Adi-Nebri'ed area produced by ground traverse surveys across the strike of the metamorphic units (B) Cross-section along A-B. Projected Coordinate System: Adindan_UTM_Zone_37N. Projection: Transverse Mercator.

3.2.1 Metavolcanic Unit

This lithological unit mainly covers the southwestern part of the study area and locally found intercalated with the slate and phyllite units; considerably covering a small area compared to other lithological units. It has fine to medium grained at hand specimen and thin section level. Since this unit is relatively massive and less deformed, it is not highly impacted by quartz veins. It shows weak foliation development, generally trending NNE – N35^{0}E with some NW strike and dipping sub vertically to the southeast. The contact it makes with adjacent units (metavolcaniclastic) is more of gradational type and sharp contact has been observed when it is intercalated with metasedimentary rocks.

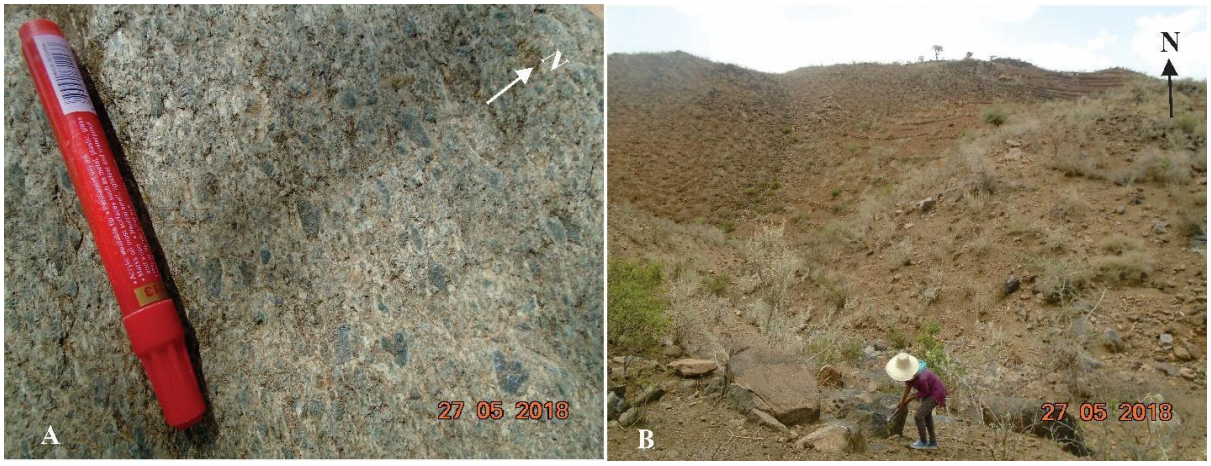

Figure 3.11: Field photographs of metavolcanic rock units. (A) Outcrop photo of metavolcanic units in south Eastern part of the study area and (B) Outcrops of massive metavolcanic rock characterized by ridge topography and hillside exposure along the river cut.

The gabbroic plug, representing a metavolcanic intrusive body, is exposed at Imba Tsiwa Ridge in the northwestern part of the study area. It is typically medium- to coarse-grained and dark-colored (mafic), composed predominantly of plagioclase and pyroxene, with minor olivine and opaque minerals. The contact with surrounding metavolcanic rocks is generally sharp, indicating its intrusive nature, and it may display minor jointing. Structurally, the plug is relatively resistant to weathering, forming prominent ridge features compared to the surrounding rocks. Meta-rhyolite unit is found around Midre-felasi ridge forming cliff topography, with light gray to reddish color, disintegrated to elongated rock fabrics.

The petrographic analysis from the metavolcanic rock sample (RS#10) showed that, the unit is mainly composed of quartz, plagioclase, sericite, epidote, biotite, chlorite, feldspar and some mafic minerals together with few rock fragments (clasts). It displays weakly developed foliation with anastomosing type and the fragments and phenocrysts are being wrapped by the mica minerals. The average modal composition (thin section RS#10) showed that 23% muscovite, 22% plagioclase, 10% quartz, 18% sericite, 16% biotite, 8% chlorite, 3% epidote, and 5% opaque (Fig. 3.12 & 3.13). Epidotization and sericitization are the most common alteration process in this unit. The rock sample from the meta-rhyolite unit (RS#2) shows 95% quartz and 5% opaque. Besides, the quartz grains are recrystallized and deformed. These quartz grains have angular to sub angular shape and exhibiting undulate extinction. Minerals like

biotite, muscovite, quartz and feldspar are active minerals in alteration. The plagioclase feldspar shows alteration to calcite and sericite with remnant albite showing twinning.

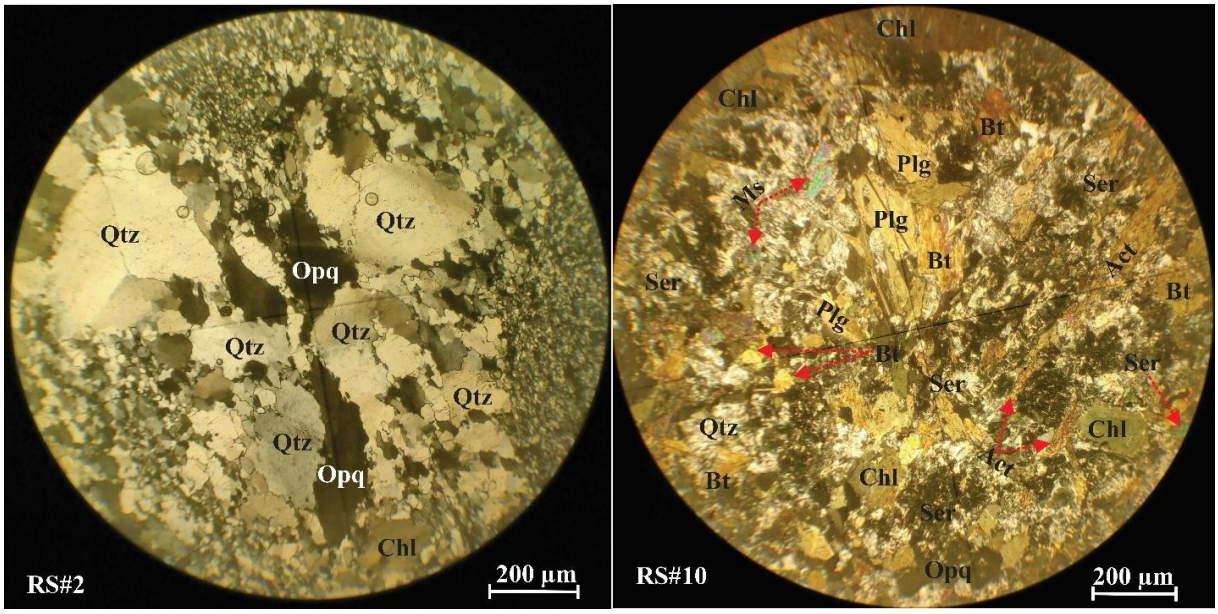

Figure 3.12: Microphotographs of metabasaltic andesite showing alteration and replacement, (A) quartz grains showing undulose extinction in meta-rhyolite, (B) randomly oriented actinolite/ tremolite mineral, and replacement of mafic mineral by secondary minerals of calcite and quartz.

Later deformation causes undulose extinction and a sutured border in recrystallized anhedral to subhedral quartz grains. Minor, randomly oriented hornblende porphyroblasts, shattered feldspar (plagioclase), massive sericite grains, and xenoblastic calcite are also found. Plagioclase that has been changed and broken up, devitrified volcanic glass, coarse calcite, and quartz all contributed to the development of the decussate structure. The metamorphic nomenclature quartz-muscovite-sericite schist is derived from these mineral assemblages.

Broken, fractured crystal of quartz is common indicating pre-tectonic structure. Certain minerals like quartz, mica and opaque are enclosed in the bigger porphyryoblast of biotite and muscovite and hornblende giving a spongy appearance poikiloblastic structure. Based on the mineral assemblages the metamorphic name gives as muscovite-plagioclase-sericite schist

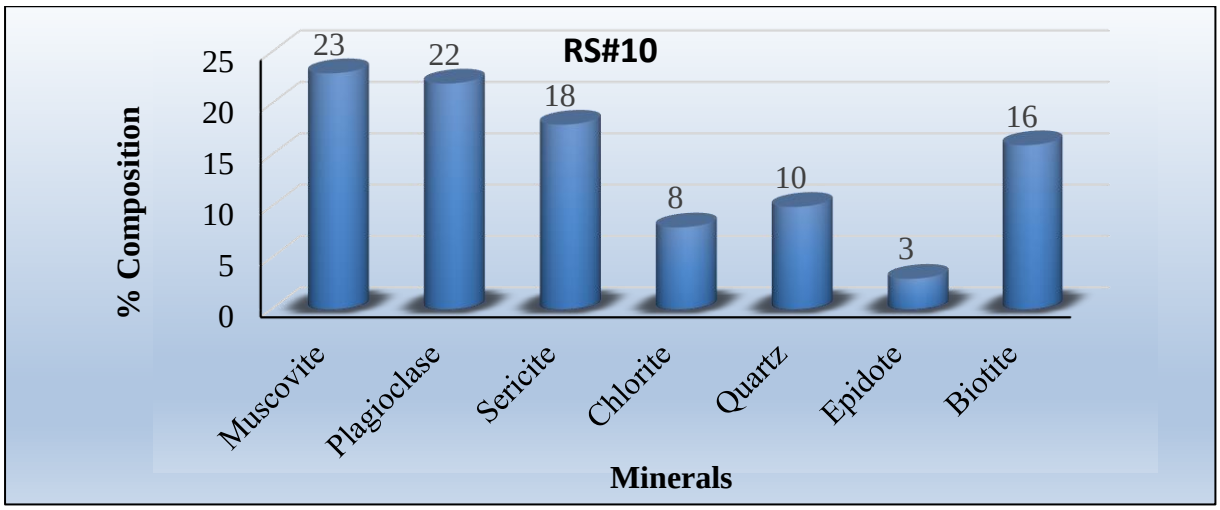

Figure 3.13: Column chart showing the modal proportion of minerals on the metavolcanic unit

3.2.2 Metavolcaniclastic Unit

This is the most dominant lithologic unit occurring extensively in the North, Northwest and Southwest part of the study area. It is characterized by hill forming in the NW part and somewhat gentle topography in the SW part of the study area. The exposure is continuous and blocky affected by series of quartz veins. The color of this exposed outcrop is dark and grayish weathered, but the fresh sample shows variation in color depending on the amount, type and size of the clasts and fragments (Fig. 3.14).

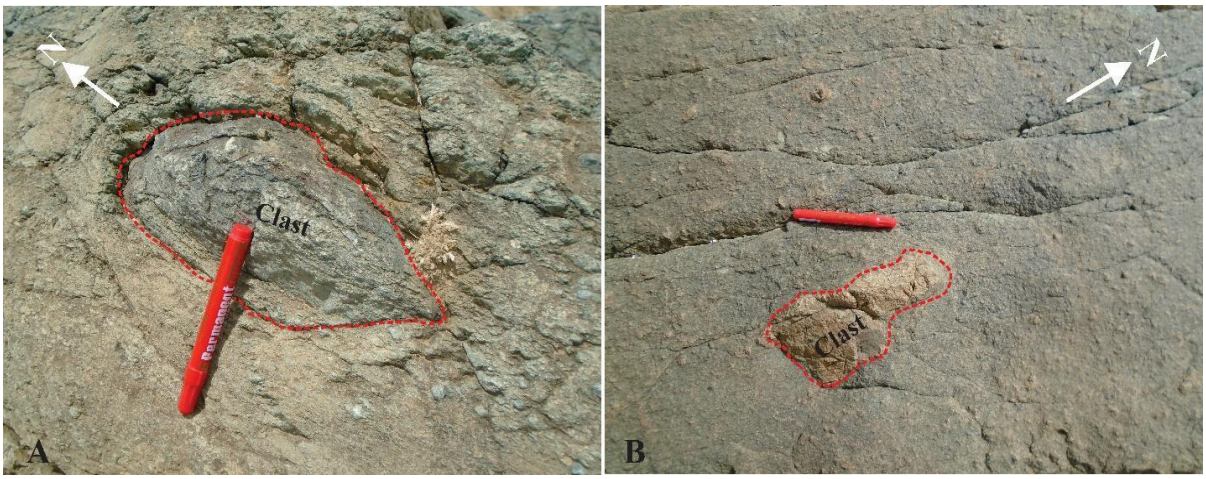

Figure 3.14: Outcrops of metabreccia; (A&B) Metabreccia rock with sub-rounded to sub-angular black to grayish volcanic clasts within the fine to medium grained matrix.

The size of the clasts ranges from 2 – 15 cm most of which are sub-rounded to sub-angular in shape. There are also large clasts and fragments that reaches up to 60 cm in diameter. The

metabreccia unit exhibits sharp contact with the adjacent meta-andesitic units. Furthermore, it is rarely encountered intercalated with phyllitic, graphitic and talc schists, and micaceous slate. Although it displays a general alignment of N-S to $N30^0E$, it also displays a local alignment of $N15^oW$ to $N30^0W$ with a dip of 65^0 to 80^0 towards SW.

Petrographic analysis revealed that the samples ((Fig. 3.15, RS#15 A & B) from this outcrop dominantly consists of an average modal composition of 18% quartz, 15% sericite, 15% muscovite, 13% calcite, 8% epidote, 10% opaque, 7% actinolite/tremolite, 7% plagioclase, 5% clasts and opaque minerals.

Later deformation causes undulose extinction and a sutured border in recrystallized anhedral to subhedral quartz grains. Minor, randomly oriented hornblende porphyroblasts, shattered feldspar (plagioclase), massive sericite grains, and xenoblastic calcite are also found. Plagioclase that has been changed and broken up, devitrified volcanic glass, coarse calcite, and quartz all contributed to the development of the decussate structure. The metamorphic nomenclature quartz-muscovite-sericite schist is derived from these mineral assemblages.

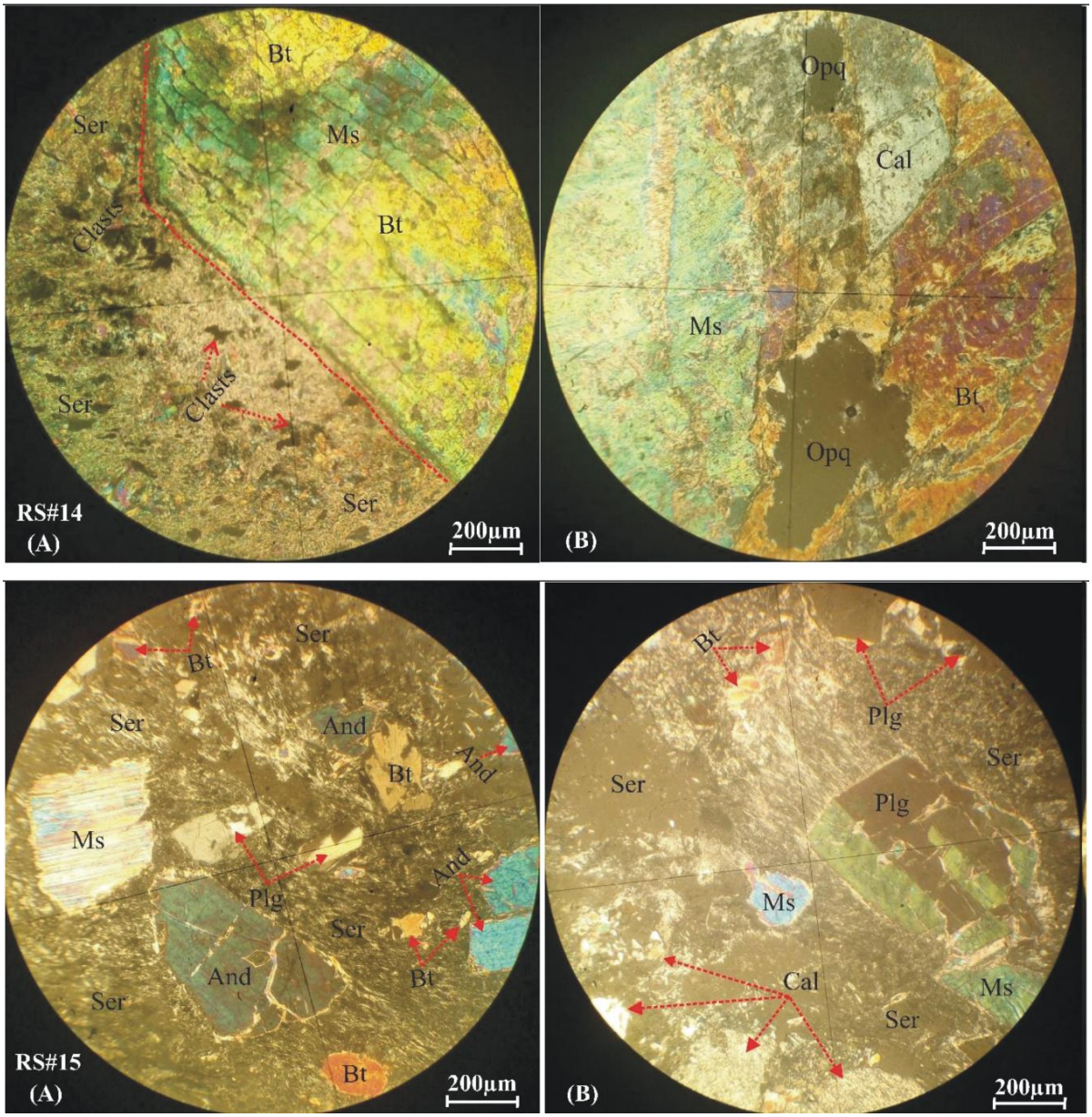

Figure 3.15: Thin section of meta-andesitic units. Secondary minerals of alteration of plagioclase into sericite minerals replacement in meta-andesite, and recrystallized of epidote, chlorite and muscovite minerals.

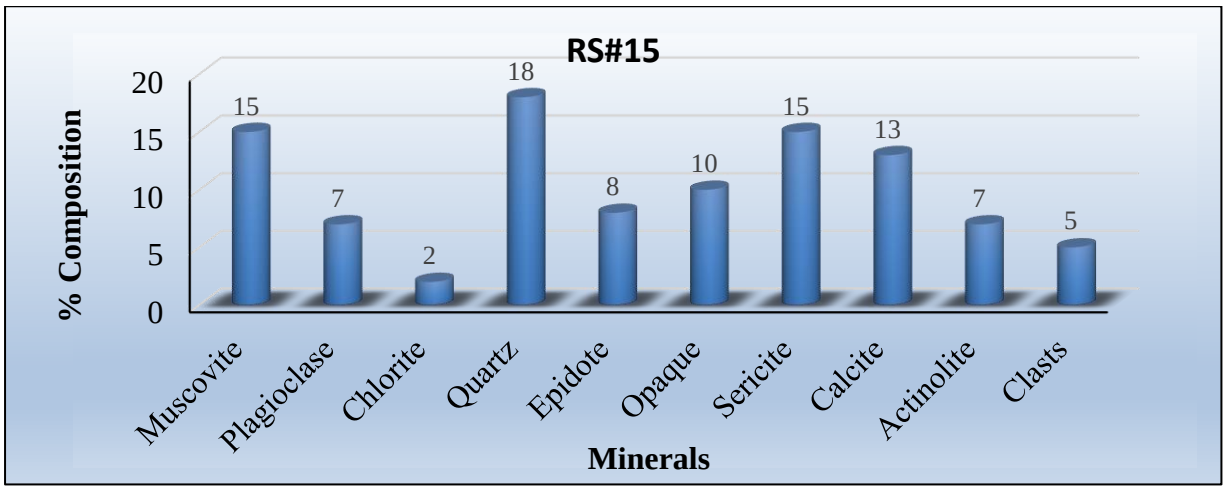

Figure 3.16: Column chart showing modal proportion of minerals on the Metavolcaniclastic unit

3.2.3 Phyllitic, Graphitic and Talc Schist Unit

Phyllite represents a low-grade metamorphic rock formed through the progressive metamorphism of slate under increasing temperature and pressure conditions. It is characterized by the development of fine-grained mica minerals, such as muscovite and chlorite, which shows a well-developed foliation known as phyllitic cleavage. Unlike slate, phyllite displays a distinctive silky to glossy sheen resulting from the preferred orientation of very fine mica flakes. This mineral alignment also enables the rock's tendency to split easily into thin sheets along foliation planes.

Graphitic schist is a dark gray to black color and a greasy feel. The presence of graphite indicates an organic-rich sedimentary protolith and suggests metamorphism under reducing conditions. Similarly, talc schist is composed predominantly of talc, formed through hydrothermal alteration or metamorphism of ultramafic or magnesium-rich rocks. It is typically soft, soapy in texture, and exhibits a well-developed schistosity. This unit is situated locally between the micaceous slate, metavolcanic and metavolcaniclastic units, and it has gradational contact with all the rocks of the area. This unit's characteristic color ranges from dark to gray, with light greenish gray and shining gray in some places, as well as micaceous minerals that form fabric and have shiny surfaces. It is also characterized by high levels of foliation and crenulation throughout the exposures, with the foliation primarily striking to NE direction and dipping 30^0–40^0 NW. In comparison to the entire mapped area, this unit is found on the flat to gently sloping areas, and quartz veins are widespread across the foliation direction.

In the study area, this assemblage of low-grade, foliated metamorphic rocks is predominantly exposed in the central to northeastern parts of the mapped area. These rocks commonly display well-developed foliation, local folding, and shearing, reflecting the regional deformation history. Their spatial distribution and structural characteristics suggest their significant role in recording the tectono-metamorphic evolution of the area.

Figure 3.17: Field photographs of phyllitic, graphitic and talc schist outcrops. (A) Phyllitic and talc unit characterized with grey, green, fine grained and highly foliated and crenulated textures, (B) outcrop photo of pencil like highly foliated graphitic schist.

Its flat, smooth surfaces are prone to deterioration. Some locations, such as Midre-Felasi, have rugged topography due to the soft phyllitic and graphitic schist with minor graphitic forming linear ridges and nearby small strike-parallel gullies that are easy carved by the seasonal rainfall and minor small streams. Furthermore, foliated talc schist, which trends from NE to SW, is located in the northwest portion of the study area. This talc schist has a grayish-green color, a well-developed schistosity, fibrous fracture, and a greasy texture. It also contains a lot of talc. Various alteration zones were identified based on variations in the host rock's texture and color. According to petrographic analysis, this unit is constituted of 35-38% biotite, 25-30% muscovite, 20-25% sericite, 5% opaque, and 2% quartz (Fig. 3.18). The foliations of this unit are displayed by preferred alignment of minerals and concordant with compositional layering. It is evident from the crenulation cleavage in Figure 3.18 that the rock has undergone at least two stages of deformation. Additionally, the favored orientation of platy minerals indicates well-developed schistosity. Presence of pyrite crystals with cubic outline is quite conspicuous in these rocks. In majority cases, these are altered to limonite (pseudomorphs) and show red color.

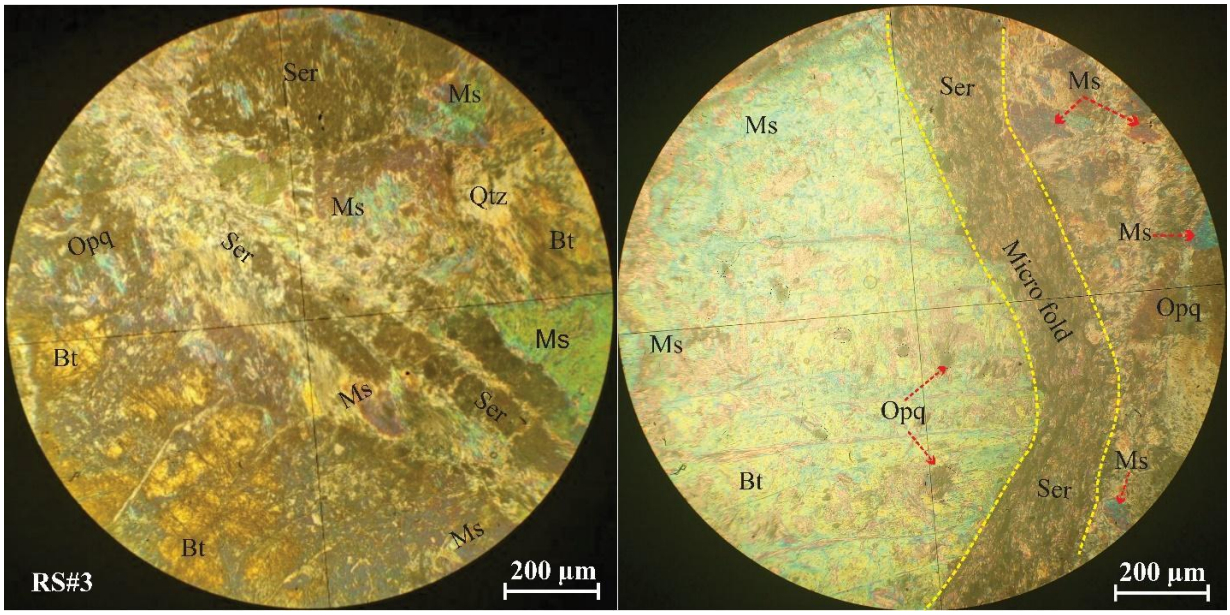

Figure 3.18: Microphotographs of phyllite rock unit; (A) Plagioclase showing S_1 and S_2 crenulation cleavage, (B) Micro folding and plagioclase porphyroblast.

Additionally, the RS#3 shows S_2 crenulation cleavage and well-developed S_1 foliations. The S_1 foliation is horizontally oriented and strongly developed in figure 3.18. The cleavage domains created by D2 deformation (flanks of micro-folds) and micro-lithons (fold hinge) characterize the crenulation cleavages (S_2). The migration of minerals or the transfer of solutions in response to the stress gradient during the creation of microfolds is what caused this crenulation cleavage (Alene, 1993).

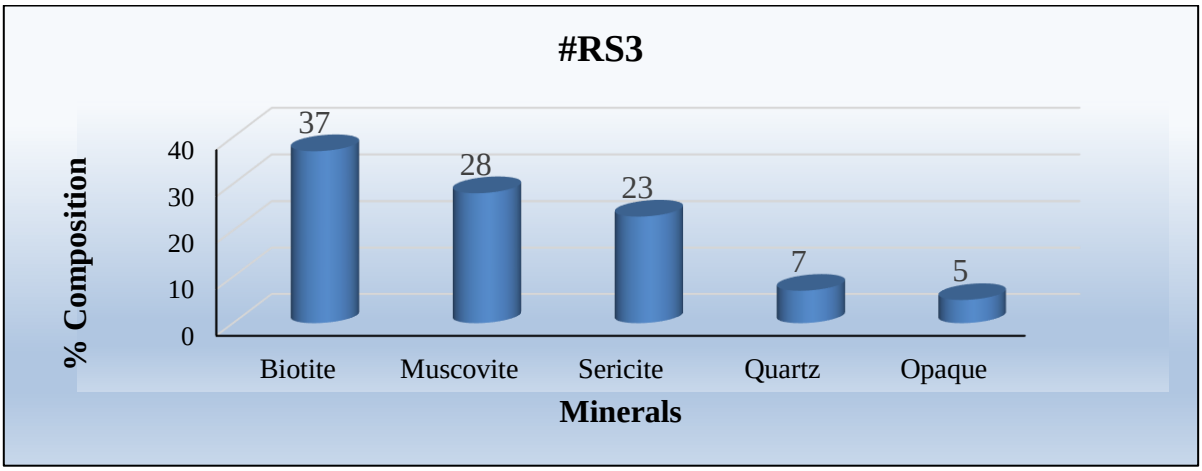

Figure 3.19: Column chart showing the modal proportion of the minerals on the Phyllitic and graphitic schist unit.

3.2.4 Micaceous Slate Unit

It is a fine-grained, well-foliated unit that has variegated colors. In comparison to other units, it creates gentle topography. This unit is intermittent and intercalated with other (Fig. 3.20). The overall foliation trend is N-S to N10ºW, with a moderate to sub-vertical dip to the east and west. There are spots where this unit is impacted by quartz veins and joints that are closely spaced. Field observations at the outcrop and hand specimen levels demonstrate that the presence of dark green glossy minerals and elongated white shining minerals indicates both sericitation and mineral alteration (chloritization). The presence of mafic metamorphic minerals (epidote and chlorite) in the thin section examination suggests that the slate originated volcanically or volcanoclastically at the current scale of observation. Quartz, feldspar, and sericite crystal fragments make up the majority of this unit, with trace amounts of epidote and chlorite. However, quartz and sericite are the two main minerals found in this unit.

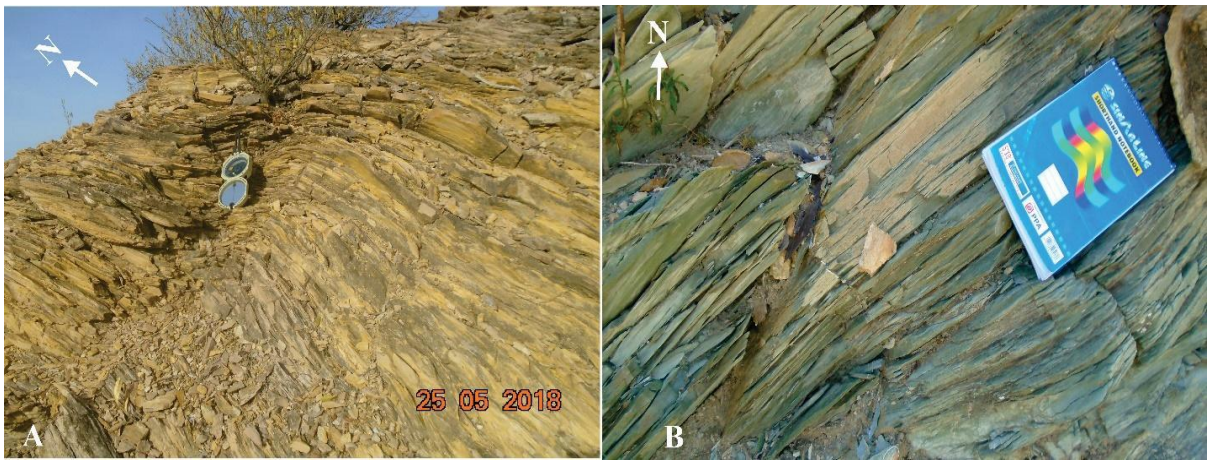

Figure 3.20: Fine grained and well laminated outcrop of slate: (A) slate unit that displays slaty cleavage from south east of the study area, (B) slate showing closely spaced joints.

Petrography of a thin section of this slate reveals that it is composed of 50-55% sericite, 15-20% fine-grained chlorite, 18% chlorite, 10-15% muscovite, 5% quartz and opaque, and less than 2% epidote. Some quartz crystals exhibit a weakly developed S_1 foliation and unpredictable orientation. Sericite is a fine-grained groundmass that is primarily an altered result of quartz and feldspar, with some specimens having a medium texture (Fig 3.21). The foliation of the majority of the minerals is well developed. The metamorphic nomenclature sericite -chlorite- muscovite schist derived from these mineral assemblages.

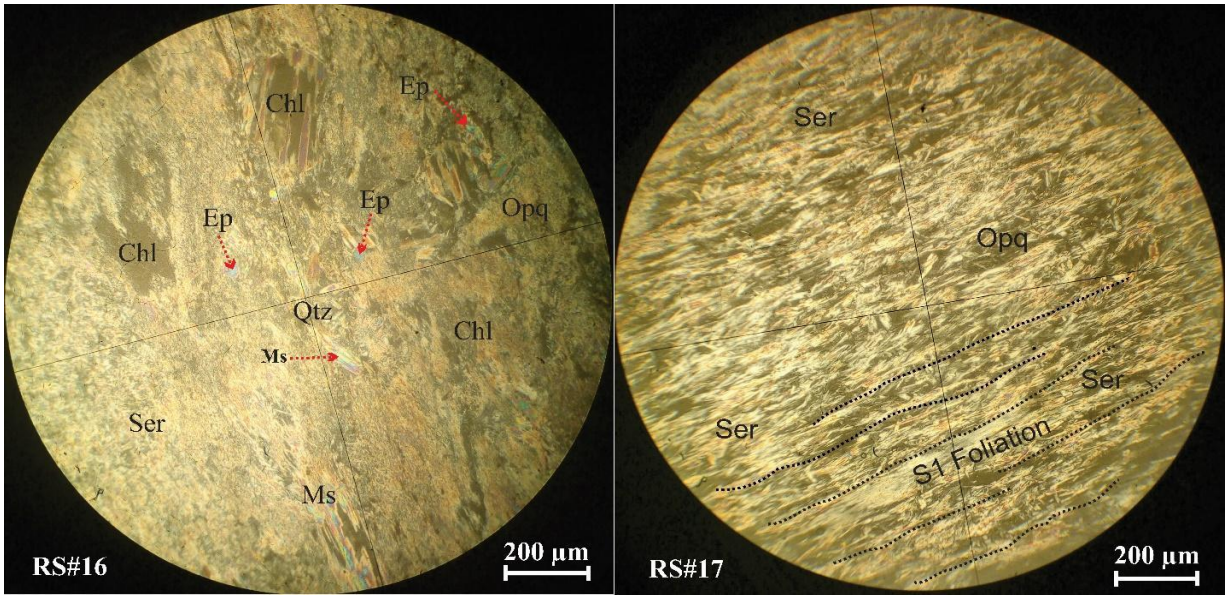

Figure 3.21: Microscopic pictures of slate unit that shows S1 foliation, and Crystal fragments of quartz, feldspar and sericite with small amount of epidote and chlorite.

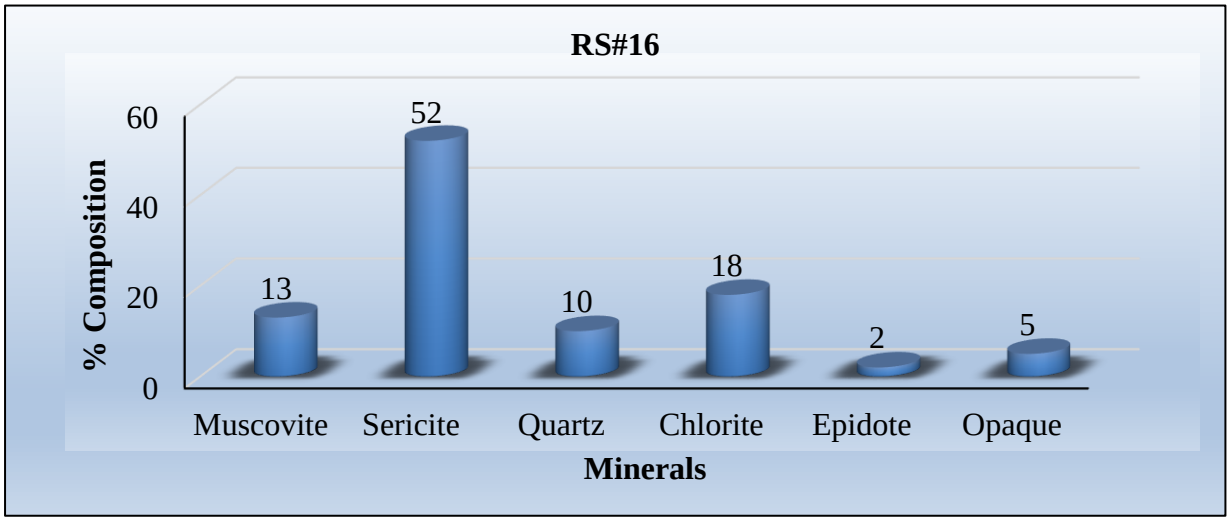

Figure 3.22: Column chart showing the modal proportion of the minerals on the micaceous slate unit.

3.2.5 Meta-limestone Unit

This unit is composed primarily of calcite, a sedimentary rock that has undergone weak metamorphism. Decomposed small fossils, shell fragments, and other fossilized debris are frequently its constituents.

This weakly metamorphosed limestone conformably overlaying the phyllitic rock and it is located in the southwest part of the study area. Additionally, this unit includes siltstone and mudstone that have undergone minor metamorphism (i.e., as intercalations). It is characterized by a white color, highly fine-grained and massive texture that exposed over a segment that is

60 meters thick and is impacted by several joint sets, and minor tight folds (Fig. 3.23). This meta-limestone is highly coorelated with the Mai-kenetal limestone due to its slight metamorphism, and white in color.

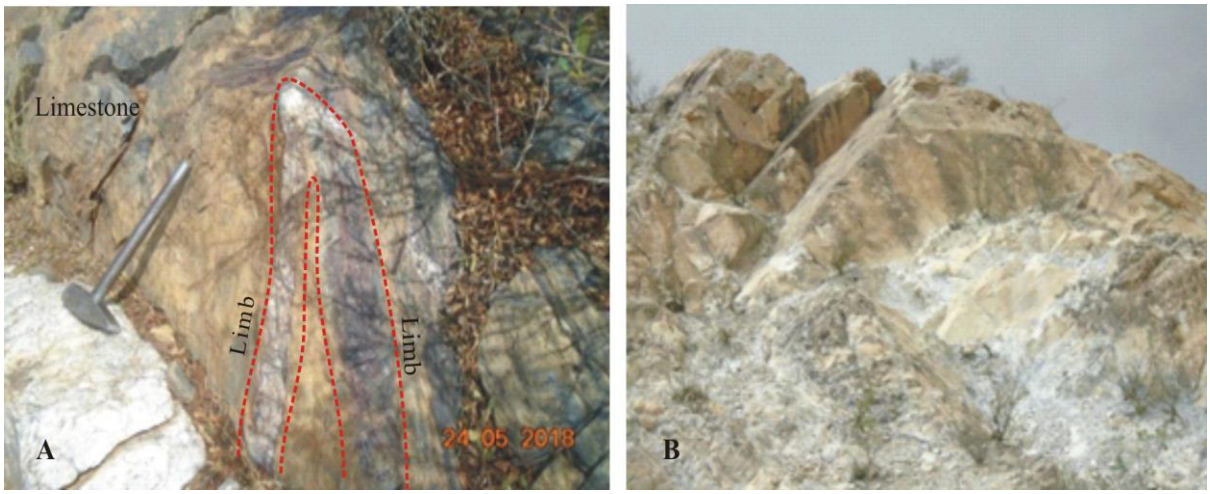

Figure 3.23: Field photographs of meta-limestone from southwestern part of the study area.

3.2.6 Ferruginous Sandstone

The ferruginous sandstone rock unit is exposed in the southeastern part of the mapped area (Fig. 3.10). This unit is also be found between the phyllite and meta-limestone units. It has a distinctive reddish to brown tint with mica minerals that form fabrics and have shiny surfaces (Fig. 3.24). It is distinguished by the fact that the entire unit is non-foliated.

Figure 3.24: Ferruginous sandstone rock unit exposed in southeastern part of the study area

The round to sub-round quartz grains (Fig. 3.24) of this unit normally have a thin red hematite rim. The reddish and pink-brown grains predominate, with fewer white and black grains. It has

been found shining, sorted and glued properly. The hand specimen of this unit does not have acid fizzing, and hence there is little carbonate present. In some samples, its heavy and massive nature indicates that this unit is composed of iron, which needs a further detailed investigation for iron ore exploitation.

3.2.7 Granitic Intrusion

The Adi Nebri'ed and Chila Blocks contain the majority of the granitic intrusives. However, the Shiraro and Adi Hageray Blocks also include variable-dimensional granitic intrusions. Their diameters range from one to 6 kilometers, and their forms range from elliptical to sub-rounded. Regarding the main regional fabric, these bodies exhibit a variety of structural interactions (Tadesse, 1997; Tadesse et al., 1999). In the study area, felsic intrusive rocks widely intrude into the metavolcanic, metavolcaniclastic and metasedimentary rocks. The deformation patterns and preferred orientation of constituent minerals in the felsic intrusive indicates that they are post-tectonic in origin. The study area rocks have granite unit exposed on the eastern and northeastern flanks.

The Adi Nebri'ed granite is light gray, pale to pink in color and has medium to coarse-grained size texture (Fig. 3.25) owing to the presence of randomly oriented K-feldspar phenocrysts. This unit is located close to the Adi Kilte locality in the northeastern uppermost corner of the study area, facing the Mereb River and the southeast around Midre felasi village. These granites have sub-rounded shapes and are over 2 km across. The exposure of these granites form a rugged topography, slightly to highly weathered, dissected by series of joints and exfoliation fractures, and which is dissected by deep gully-forming streams producing dendritic drainage pattern. The exfoliation produced rounded massive blocks. Most of the faults documented in this unit dips towards south of the Mereb River and trends east to west. It penetrates the basement rocks along the weak zones, allowing minerals to be carried and transported by hydrothermal solutions. As a result, the base metal mineralization is probably deposited somewhere in the favorable environment.

A fresh rock sample (Sample No. RS#29) was collected from the Adi Kilte locality from the southern part of the intrusion. It consists mainly of 40% K-feldspar, 20% plagioclase (albite-oligoclase), 25% quartz, 10% biotite and 5% hornblende. Accessory minerals include sphene, zircon, trace of epidote, allanite, apatite and iron oxide. K-feldspar is mainly microperthitic microcline. Most of plagioclase grains show zoning. The core of zoned plagioclase grains are

severely affected by secondary alteration and hence have cloudy appearance. Biotite is generally brownish and rarely altered into chlorite along the margins and cleavages.

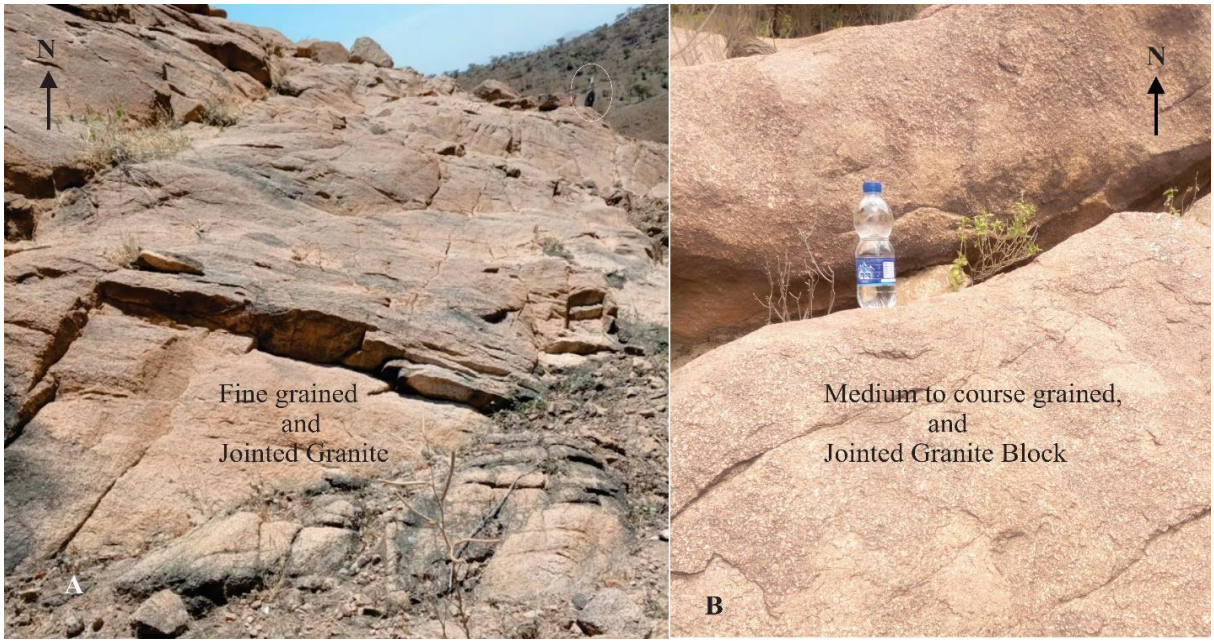

Figure 3.25: Pinkish Granite intrusion found in North of Adi-Nebri'ed area near Adi-kilte locality towards River Mereb.

4. STRUCTURAL AND DEFORMATIONAL HISTORY OF THE AREA

Northern Ethiopia's basement rocks have experienced at least two significant deformational events. Pervasive regional foliation, tight minor folds, and E–W trending recumbent folds, the results of early N–S compression (Alene et al., 2006). These polyphase deformation structural patterns are marked by the existence of NE striking foliation, lineation, folds, faults, joints, dykes and quartz veins. The existence of foliation (S_1) and the original layering (S_0) representing first phase of deformation (D1), which are parallel to each other.

4.1 Geological Structures

A number of secondary structures impacts the study area (Fig. 4.9). These consist of normal, inferred, and thrust faults, NE to SW and E to W striking foliations, NE to SW striking shear zones, quartz veins, dykes, and joints. Along with other kinds of structural features such strike-slip faults and crenulation cleavage are also noted. These structures are described in depth in the section that follows.

4.1.1. S_1 Foliation

This structure is predominantly developed over the slate unit. Slaty cleavage and developed continuous cleavage in phylitic, graphitic and talc schists are examples of S_1 foliations (Fig. 4.1). However, on metavolcanic and metavolcanoclastic units, weak S_1 foliations have developed. Locally, there is some fluctuation, but overall, the foliation exhibits a general trend of $N10^0E$ to $N50^0E$ dipping $S30^0 – 60^0E$ and/or NW. Typically, it is parallel to the original lithological stratification (S_0). In metasedimentary rocks, compositional banding in outcrops identifies primary bedding (S_0).

Furthermore, as can be seen in the outcrop geology of the study area, and from the microphotograph of RS#17 (Fig. 3.21), the preferred alignment of muscovite, chlorite, epidote, sericite, plagioclase, quartz, and opaque minerals defines S_1 foliations as observed in thin sections. The primary structural characteristic in the study area is S_1 foliation, which also exhibits a general trend of northeast striking and varying northwest to southeast dipping. Hence, according to Alene et al. (2006), these structural components have a regional correlation with the first phase of deformation (D1) due to N-S compression.

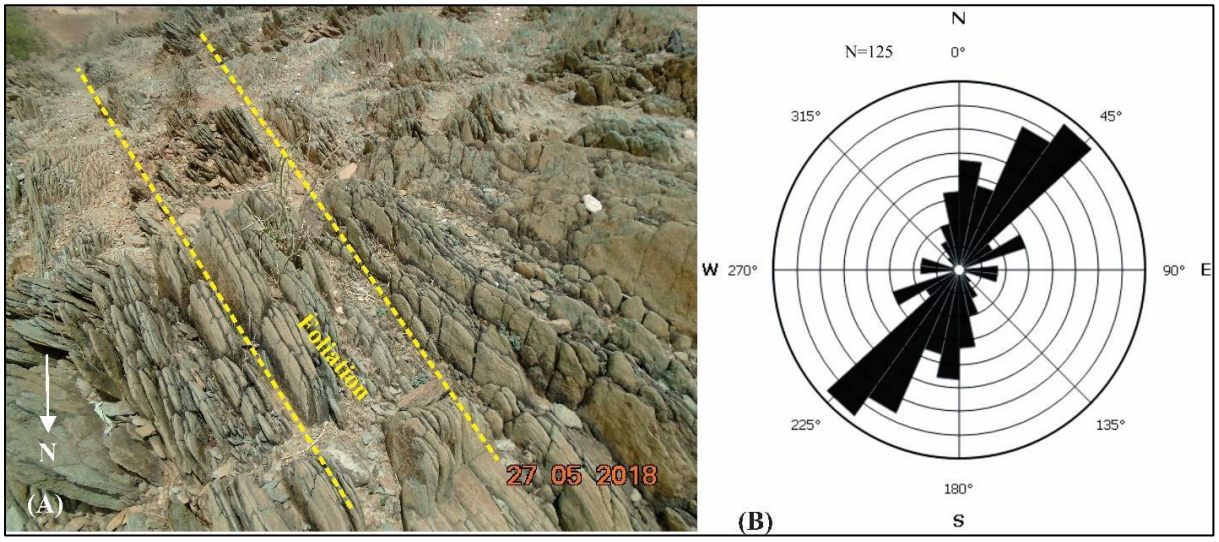

Figure 4.1: Field photographs and Rose diagram of graphitic slate unit with slaty cleavage, (A) outcrop photo of pencil like graphitic slate foliation, (B) Rose diagram for the foliations

The longest wedge of the rose diagram represents $N45^0E$, in which this value indicates that the mean value of the strike direction of foliations in the study area. Consequently, three significant foliation trend ranges have been noted. These are foliation trending: $N20^0$-30^0E, $N30^0$-45^0E, and $N5^0$-15^0W. Of these, the $N20^0$-45^0E trend constitutes the majority of the foliation (trending 20^0-45^0 and dipping 50^0-65^0 towards the southeast). It is identified by the planar characteristic and S_1 foliation that are present in the phylitic, graphitic and talc schist and metavolcaniclastic unit (Fig. 4.1). This structural feature shares characteristics with Asgede's D1 deformation (Taddese, 1999), which may be related to the regional D1 deformation brought on by N-S compression (Alene et al., 2006).

4.1.2 S_2 Foliation

The S_2 foliation is a prevalent ductile-type structure common in the current study area's slate-phyllite unit. According to microstructural investigation under thin section, S_2 foliation is identified by continuous realignments of fine-grained platy minerals and has a cross-cutting relationship with the regional S_1 foliation. The E-W trending sheared and less deformed barren quartz vein and the scattered, E-W trending fracture cleavages and cut in the S_1 fabric are indicative of S_2. Locally, quartz veins exhibit as discordant relationships and primarily manifest as fracture filling.

The fracture filling quartz veins are folded by D2, which causes the host rock to develop open, shallow plunge folds. It is observed that foliation was produced due to D1 deformation (D1),

and subsequent microfolds with a parallel fold axis were crenulated by the later D2 deformation. Additionally, as it was highlighted in the geology of the study area, and microscopic analysis of the thin sections made from slate phyllite units reveal that the development of crenulation cleavage is due to the second phase of deformation (D2). Chlorite, graphite, sericite, talc and opaque minerals shows the crenulation cleavages (S_2).

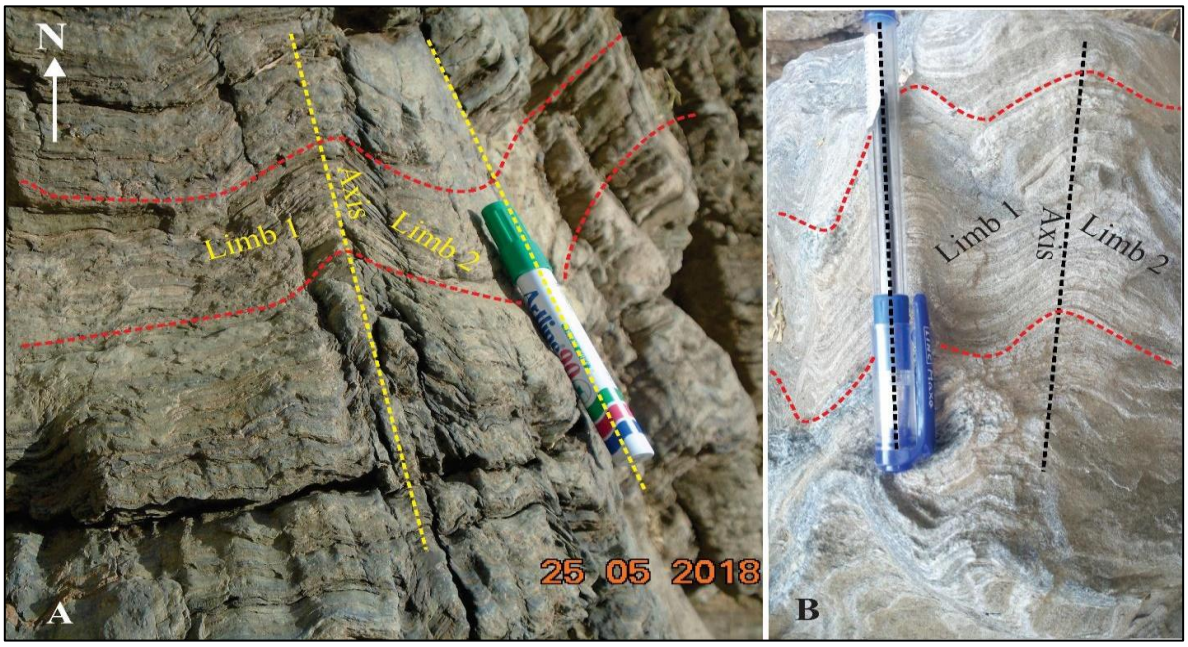

Figure 4.2: Field photos and mesoscopic folds with horizontal to sub horizontal fold axes. (A) Upright harmonic fold within phyllite rock unit of the study area (B) Crenulated fold within phyllite hand specimen

4.1.3 Folds

In the study area, there are numerous lithologic units with clearly visible small-scale micro-folds. These folds frequently show sub-horizontally to moderately dipping and are kink folds (Fig. 4.2). The fold axis of the study area typically has 10^0 to 30^0 plunges, although in some locations, such as Midre-Felasiy, it can reach 80^0 to 90^0. They are also observed on phyllitic schist (Fig. 4.3 A&B) and meta-limestone rock types (Fig. 4.3 D) in the north and southeast of the study area.

This deformation phase includes thrusting and disharmonic crenulation cleavage as well. The meta-limestone and slate unit's microfolds plunge from north to south and have sub-horizontal to horizontal fold axes. In addition, according to Alene et al., (2006), all folds plunging N-S directions are correlated to D2 that resulted from E-W shortening.

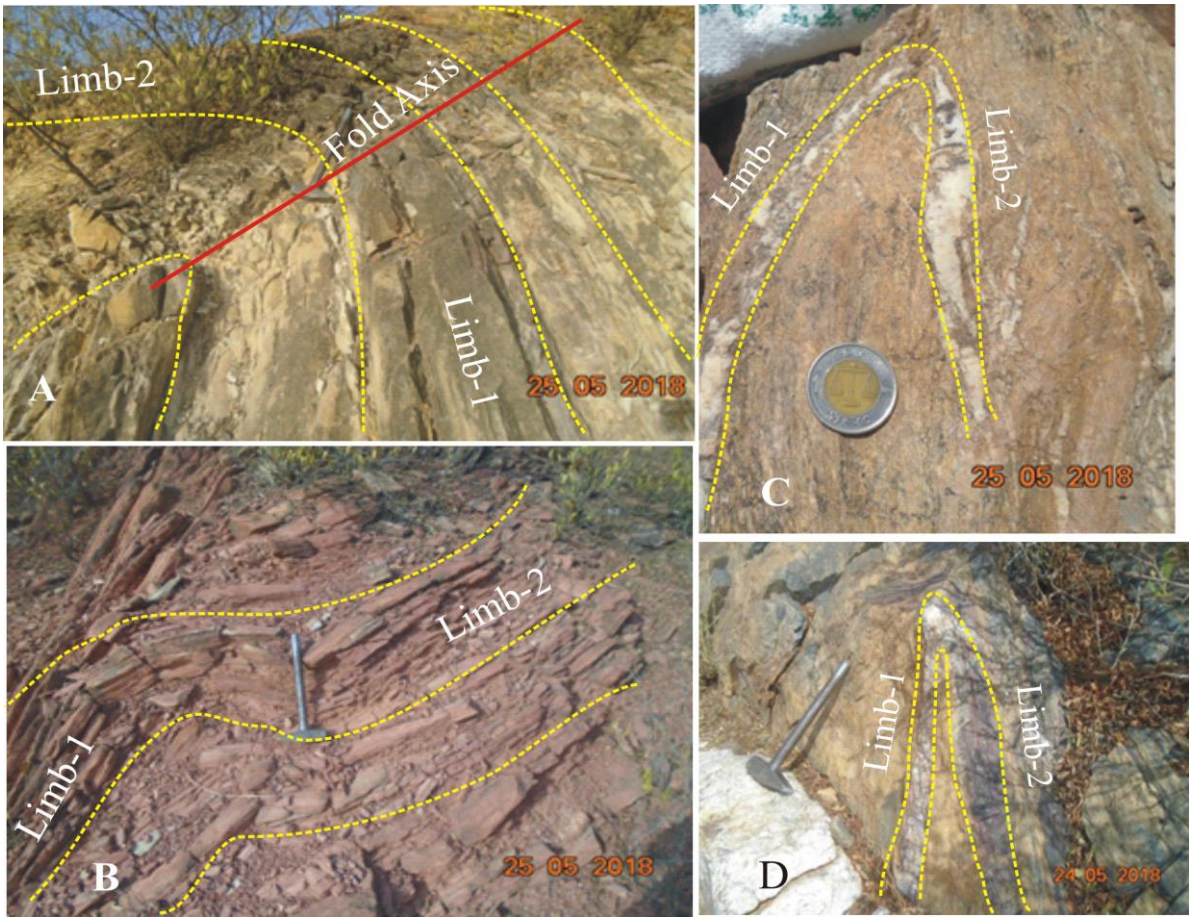

Figure 4.3: Field photos of folds, (A) The fold axes are plunging with shallow degree towards the south, (B) Recumbent fold on the slate-phyllite unit (C) Mesoscopic upright fold on Phyllite unit (D) Mesoscopic upright fold on Meta-limestone rock

4.1.4 Shear Zones

According to the current field investigation, the shear zones in Adi-Nebri'ed area are linked to faulted rocks with measurable displacements and are mostly found on the walls of the faults. These severely distorted rocks might have developed as pieces of brittle rock slipped past one another, shearing the rocks as well. It is easy for the naked eye to detect cataclastic brittle rock with randomly oriented fabrics in this specific narrow spaced shear zones. These thin localized spots of severely deformed rocks are most commonly found north, northeast, and northwest of Adi-Nebri'ed localities (See structural map on Fig. 4.9). Furthermore, the rigid clasts exhibit deterioration, resulting in fissures that caused by rotation and stretching. The fine-grained matrix subsequently fills them. Other features that show varying densities of foliation planes within the foliated rocks include sericitization, increased quartz vein activity, and rather well-developed foliation/crenulations are common in the study area. In general, presence of shearing

in the area indicated by the development of crenulation, strong foliations, veins, and quartz porphyry with rotated quartz (Fig. 4.4). The extensively fractured rocks in these confined areas are signs of deformation.

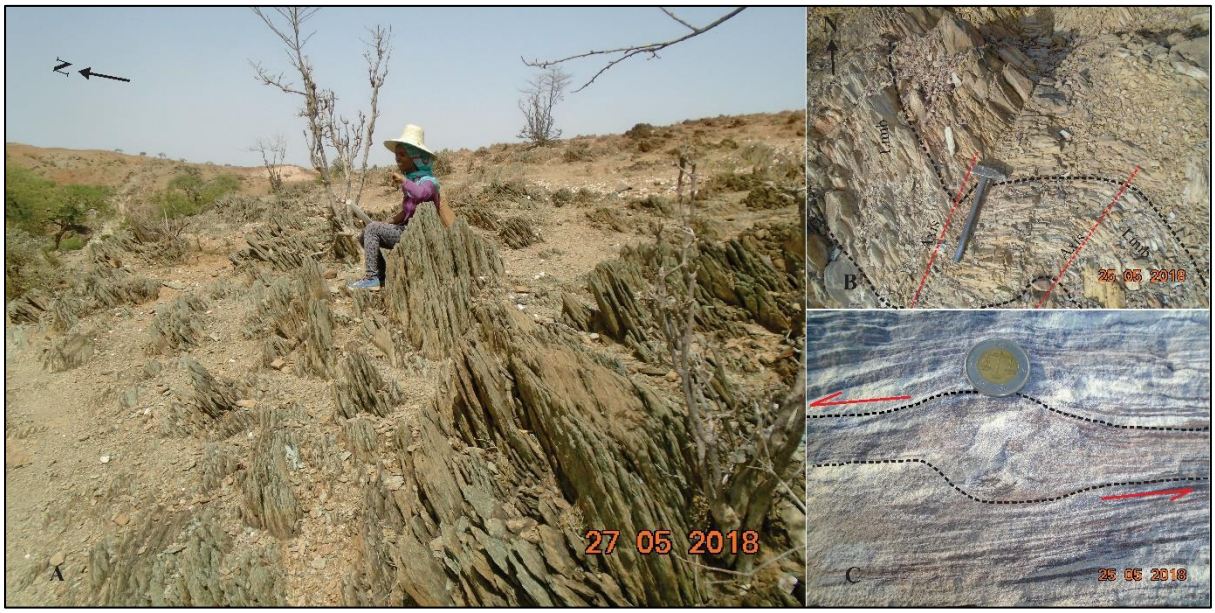

Figure 4.4: (A&B) Sheared phyllitc rock with well-developed foliation and fold found around Godfey and Adi kilte, respectively, and (C) Centimeter-scale dextrally rotated rock fabric (Mylonite) found northeast of Adi-Nebri'ed, Midrefelasi ridge

In addition to the brittle deformation, the centimeter-scale dextrally rotated breccia (mylonite) found at the toe of the intrusion (in the fine grained, foliated and faulted phyllitic rock) is a straightforward indicator of the ductile shear zone of limited Adi-Nebri'ed area, Midrefelasi ridge (Fig. 4.4C). The existence of non-ideal simple stress tails characterizes the N-NE trending zones. During the shearing of the matrix, the stiff clasts (lithic fragments) exhibit rotation and produced fissures. The layers or tails that rolled around the rigid clasts indicate the rotation of the clasts, and the pressure shadows or tails extend on either side of the clasts (Shelly, 1993). D2 deformation was caused by a similar orientation of regional compressive stress (Alene et al., 2006). Thus, there is a correlation between D2 deformation and the NE oriented brittle-ductile shear zones. At several locations, signs of a second, weakly developed shear deformation phase are perceived.

4.1.5 Faults

Major faults were not easily detected in the study area because of the area's limited exposures, extreme complexity and deformation. However, the ground observation revealed that the

majority of the thrust faults are recorded along the mafic-ultramafic belt spanning between the Adi Nebri'ed and Adi Hageray blocks, which is N and NW part of the study area. Furthermore, inferred faults and minor normal faults actually correspond to ridges, valleys, and rivers; as a result, they were digitized and adopted as lineaments (Fig. 4.5 and 4.9). Apart from these faults, sinstral-strike slip movements were observed manifested on veins, dykes and joints.

The northern, northeast, northwest, and center regions of the study area are where these small faults are located. The final stage of deformation (D3) in the area is responsible for these minor faults, which are oriented from $N20^0$ - 60^0E (NE-SW trend) with a sinistral sense of displacement and are found in slate-phyllite and metavolcaniclastic units. These faults, which are linked to the contacts of the rocks are distinguished by a series of intense shearing events that vary in magnitude and length, spanning from a few meters to kilometers (Fig. 4.9). Generally speaking, most of the sinstral-slip faults that have been seen dipping southeastward with a moderately steep dip and noticeable displacement. Previous attempts have suggested the presence of typical faults in the area, and the latest investigations have confirmed this fault extension. The frequent development of similarly oriented minor fractures and joints is likewise caused by the stress field that produced the larger regional fault trends. They all significantly affect the area's shearing, metamorphism, and modification. A careful examination shows that the supposedly large, longest faults are actually composed of many small fault segments that are spreading laterally and growing in size and displacement.

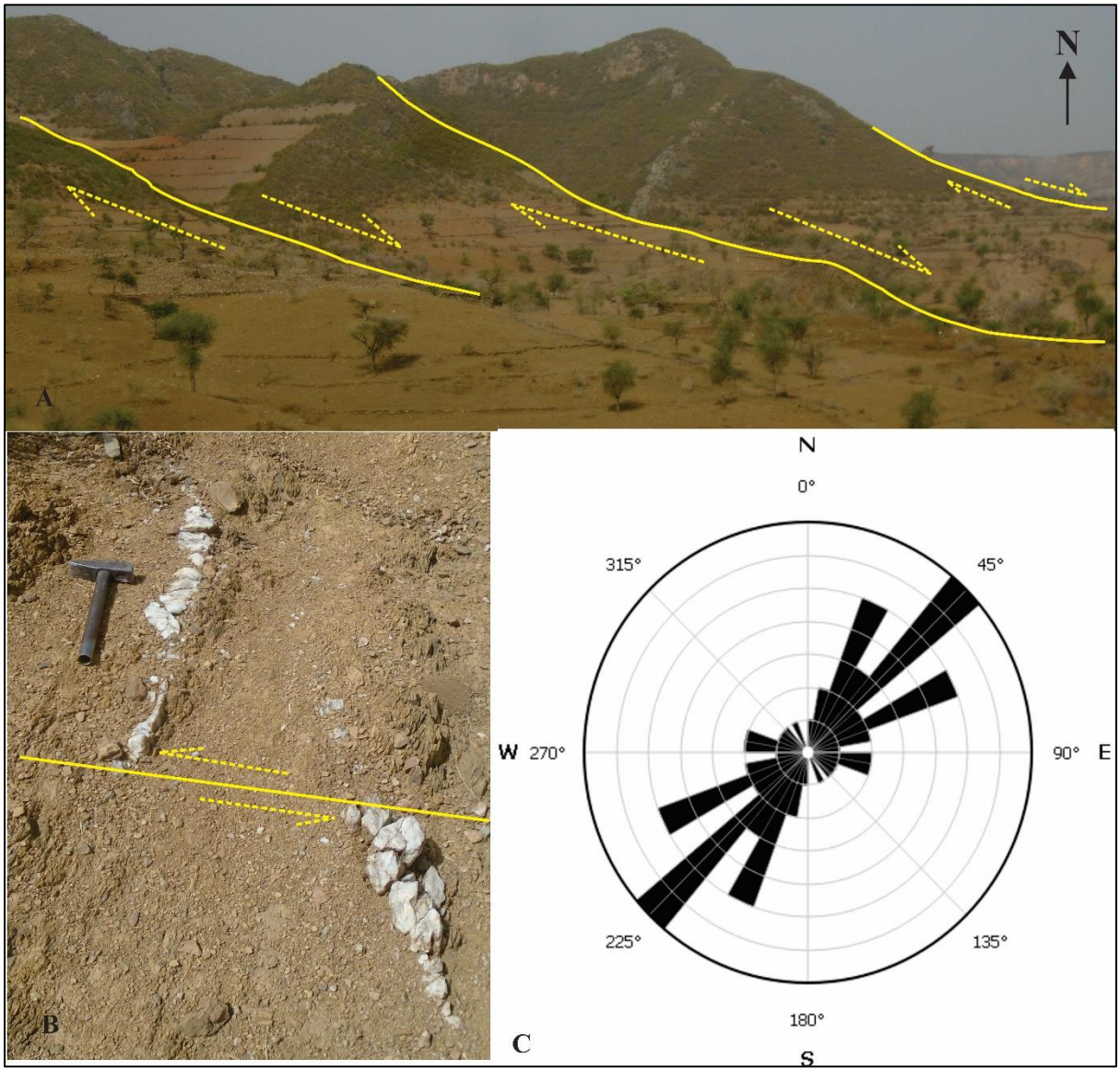

Figure 4.5: Simple measured faults (A=Normal fault and B= sinstral-strike slip fault) of Adi-Nebried area and (C) Rose diagram of all studied faults.

4.1.6 Joints

The other dominant structures in the study area are the joints, which takes many different forms and has extremely complicated large range of dip/strike variations. These joints have a moderate to sub-vertical dipping trend. They often occur in sets, with each set consisting of parallel to sub-parallel orientated to one other, and are formed as a result of tensional pressure on the outcrops. These conjugate brittle structures primarily affect metavolcanic (Fig. 4.6), metavolcaniclastic, metalimestone, and slate-phyllite units. They have at least three sets of joints (NNE, NE, and to a lesser extent NW joints), most of which are at a high angle to the D1

and D2 structures. They describe the last and youngest deformation phase (D3 deformation) by crosscutting the local and regional foliations.

As demonstrated by the diversity in their occurrence and distribution, the joints in the rocks locally display cross-cutting connections that suggest the presence of polyphase deformation. In general, although some of the joins are only 10 to 15 cm apart, and their spacing ranges from 10 to 160 cm. A total of more than 92 joint measurements have been made throughout the study area.

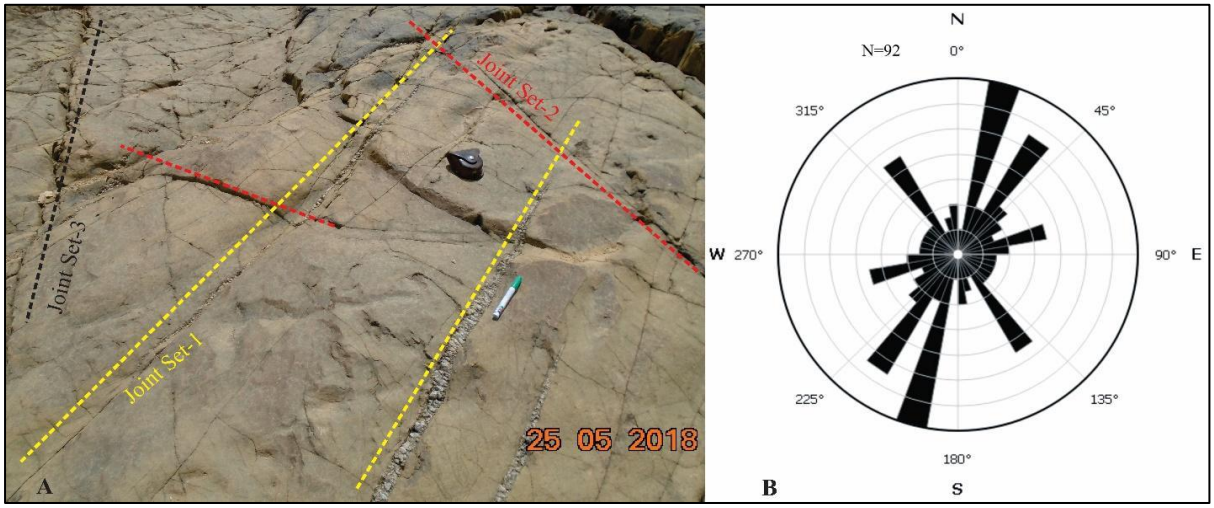

Figure 4.6: Joints and their orientation, (A) Regular joint sets on phyllite rock, which cut each other and filled with silica, (B) rose diagram of joints

The inventoried fractures are distributed throughout the first and third quadrants. In addition to notable N-S, NE-SW, and NW-SE trending fractures, a single prominent fracture orientation ($N10^0$-45^0E) is recorded. Compared to other fractures, those trending E-W appear to be older. The longest wedge of the rose diagram $N15^0$-20^0E, $N30^0$-42^0E, and $N30^0$-40^0W represents three sets of the joint system indicating that mean value of the strike direction (4.6B).

4.1.7 Quartz Veins

Quartz veins are widespread in the area, showing obvious contacts with the metamorphosed host rocks and are primarily fracture-related. The shear zone and the contact between the metavolcaniclastic and metasedimentary rocks are where quartz veins commonly found. The majority of the quartz veins in the area (Fig. 4.9) are typically show narrow width (30-50 cm thick) and run parallel to S_1, the main foliation. However, they are also visible as thick as 1 m and higher (Fig. 4.7A). Each exhibits a distinct attitude, with NE, NW, and occasionally EW trends. The metavolcanic, metavolcaniclastic and slate-phyllite units contain enormous,

continuous quartz veins that range in thickness from 50 - 130 cm. While some are depicted and represented on the geological map, but the majority of them being small are not shown on the map.

The generations of quartz veins were identified locally based on their occurrence in relation to the host rocks' foliation and their intersection relationship. In general, there are three generations of quartz veins that are concordant and/or discordant to the regional S_1 foliation. Unlike the unfolded second and third generations, the first-generation quartz veins are less common and folded by D2. The second generation quartz veins are found in association with fractures, and runs parallel to the regional foliation. The majority of second-generation quartz veins are larger in size, frequently barren massive veins, and attenuated quartz shear veins that appear as crashing and filled the E-W fractures and foliations. The formation of these quartz veins in the studied area is also due to D2. The third generation of quartz veins crosses the regional trend and is set up in conjunction with fractures and joints. The veins in the second and third generations are not severely deformed and propagate in a similar manner as the joints and fractures. The veins of the second generation of quartz are crossed by those of the third generation. The third generation veins are narrow, mineralized, and are part of the D3 deformation event. They often cut the E-W trending veins and the majority of the rock units, which are primarily quartz sericite schist and quartz porphyry. According to field observations of vein cross-cuttings, veins trending $N45^0E$ and EW are comparatively older than veins striking at $N20^0W$ and $N65^0W$ orientations. In general, the majority of the quartz veins are observed to be in harmony with the regional foliation. Since the basement rocks in the study area are being affected by progressive deformation, the veins are severely distorted in several locations.

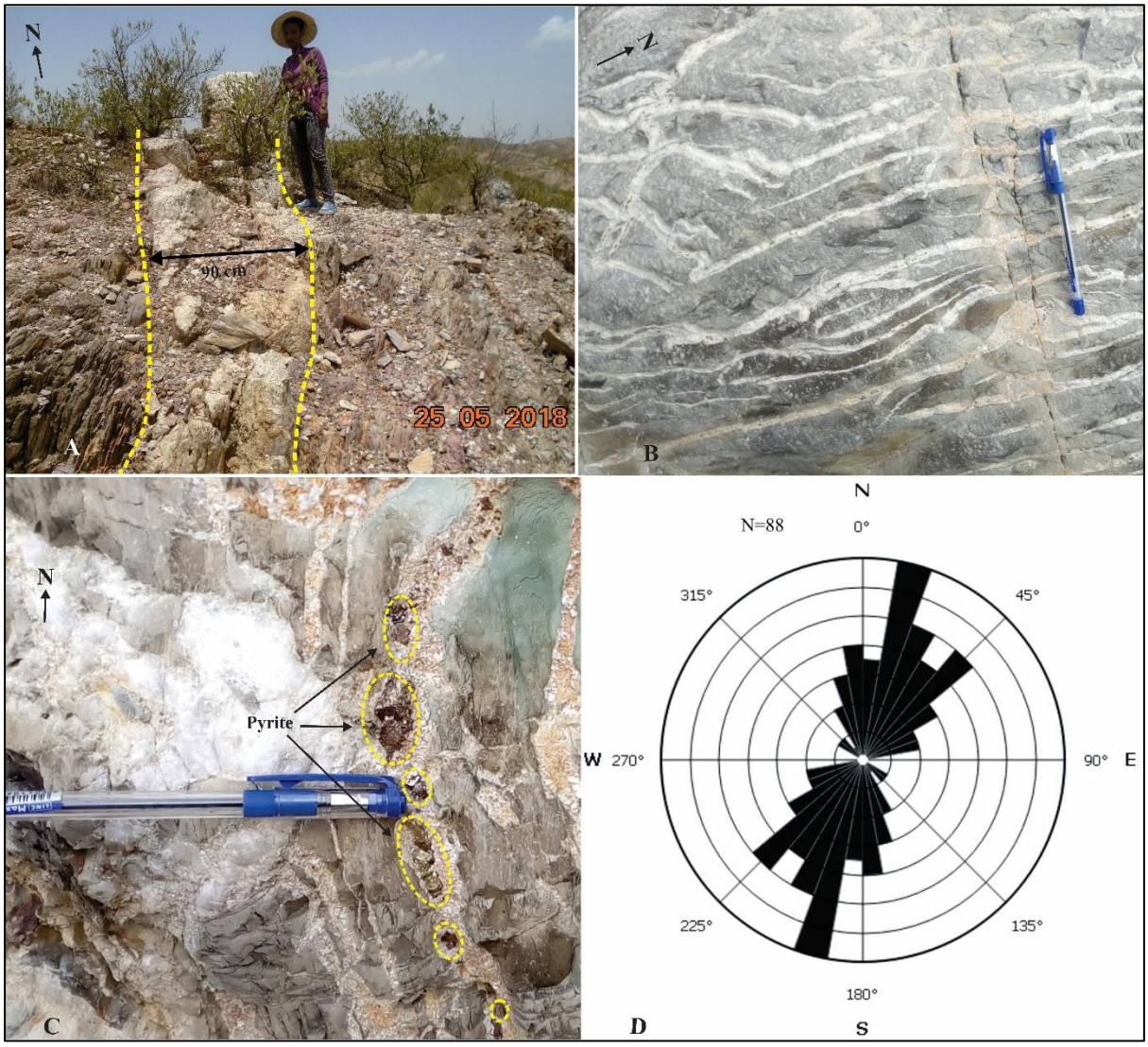

Figure 4.7: Quartz veins: (A) Field photographs showing quartz veins in the phyllitc outcrops, (B)Thin and elongated quartz veins discordant each other, (C) Sheared phyllitc rock filled by silica and pyrite minerals, (D) Rose diagram showing strike of the veins (N=88 represents the number of measurements).

4.1.8 Dykes

The dykes have variable width and strike extent. Individual dyke have varied texture and different composition. In this case, a number of mafic and felsic dykes, ranging in thickness from 35 centimeters to 2 meters, cut through practically all of the metavolcanic, metavolcaniclastic and metasedimentary rock units in the study area. The majority of the mafic dykes (Fig. 4.8A) are composed of primarily olivine and pyroxene, fine to medium grained, and its color ranges from gray to dark. They are moderately to severely weathered on their jointed outcrop surfaces.

Figure 4.8: Dykes: (A) Mafic dyke that dissected to the phyllitic rock at river cut exposure around Adi-kilte area, and (B) Felsic dyke discordant to the massive slate-phyllite unit in Midre-felasi area

In addition, the aplitic (felsic) dykes were detected having discordant relationships with the regional foliation (Fig. 4.8B). These acidic dykes are primarily composed of quartz and K-feldspars, with fine to medium grain sizes. They are typically found as late-stage intrusions associated with the existing granite rock, where its weathered surface exposures show kaolin formation. Generally, nearly all dykes have a similar orientation, which is parallel to the rocks typical foliation orientation (NNE-SSW) (as shown in Fig. 4.9).

4.2 Deformation History

According to field observations of geological features and the cross-cutting interactions between structures, at least three phases of deformation, designated as D1, D2 and D3, have displaced the study area. In metasedimentary rocks, compositional banding in outcrops identifies primary bedding (S_0).

4.2.1 First Phase of Deformation (D1)

The foliation and planar features of schist and metavolcaniclastic rocks are indicative of the first phase of deformation event. The area's primary structural component is the S_1 foliation, where its overall trend is NE-SW and E-W, and parallel to the regional foliation trends. The northeastern side of the study area also shows dips from $N20^0 – 45^0E$, as well as NE-SW trending parasitic folds and elongation lineation.

According to Alene et al. (2006), the rocks that have undergone metamorphism and deformation during the previous deformational phase (D1) because of N-S compression and the collision of East and West Gondwanaland produced moderate to strongly developed sub-

vertical S_1 foliation and sub-vertical tight folds. In order to preserve the natural layering and bedding, the S_1 foliation lies subparallel to the slate unit's initial lithological layer (S_0).

4.2.2 Second Phase of Deformation (D2)

The development of fold in the slate-phyllite, quartz-feldspar-sericite schist in the center, north, and northeast and meta-limestone in the southeastern part of the study area are indicative of the second deformation event. The S_1 foliations are folded around these minor folds, which have a general hinge line that trends N60°W and plunges by 50°. This stage of deformation also includes thrusting and disharmonic crenulation cleavage. The E-W trending sheared and less deformed barren quartz vein, E-W trending fracture cleavages and cut the S_1 fabric are indicative of D2.

4.2.3 Third Phase of Deformation (D3)

The third stage of deformation event is characterized by brittle ductile shear zones that dip sub-vertically and strike from NE to SW direction within almost all local units. In the shear zones, the rocks are heavily silicified, frequently followed by mineralized quartz veining and sulphidization. In the shear zone, elongation lineation and horizontally E-W plunging mineral aggregate, along with rotated σ structures, always show a dextral strike slip sensation of movement during the D3 deformation.

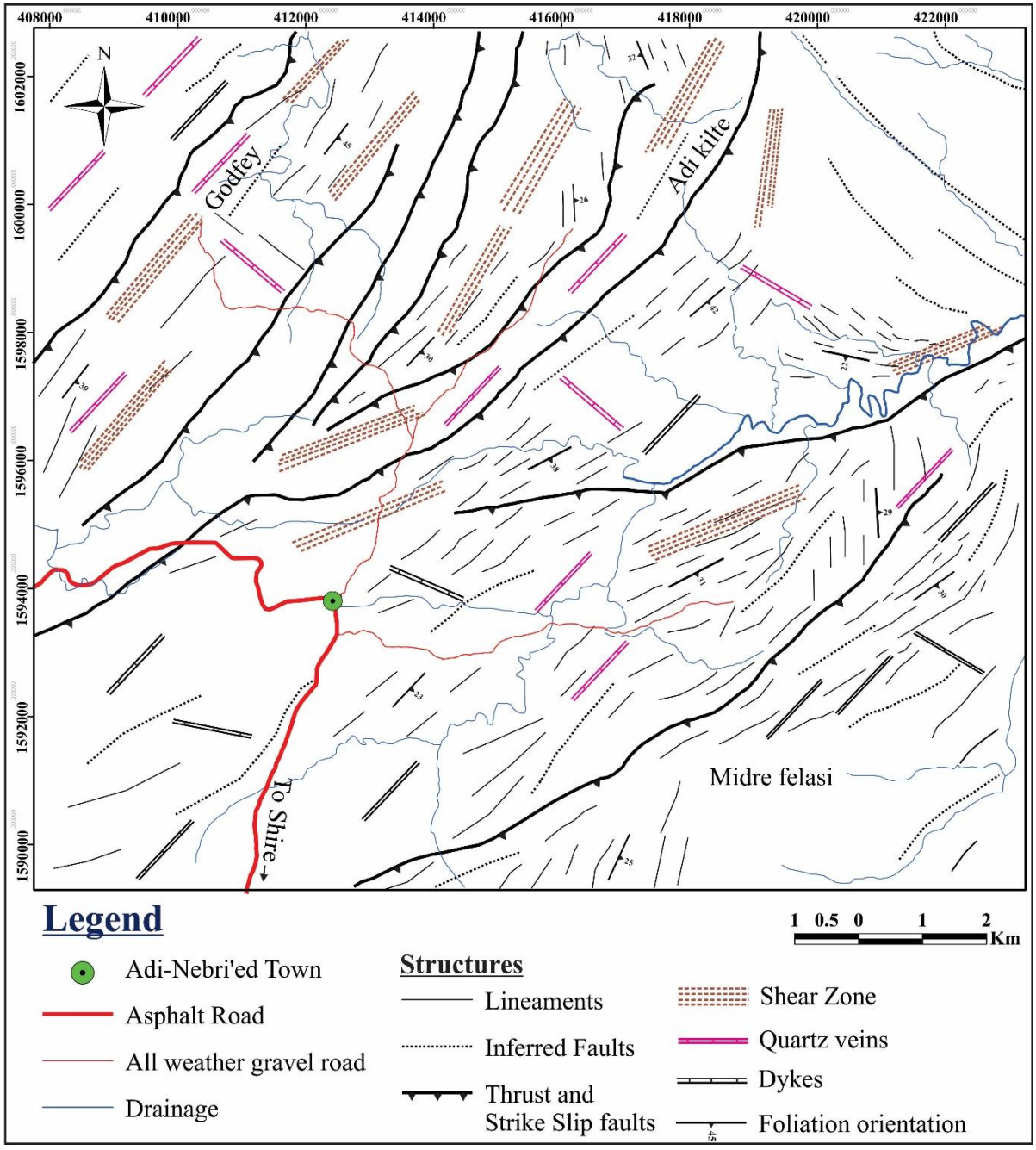

Figure 4.9: Structural map of Adi-Nebri'ed area produced by ground traverse surveys and structural measurements across the strike of the lithological rock units. Projected Coordinate System: Adindan_UTM_Zone_37N. Projection: Transverse Mercator.

5. GEOCHEMICAL ANALYSIS OF THE ROCKS OF ADI-NEBRI'ED AREA

5.1 Whole Rock Geochemistry

Fourteen (14) samples from the Adi-Nebri'ed area are collected and examined for whole-rock geochemical analysis. The main objective of analyzing and interpreting geochemical data is to understand the overall chemistry, origin and tectonic setting of the metavolcanic and/or metavolcaniclastic rocks of Adi-Nebri'ed area. From this geochemical data, Harker variation diagrams of MgO versus major oxides, MgO versus trace elements chondritic normalized rare earth element (REE) abundance pattern, and multi-element variation diagram have been produced.

The major, trace and rare earth elements abundance in fourteen (14) samples (shown in Table 5.1) are used in construction of discrimination and variation diagrams in order to understand their geochemical signature and reconstruct the tectonic setting of the area.

Major element data have a limited application in understanding the petrogenetic evolution of hydrothermally altered metamorphosed rocks because they are mobile and sensitive to weathering, hydrothermal fluid activities, and metamorphic processes unless they are used in conjunction with the immobile elements (Barrett & MacLean, 1994). Therefore, the present study utilizes immobile elements, which, when applied in discrimination diagrams, are normalized to an anhydrous basis.

Table 5.1: Whole-rock major and trace element geochemical data for selected representative rock samples from the Adi-Nebri'ed Area (major oxides in %, trace elements in ppm).

Sample	Metavolcanic rocks					Metavolcaniclastic rocks						Metasedimentary rocks		
	RS-2	**RS-6**	**RS-10**	**RS-12**	**RS-16**	**RS-3**	**RS-14**	**RS-15**	**RS-17**	**RS-21**	**RS-32**	**RS-8**	**RS-25**	**RS-37**
SiO2	88.8	46	45.9	59.6	46.4	44.4	47.2	45.4	53.90	52.50	51.68	67	59.53	55.23
TiO2	0.01	1.09	0.74	0.6	0.28	0.36	0.76	0.59	0.59	0.95	0.90	1.22	0.91	0.874
Al2O3	2.07	14.3	17.85	15.05	6.24	13.5	7.69	10.5	11.57	14.70	13.14	21.7	16.55	13.5
Fe2O3	3.29	11.95	11.35	4.25	10.05	8.3	9.64	11.75	8.65	8.30	8.64	0.57	3.73	11.22
MnO	0.03	0.03	0.03	0.03	0.03	0.03	0.03	0.03	0.03	0.02	0.03	0.03	0.03	0.03
MgO	<0.01	11.55	6.01	2.79	21.4	5.71	12.4	14.75	8.87	7.37	8.55	0.02	7.15	3.9
CaO	0.04	9.2	11.35	3.53	8.94	8.15	16.55	9.9	8.39	6.57	8.91	0.03	3.00	7.61
Na2O	2.01	2.56	2.33	4.63	0.06	1.22	0.41	1.39	2.08	3.60	2.80	0.02	0.03	2.45
K2O	<0.01	0.29	1.18	3.1	0.03	2.65	0.26	0.47	1.33	1.70	1.34	<0.01	0.20	1.5
P2O5	<0.01	0.09	0.34	0.25	0.06	0.11	0.08	0.13	0.17	0.17	0.15	0.05	0.05	0.23
LOI	2.12	1.6	2.36	6.32	5.37	13.8	3.2	4.89	4.90	3.96	3.77	8.32	7.34	2.9
Cr2O3	0.027	0.087	0.016	0.028	0.273	0.032	0.124	0.138	0.06	0.06	0.07	0.018	0.10	0.075
SrO	<0.01	0.02	0.08	0.06	<0.01	0.03	0.03	0.03	0.04	0.04	0.04	0.01	0.04	0.11
BaO	<0.01	<0.03	<0.05	<0.06	<0.09	<0.02	<0.07	<0.08	< 0.09	< 0.01	<0.01	<0.04	1.50	<0.1
Total	**98.43**	**98.92**	**99.75**	**100.35**	**99.24**	**98.44**	**98.51**	**100.14**	**100.57**	**99.9**	**100.01**	**98.96**	**100.16**	**99.63**
V	9	240	350	102	139	257	344	228	218.57	171.0	214.3	291	240.3	193.8
Cr	170	610	110	180	1900	220	870	960	445.71	395.0	513.8	120	713.3	522
Ga	2.2	16.8	20.1	20.1	8.5	13.5	12.1	12.1	13.84	18.5	16.9	14.8	12.7	13.88
Rb	<0.2	4.9	26.9	70.8	0.8	55.1	3.8	9.3	28.47	37.9	29.3	<0.2	11.1	23.1
Sr	2.5	216	788	553	40.9	290	229	257	333.64	384.5	345.6	75.2	63.8	173.3
Y	0.4	17.2	19.2	9.5	6.5	10.3	17.1	12.7	12.34	13.4	14.3	8.5	7.8	13.84
Zr	7	70	58	144	17	35	44	37	56.43	107.0	91.3	289	198.3	57.4

Nb	0.2	2.9	1.9	5.2	0.4	1.2	0.8	1.1	1.90	4.1	3.2	10	6.8	2.36
Sn	<1	1	1	1	<1	1	<1	1	1.00	1.0	<0.5	2	<0.5	1.5
Cs	0.05	0.2	0.57	1.61	0.14	1.01	0.08	0.34	0.55	0.9	0.7	0.01	0.1	0.17
Ba	18.8	100.5	475	723	4.4	386	72.9	143.5	274.24	411.8	327.0	31.3	22.3	84.16
Hf	0.2	1.9	1.5	3.6	0.6	0.9	1.4	1.1	1.51	2.8	2.4	7.1	4.9	1.56
Ta	0.1	0.2	0.1	0.4	<0.1	<0.1	<0.1	<0.1	0.20	0.3	0.2	0.8	<0.7	0.18
W	1	1	2	<1	<1	<1	<1	5	2.25	<0.1	1.0	<1	<0.1	1
Th	0.06	0.33	1.36	5.1	0.31	0.82	0.19	0.48	1.19	2.7	2.1	3.11	2.2	0.276
U	0.15	0.1	0.26	1.61	0.08	0.32	0.06	0.18	0.38	0.9	0.7	1.17	0.8	0.11
La	0.5	4.6	9.5	19.8	2.8	4.9	2.5	4.6	6.63	12.2	9.8	10.6	8.0	3.78
Ce	0.7	11.6	23.4	41.3	6.2	10.7	5.2	11.5	14.91	26.5	21.1	20.1	15.5	9.42
Pr	0.05	1.65	3.22	4.79	0.88	1.41	0.91	1.59	1.95	3.2	2.6	2.04	1.7	1.33
Nd	0.2	8.6	15.2	18.1	4.4	6.3	5.2	7.7	8.76	13.4	11.3	6.7	5.9	6.92
Sm	<0.03	2.68	4.11	3.22	1.18	1.61	1.88	2.02	2.59	3.0	2.7	0.99	1.1	1.5
Eu	<0.03	0.92	1.32	0.9	0.33	0.53	0.78	0.74	0.87	0.9	0.9	0.25	0.3	0.27
Gd	0.06	3.2	4.46	2.95	1.28	1.81	3.01	2.35	2.55	3.1	3.1	0.85	1.0	2.572
Tb	<0.01	0.49	0.64	0.31	0.17	0.3	0.49	0.4	0.44	0.4	0.4	0.17	0.2	0.49
Dy	<0.05	3.24	3.64	1.99	1.15	1.98	3.25	2.54	2.77	2.6	2.8	1.33	1.3	4.54
Ho	<0.01	0.66	0.75	0.37	0.23	0.39	0.66	0.5	0.56	0.5	0.6	0.3	0.3	0.86
Er	<0.03	1.82	2.05	0.89	0.61	1.12	1.87	1.47	1.54	1.4	1.5	1.03	0.9	2.22
Tm	<0.01	0.25	0.31	0.13	0.1	0.18	0.25	0.2	0.22	0.2	0.2	0.2	0.2	0.35
Yb	<0.03	1.61	1.9	0.82	0.7	1.13	1.69	1.22	1.40	1.2	1.3	1.37	1.1	1.81
Lu	<0.01	0.21	0.26	0.09	0.07	0.14	0.21	0.16	0.18	0.2	0.2	0.21	0.2	0.31

5.2 Major Oxide Characteristics

According to Le Bas et al. (1986) TAS diagram; majority of the metavolcanic and metavolcaniclastic samples of the study area lie in the subalkaline/tholeiitic region, with a few trending toward the alkaline region. The subalkaline nature indicates a tectonic setting possibly related to mid-ocean ridges, island arcs, or continental margins, where tholeiitic magma series are common. Furthermore, most of these samples plot in the basalt, basaltic andesite, and andesite fields, indicating they are basic to intermediate in composition; suggesting derivation from mantle-derived magmas with varying degrees of evolution, (Fig. 5.1) (i.e. in our case: metabasalt and metabasaltic andesite). However, one sample plots in the trachyte/trachydacite field, indicating a more evolved, silica- and alkali-rich composition.

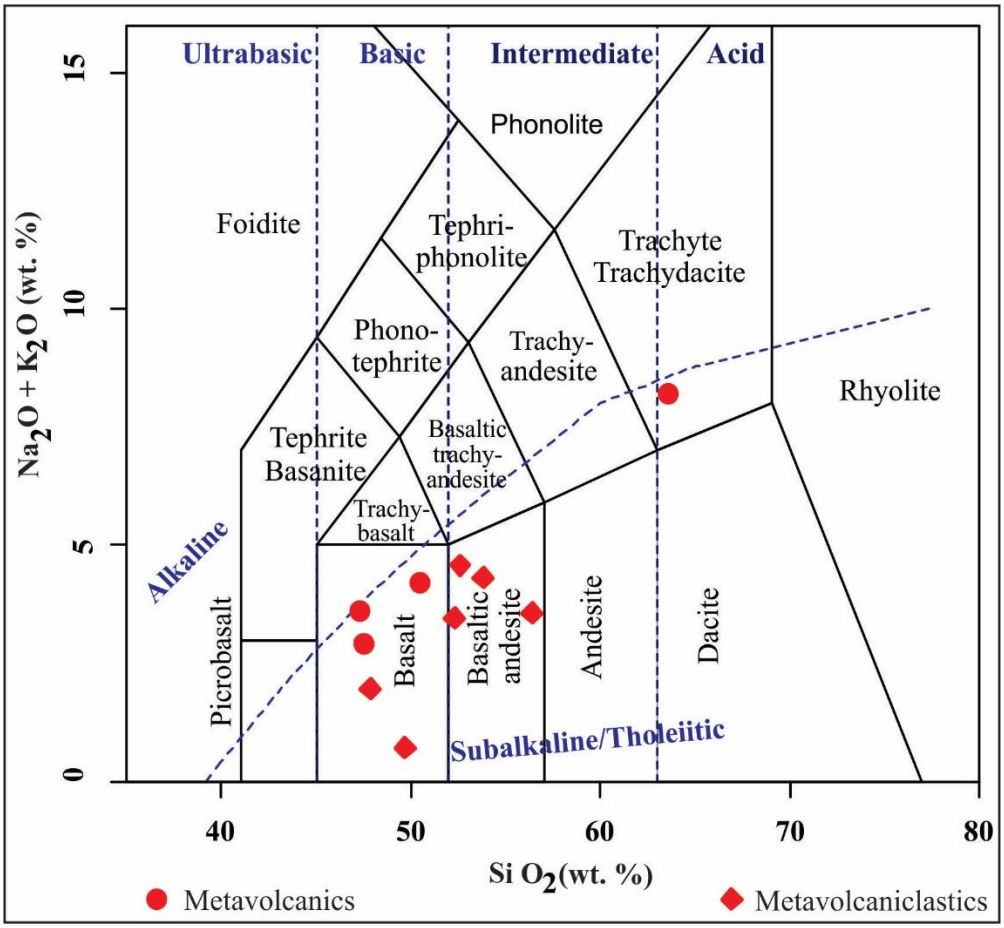

Figure 5.1: TAS classification of the Adi-Nebri'ed rocks. SiO_2 Wt. % versus total alkali (Na_2O+K_2O Wt. %). Line between subalkaline and alkaline after Le Bas et al., (1986).

The presence of an alkaline trachyte sample suggests either a different magma source or greater magma evolution (fractional crystallization or crustal assimilation). Almost all of the samples

collected from the area show high content of Fe_2O_3 (8.3 - 11.95 Wt. %) that reflects the abundance of opaque, and the SiO_2 contents ranges from 44.4 to 88.8 wt. %. The metavolcanic and metavolcaniclastic rocks of Adi-Nebri'ed area also show 0.01-4.63 wt. % of Na_2O and 0.03 - 16.55 wt. % of CaO (Table 5.1). The major element oxides show good correlation with SiO_2 (Fig. 5.1).

Harker variation diagram is also described by using the relationships between concentration of MgO versus all major oxides wt. % (Fig. 5.2) to describe the origin and behavior of magma. Some major oxides such as TiO_2, CaO, and Fe_2O_5 shows increasing trend with increasing MgO, and other major oxides such as SiO_2, Al_2O_3, K_2O, and P_2O_5 and show negative correlation with MgO. The positive and negative correlation of major oxides with MgO may indicate the fractionations of basic magma during its origin. However, MgO versus Na_2O (Fig. 5.2) shows scattered pattern suggesting later alterations due to the high mobility of Na (Tadesse and Allen, 2005). MgO versus CaO plot shows a positive pattern showing simultaneous removal of these two oxides from the parent magma, most probably accomplished by fractionation of clinopyroxene. The metavolcanic rocks of the study area have SiO_2 content ranging from 44.4 to 88.8 wt. %, and Al_2O_3 (2.07 to 21.7 wt %), Fe_2O_3 (3.29 to 11.95 wt %) and CaO (0.04 to 16.55 wt %). MgO content ranging between 0.01 to 21.4wt. %.

The abundances of Na_2O (mostly 1.80 - 4.60 wt %), K_2O (0.3 - 3.1 wt %), P_2O_5 (0.11 - 0.34 wt. %) and the Na_2O/K_2O (mostly between 1 and 3) are low. This can be attributed to a loss during alteration and metamorphism. The majority of samples show relative high abundance of MgO ranging between 0.02 to 21.4 wt.% and CaO 0.03 to 16.5 wt.% ranging between which may be related to the presence of Mg rich chlorite, epidote and the non-intensive metamorphism.

In general, figure 5.2 is likely used to support a petrogenetic interpretation (i.e. volcanic arc environment, alteration, or metamorphic overprint) and to distinguish between igneous-derived (metavolcanic) and sedimentary-derived (metasedimentary) protoliths based on major oxide geochemistry.

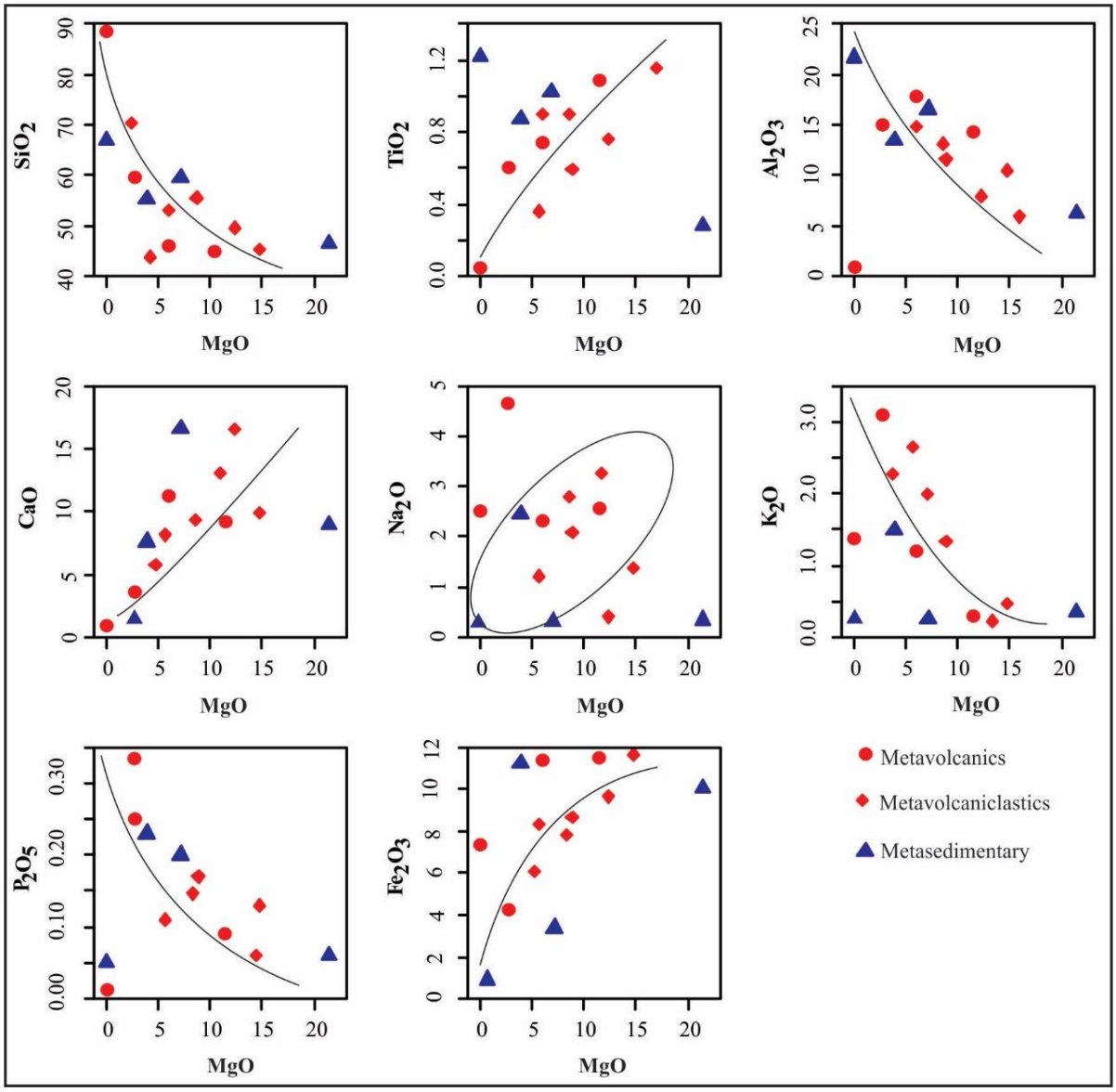

Figure 5.2: Harker variation diagrams of MgO wt. % versus major oxides wt. % for selected rock samples of the Adi Nebri'ed area.

5.3 MgO versus Trace Elements Variation Diagrams

The MgO versus selected trace elements plots show variation between trace elements and MgO (Fig. 5.3). Most of the incompatible trace elements form a negative correlation with MgO. Trace elements such as Rb, Sr, Hf, Zr, Ba, La, and Ce are showing negative trend with MgO. However, compatible trace elements like Cr and Y are showing positive trend with MgO. The positive correlation between Cr content and MgO indicating fractionation of the parental magma (Yihunie & Hailu, 2007). In general, the positive and negative patterns of the

compatible and incompatible elements with MgO may reflects the differentiation and fractionation of Mg and Fe bearing minerals such as olivine and pyroxene.

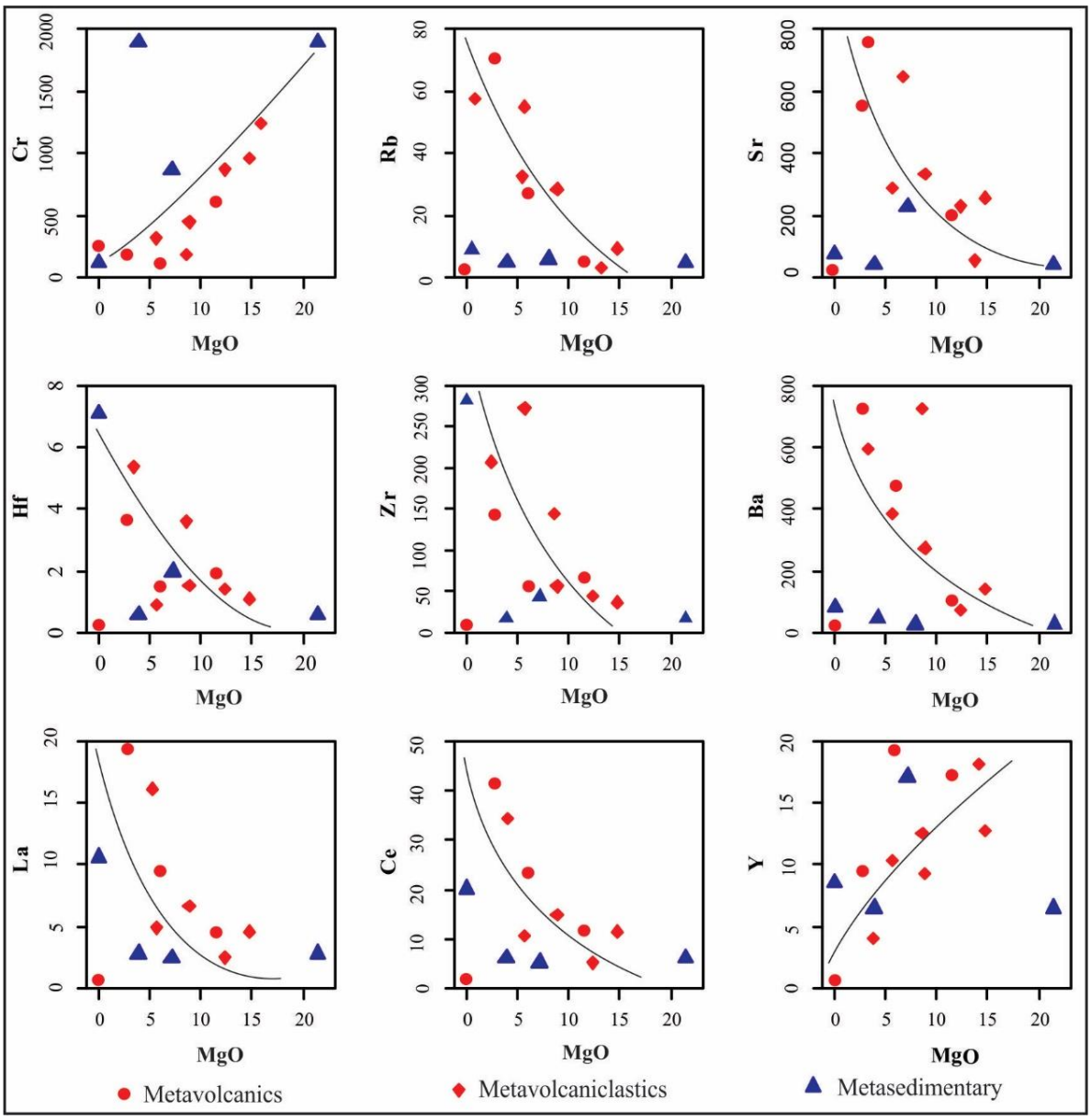

Figure 5.3: Harker-type variation diagrams of selected trace elements (ppm) versus MgO (wt. %) of the study area rocks.

5.4 Trace Elements Geochemistry

The abundances of trace elements used to distinguish the crystals that were present during melting or fractional crystallization of the magma. To identify those trace elements involved in the melting or in fractional crystallization of the magma, chondritic normalized rare earth

element (REE) abundance pattern and multi-element variation diagram pattern are plotted as shown in Figure 5.4. The REE trend indicate slight enrichment in light rare earth elements (LREE) but two samples show depletion in LREE. However, all rock samples show slight depleted pattern for heavy rare earth elements (HREE). The enrichment of LREE and slight depleted pattern in HREE (Fig. 5.4) indicates fractionations of the basic magma.

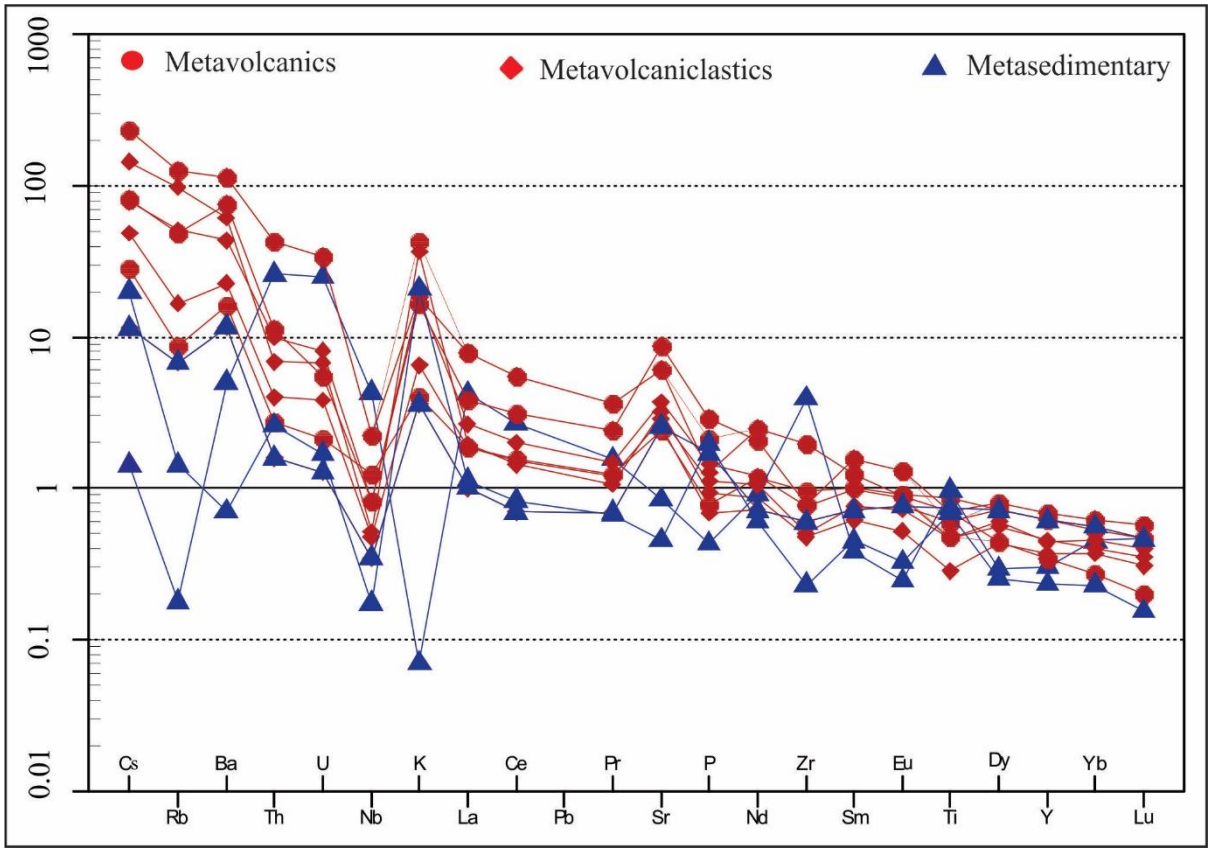

Figure 5.4: Primitive-mantle-normalized incompatible element patterns for the host rocks. The samples are normalized to the primordial mantle of value determined by Sun and McDonough (1989).

5.5 Tectonic Setting

Tectonic discrimination diagrams of geochemical data for the metavolcanic and metavolcaniclastic rocks of the study area displays the chemical characteristics of the magmas generated at subduction-related settings. According to the Zr versus Ti binary (Pearce and Cann, 1973) and Th-Hf-Nb tertiary (Wood, 1980) geochemical discrimination diagrams of metavolcanic and metavolcaniclastic rocks, the area indicates that these rocks are subduction-related arc types. The tectonic setting assessed using discrimination diagrams utilizing the alteration resistant elements including Nb, Zr, Ti, Y, La, Hf, Ta, and Yb (Pearce & Cann, 1973; Wood, 1980). Based on the above listed geochemical discrimination diagrams, most of the

samples are plotted within the volcanic arc basalt field. Such behavior is the characteristic of back-arc basin basalts.

The tectonic environment of the rocks in the Adi Nebried area has been defined using fewer mobile components during hydrothermal alteration and metamorphism. Another supportive tectonic discrimination diagram of magma source for the metavolcanic and metavolcanicatic rocks of the study area shows that most of the examined samples are located in the volcanic arc tectonic setting. Nb/La ratio <0.5 of volcanic rocks have resulted from lithospheric mantle sources (Hofmann, 1997). Depleted magmatic sourced volcanic rocks which have not faced crustal contamination and magma mixing show lower incompatible trace element contents compared to OIB and lower crust derived magmatic rocks (Wilson, 1989). The Nb/La ratio < 0.5 (0.42), low (La/Yb) ratio (5.78), low Nb content (0.2-6.8 ppm) and lower overall trace element contents of the studied samples suggest that they are most likely derived from a depleted mantle source (Fig. 5.5 C & D). Most samples fall along or slightly above the MORB array, with a few trending towards higher Th/Yb values (Fig. 5.5C), implying that dominantly shallow mantle melting sources, and minor crustal contamination or subduction input in some samples.

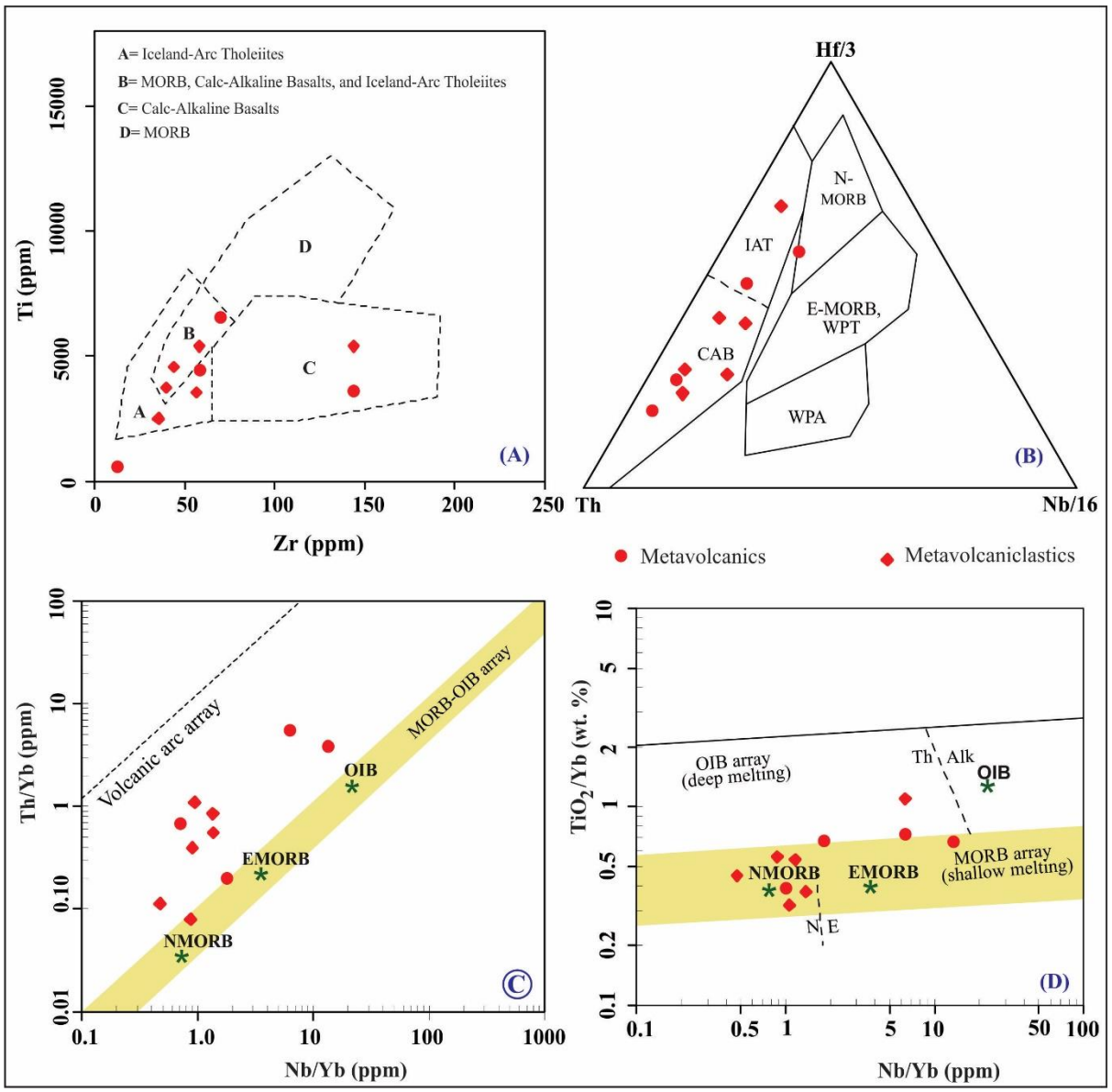

Figure 5.5: Tectonic discrimination diagrams for the selected metavolcanic and metavolcanilcatic rocks of the study area. Diagrams after (A) Pearce and Cann (1973), (B) after Wood (1980), (C) Nb/Yb vs Th/Yb (Pearce, 2008), and (D) Nb/Yb vs TiO2/Yb ((Pearce, 2008) Where, (MORB = mid-ocean ridge basalt, VAB = volcanic-arc basalt, WPB = within plate basalt, IAT= Island-Arc Tholeiites, CAB= Calc-Alkali Basalts, OIB= Oceanic Island Basalt).

6. DISCUSSION

6.1 Geological Setting of Adi Nebri'ed Area

The basic Neoproterozoic stratigraphic framework for northern Ethiopia and Eritrea was established by Beyth (1971, 1972). The basement rocks of Northern Ethiopia are part of the southern Arabian-Nubian Shield of Neoproterozoic (0.85-0.50Ga), which is characterized by the widespread occurrence of low-grade, volcanic and volcano-sedimentary rock assemblage (Beyth, 1972, Kazmin et al., 1978, Tadese et al., 1999). This assemblage belongs to the upper Proterozoic Red Sea Fold Belt of Ethiopia (Kazmin et al., 1978) or more broadly to the Neo-Proterozioc Pan-African Arabian-Nubian Shield (De Wit and Chaweka, 1981), and is intruded by syn-tectonic composite granitoids and post tectonic pink granites. Furthermore, the N-S trending Neoproterozoic volcano-sedimentary-plutonic associations in Eritrea are part of the Arabian-Nubian Shield.

Additionally, the basement complex of Sudan includes reworked Precambrian inliers reactivated during Pan-African tectono-thermal activities, namely the Nuba Mountains, the Darfur block and the Bayuda and Nubian deserts. In the later era, high-grade granitoid gneisses with minor inliers of high-grade metasediments were migmatized and intruded by voluminous granitoids in late Pan-African times. Small inliers of amphibolite-facies gneisses and metasediments occur also within the low-grade volcanogenic ophiolite assemblages of the Red Sea Hills of the country (Anonymous, 1981).

The most noticeable Neoproterozoic tectonic feature in Eritrea is the Augaro-Adobha Belt (AAB) (Fig. 6.1). It extends over 300 kilometers from the northern Sudanese border down to the Barka River valley (Gherardi, 1951; Mohr, 1979; Ghebreab et al., 2009) and then southward to northwestern Ethiopia (Ghebreab et al., 2009). The belt contains mega-shear pods of gabbroic and syn-shearing granitoid intrusions (Ghebreab, 1996). The eastern convex boundary of the AAB is often where the mineral deposits are found (Augaro–Bisha–Zara mineral belt). The predominant rock types in the Augaro area, western Eritrea are supracrustal rocks of sedimentary origin with subordinate volcanic rocks of basaltic to basaltic-andesite composition (Teklay et al., 2003).

The Asmara-Nakfa Belt (ANB) has an average width of 5–20 km and a trend of NNW–SSE for more than 200 km, extending from south of Asmara via Nakfa to northernmost Eritrea. It

joins the northward-trending Augaro-Adobha Belt (Fig. 6.1), where the Cenozoic Red Sea escarpment's shape was determined by the ANB's steep, NNW-trending Pan-African tectonic grain. The ANB is a deformation zone dominated by sinistral strike-slip shearing (Ghebreab, 1996; Ghebreab et al., 2009). According to Woldehaimanot (2000), greenshist facies metavolcanic rocks,meta sediments and pre-tectonic mafic and ultramafic intrusives form the dominant rock units in the Nakfa Terrain.

The Alid-Zula Belt (AZB) is another major NNW-trending Neoproterozoic structure mostly buried under volcanic rocks, and complexly reactivated by Cenozoic rifting events (Fig. 6.1). The Red Sea rift is breaking through along this pre-existing belt to make its way into the Danakil depression. Neoproterozoic structures are known to control the development of the Red Sea-related structures in this area (Drury et al., 1994; Ghebreab and Talbot, 2000; Ghebreab et al., 2009). This belt also stretches across the Danakil depression in Eritrea to the Afar escarpments in Northern Ethiopia.

The study area form part of Adi Nebri'ed block, which is the southern extension of the Asmara-Nakfa Belt and/or Nakfa Terrain (Fig. 6.1) where it comprises of rocks with low-grade domains. According to Tadesses et al. (1999), there are two major belts of mafic and ultra-mafic rocks, that form part of Zager Belt (ZB) and the Daro Tekli Belt (DTB). In addition, there is a thin (<1 km wide) NE–SW belt of ultramafic me´lange zone situated along the central steep zone.

Zager belt (ZB) trends NE–SW and bounds the Adi Hageray metasediment-dominated block on the west and the Adi Nebri'ed volcanic-dominated block on the east (Tadesse et al., 1999). It can be traced for the entire NE–SW length of the mapped area. It also appears to have significant strike continuation outside the study area, perhaps as far north as Asmara and Keren in Eritrea from remote sensing observations (Tadesse et al., 1999). Locally pillowed basic metavolcanics, talc-chlorite schist, sheeted dikes, layered gabbro, pockets of pyroxenite and hornblendite cumulates and serpentinite, together with tectonic slivers of siliceous metasediments make up the major proportion of this belt's rock association (Tadesse, 1996, 1997; Tadesse et al., 1999).

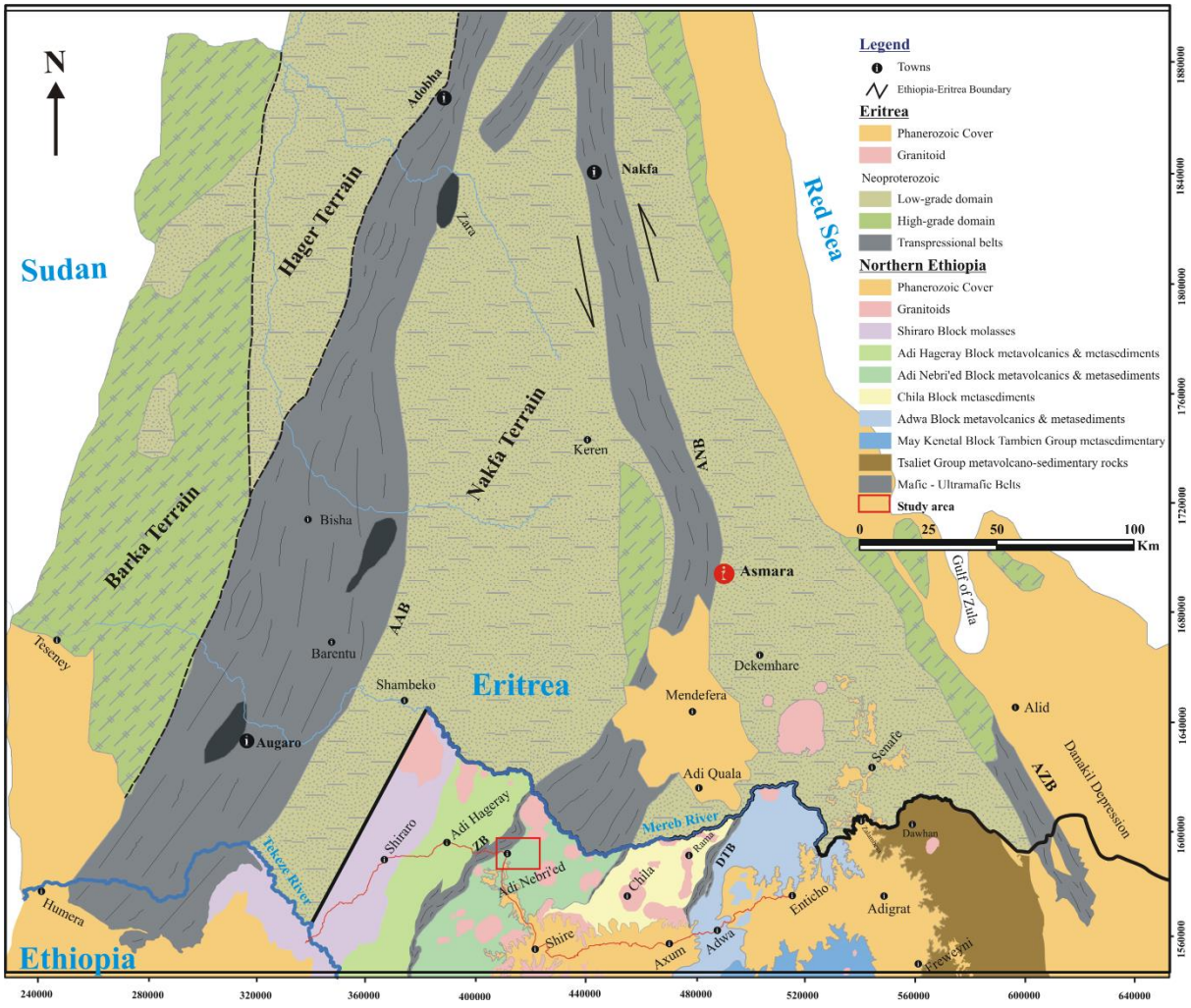

Figure 6.1: Simplified Geological map of Northern Ethiopia and Eritrea (Modified after Tadesse et al., 1999; Teklay et al., 2003; Ghebreab et al., 2009; Miller et al., 2009). Projected Coordinate System: Adindan_UTM_Zone_37N. Projection: Transverse Mercator.

The Daro Tekli belt (DTB), is situated along the Chila–Adwa block boundary (Fig. 6.1). This belt too has continuous NE–SW strike extensions. Rock types are less varied in this belt as compared to the Zager mafic–ultramafic belt. It is dominated by Behiza gabbroic complex (Tadesse, 1997). Basic metavolcanics together with chlorite schist form minor components of the belt along the southern margin of the Behiza ridge (Tadesse, 1999). In contrast to the volcanic dominated assemblages of Adi Nebri'ed block, the predominant rock types in the Adi Hageray block like the rocks in western Eritrea are supracrustal sequences of sedimentary origin with subordinate volcanic rocks (Tadesse, 1996; Tadesse et al., 1999). Based on various literatures, Tadesse et al. (1999) recommendations, and the current investigation in the Adi Nebri'ed area, the above modified map (Fig. 6.1) is produced to illustrate the extension of the

geologic units and structures. In general, this map provides insight into the geotectonic evolution of the Arabian-Nubian Shield. The different terranes represent fragments of ancient crust that accreted during the East African Orogeny, a major event linked to the assembly of the Gondwana supercontinent.

Geologically, the Zager Belt represents an ophiolitic assemblage composed of mafic and ultramafic rocks, including serpentinites, gabbros, and metavolcanics. The proximity of the study area to this belt suggests that its lithological units particularly the metavolcanic sequences-may be genetically linked to the same oceanic crustal processes that formed the Zager Belt. This implies that both units likely originated within a Neoproterozoic oceanic or back-arc basin setting prior to their incorporation into the continental crust during accretion. From a metamorphic perspective, both the Zager Belt and the study area are characterized by low-grade metamorphism, indicating that they share a similar metamorphic history. This further supports the interpretation that the study area evolved in close tectonic association with the Zager Belt during regional deformation and metamorphism. Furthermore, the meta-limestone unit is highly coorelated with the Mai-kenetal limestone due to its slight metamorphism, and white in color.

6.2 Correlation with the Regional Structures

Compared with the regional geological structures in western Eritrea and eastern Sudan, the Adi Nebri'Ed structures extremely shares the regional trending, and their genesis. The different tectonic setting in Eritrea are separated by major N–S shear zones and are distinguishable by their strongly contrasted structural styles and lithologies, in the sense of Coney et al. (1980). According to this author, the shear zone in the Asmara-Nakfa belt is continuously spanning from northeast to southwest of Eritrea, which crosses the boarder and reach to Adi Hageray and Adi-Nebri'ed blocks. Furthermore, the structure of the southeast Sudan is interpreted as a northwest trending faulted syncline, and preserving a succession of Nubian clastic sediments (largely mud rocks) topped by a sequence of extensive sheets of basalt and dolerite (Almond et al., 1984).

Tectonic thrust faults that dip slightly to moderately southeast or steeply dipping shear zones with phyllonitic fabric are the lithological boundaries of the Adi Hageray block (Tadesse, 1996, 1997; Tadesse et al., 1999). Additionally, widely spaced shear zones that strike NE-SW and have a sinistral strike slip sensation of movement influence the entire sequence of Adi Nebri'ed

blocks. In the direction of the eastern edge of the Adi Nebried block and the central steep zone, which includes the belt of ultramafic melange, the shear zones intensify and become closer together (Fig. 6.2). According to Tadesse et al. (1999), syn- to post-tectonic composite granitoids intrude into the Adi Nebri'ed sequence. Late sinistral NE-SW strike-slip shear zones and a number of SE-verging thrust faults influence the sequence in the Chila block. In general, the structural measurement of the studied sinstral-thrust faults, quartz veins and shear zones shows a regional trending synchronized with the structural extensions of the Nakfa Terrain (Eritrea), and Northern Ethiopia.

Ghebreab et al. (2009) also noted in their regional geologic context of Eritrea that lateral tectonic escape along N-S trending brittle-ductile strike-slip shear zones followed the near-vertical collapse of the thicker crust along low-angle brittle-ductile shear zones. The Augaro-Adobha, Asmara-Nakfa and Alid-Zula Belts in Eritrea are highly sheared and trending N-S, and NNE-SSW. Mainly, the ANB is a deformation zone dominated by sinistral strike-slip shearing (Ghebreab et al., 2009). The rocks of the Asmara district, multidirectional fractures are abundant, and many of them are filled with veinlets of quartz and calcite. In these rocks, the foliation typically dips sharply to the W/WNW or E/ENE. Stretching lineations are not common, but when they realized in the field, they are always parallel to fold hinges that plunge steeply (Ghebreab et al., 2009). These lineations are then deformed with transpression, creating a sequence of convex upward, moderately to steeply dipping, reverse, or thrust faults (Ramsay and Hubert, 1983).

Furthermore, Alene et al. (2006) concluded that the D2 deformation in the Arabian–Nubian shield was caused by a similar orientation of regional compressive stress. Thus, there is a correlation between D2 deformation and the NE oriented brittle-ductile shear zones. Similarly, the sheared zones in the vicinity of the Adi-Nebri'ed area are highly in synchronize with this regional shear zone alignment. These sheared zones linked to faulted rocks with measurable displacements and mostly found on the walls of faults. Additionally, some strike-slip shear zones in the low-grade domain are post-dated by local, sub-horizontal, semi-brittle shear zones along the contemporaneous axial surfaces of recumbent crenulation folds. These structures' existence suggests that strike-slip shearing did not stop vertical shortening.

The metavolcanics, metavolcaniclastics and metasedimentary rocks in the area experienced brittle-ductile shears. Furthermore, the study area is located in the Adi-Nebri'ed block, which is part of the southwest section of the ANS (Tadesse, 1997). These interpretations were used

to construct the phases of deformations in the study area. It exhibits parallel to the regional lineaments of the Mai Kenetal, Tsedia, Chehmit, and Negash syncline inliers and is trending NE-SW and NW-SE (Beyth, 1972; Alene et al., 2006).

According to Tadesse et al. (1999) and Alene et al. (2006), elongation lineation, pervasive regional foliation, and folded bedding and tight minor folds (wavelength of mm to dm) are characteristics of the first phase deformation (D1). These deformations are connected to the S_1 penetrative foliation in the current investigation. The second deformation (D2) preserves open parallel folds at long wavelengths without causing a large cleavage. Around these key F2 structures, the S_1 fabric is folded (Tadesse, 1997; Alene et al., 2006). It is believed that these second phases of deformations are linked to the creation of crenulation folding in thin section investigations of phyllite host rocks. The third phase deformation of the Adi Nebri'ed block is a NE-SW orientated shear zone (Tadesse, 1997). According to the current investigation, D3 deformations are the cause of the shear zone denoted by the closely spaced foliations and shearing suggesting structures. Moreover, the joints and faults identified in the present study could be related to the brittle structures post-dated to all the deformational phases in the block (Tadesse, 1997; Tadesse et al., 1999).

Ghebreab et al., (2009), also suggested that the quartz veins in Asmara district vary in dip from sub-horizontal to sub-vertical. The sub-vertical quartz veins are NNE–SSW, NNW–SSE and E–W trending. The NNE–SSW trending veins are relatively younger than the NNW–SSE trending quartz veins. The E–W trending veins are probably younger than the NNE–SSW trending ones. The sub-horizontal quartz veins are clearly the youngest. In the same way, the quartz veins in Adi-Nebri'ed area cross-cut each other, and they share this general regional trend.

The map (Figure 6.2) shows a highly deformed region, with numerous faults, folds (anticlines and synclines), shear zones, quartz veins, and dykes. The presence of quartz veins and dykes suggests that significant igneous and metamorphic activity has been taken place in the region. The thrust faults and composite fabric point to compressional tectonic forces, possibly related to the collision and interaction of the Nubian and Arabian plates in this part of the East African Orogen. The shear zones also indicate intense lateral deformation, possibly accommodating tectonic movement between the two plates or within continental crust blocks.

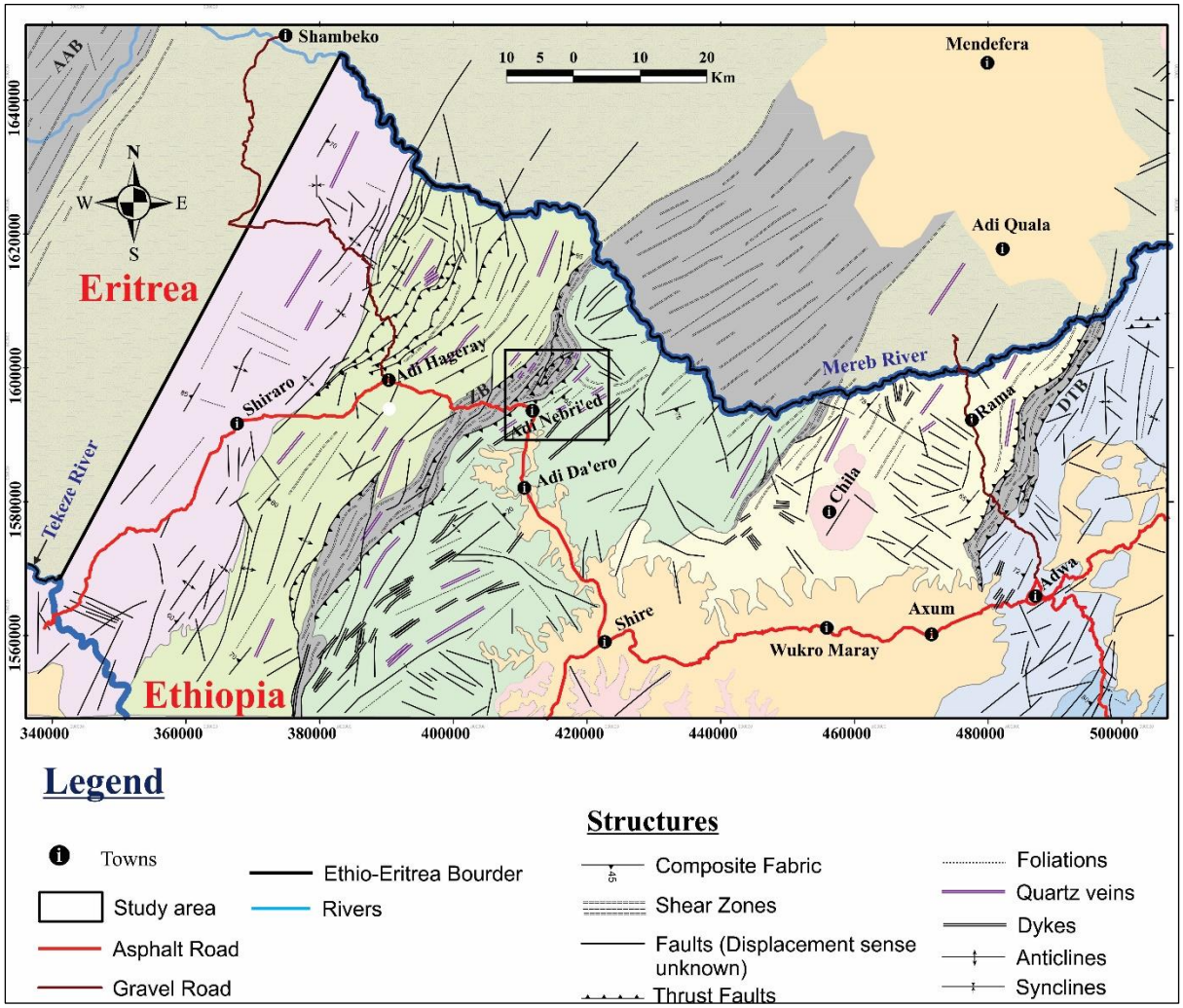

Figure 6.2: Simplified Structural map of Northern Ethiopia and Southwestern Eritrea (Modified after Tadesse et al., 1999; Teklay et al., 2003; Ghebreab et al., 2009; Miller et al., 2009). Projected Coordinate System: Adindan_UTM_Zone_37N. Projection: Transverse Mercator.

6.3 Geochemical Characteristics

On the basis of geochemical characteristics of the selected representative rock samples from the Adi Nebri'ed area, the tectonic affinities of the metavolcanics is analogous with the western and southwestern Eritrea exposures, and the area is matched to the southernmost Nakfa terrane defined in Eritrea (Drury and Berhe, 1993; De Souza Filho and Drury, 1998).

According the TAS classification diagrams (Le Bas et al., 1986), the study area's metavolcanic rocks range in composition from basalt to basaltic andesite, and fall into sub-alkaline tholeiitic rock fields (Fig. 5.1 & 6.3), demonstrates the nomenclature of normal igneous rocks on the basis of the weight percentages of SiO_2 versus total alkalis (Na_2O+K_2O). Similar findings were made by Teklay et al. (2003) in their study of the Augaro area of western Eritrea, which

reported that the metavolcanic rocks in the area ranges in composition from basalt to basaltic andesite. Their low alkali and TiO_2 contents denote a subalkaline affinity.

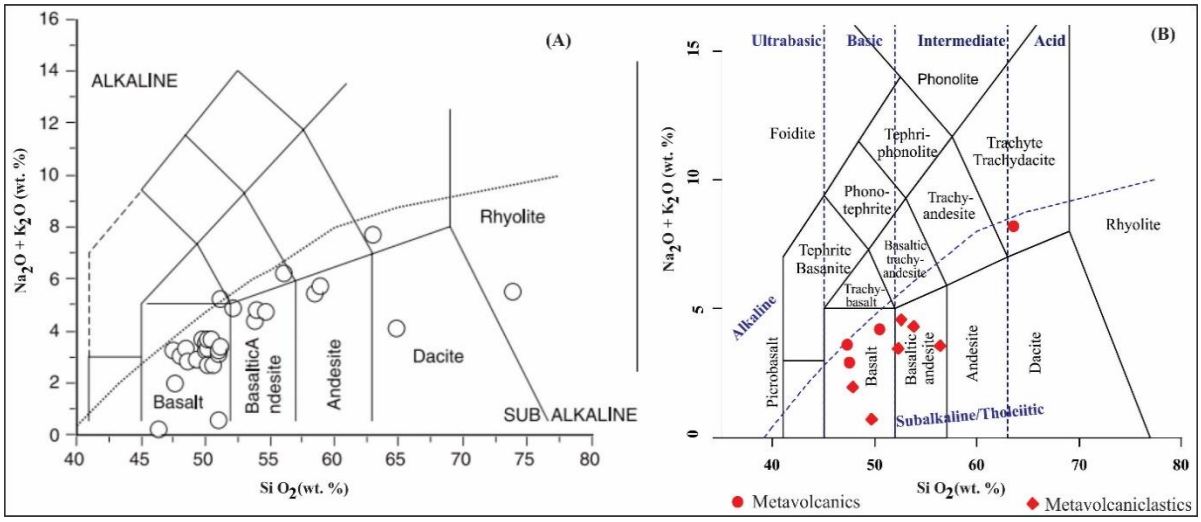

Figure 6.3: Comparative TAS classification of metavolcanic and metavolcaniclastic rocks (A) Augaro area, western Eritrea (Teklay et al., 2003), and (B) the present studied Adi Nebri'ed rocks. SiO2 Wt. % versus total alkali (Na_2O+K_2O Wt. %). Line between sub-alkaline and alkaline after Irvine and Baragar (1971), and Le Bas et al. (1986), respectively.

Major element and trace element variation diagrams, as well as REE and multi-element patterns, are crucial for characterizing Adi-Nebri'ed rocks. Hence, the study area's rock geochemical data reveals significant geochemical variance. Harker variation diagrams of major oxides like CaO, Al_2O_3, Fe_2O_5, Na_2O, SiO_2, K_2O, P_2O_5 and TiO_2 are plotted versus MgO (as shown on the results of Fig. 5.2).

The majority samples of SiO_2 vs MgO plots exhibits a weak negative linear pattern, which is expected with silica poor rocks in that silica decreases as MgO increases. This negative linear trend may reflect olivine-controlled fractional crystallization, where early removal of Mg-rich minerals influences magma evolution (Wilson, 1989). The Fe_2O_3 vs MgO and TiO_2 vs MgO diagrams show weak to strong positive correlations, which are commonly attributed to the fractionation of Fe–Ti oxide minerals, particularly ilmenite, under evolving redox conditions (Rollinson, 1993).A comparatively tight positive linear pattern in the CaO vs MgO plot indicates that these two oxides were removed from the parent magma simultaneously, most likely by fractionation of clinopyroxene. However, the scattering pattern of Na_2O vs MgO indicates subsequent changes because of the high mobility of Na (Tadesse and Allen, 2005).

In general, the rocks in the study area have similar major element contents with the rocks in the Adi Nebri'ed block as pointed out by Tadesse et al. (1999).

Trace element data indicate a small enrichment in incompatible large ion lithophile elements (LILE) compared to high field strength elements (HFSE) in the multi-element diagram (as shown on the results of Fig. 5.4) normalized to primitive mantle values. The influence of subduction fluid in the magma generation at the subduction zones is the cause of the modest enrichment in LILE and depletion in HFS (Pearce, 1982). Additionally, the diagram shows trough anomalies of Nb and P and positive anomalies of Ba. The occurrence of barite mineral at the hand specimen level linked to the mineralization may be related to the Ba anomaly, which is mobile due to its concentration in the subduction fluid (Rollinson, 2014).

The petrological classification of the metavolcanics and/or metavolcaniclastic rocks is shown on SiO_2 versus FeO*/MgO. According to this diagram, the tholeiitic nature of the rocks in the study area (Fig. 6.4 d) is very similar to the study conducted by Tadesse et al. (1999) of the Adi Nebri'ed and Adwa blocks in Northern Ethiopia (Fig. 6.4 a & b) and Teklay et al. (2003) in Augaro, western Eritrea (Fig. 6.4 c), which are dominantly found on the tholeiitic field and some of which on the Calc-alkaline affinity.

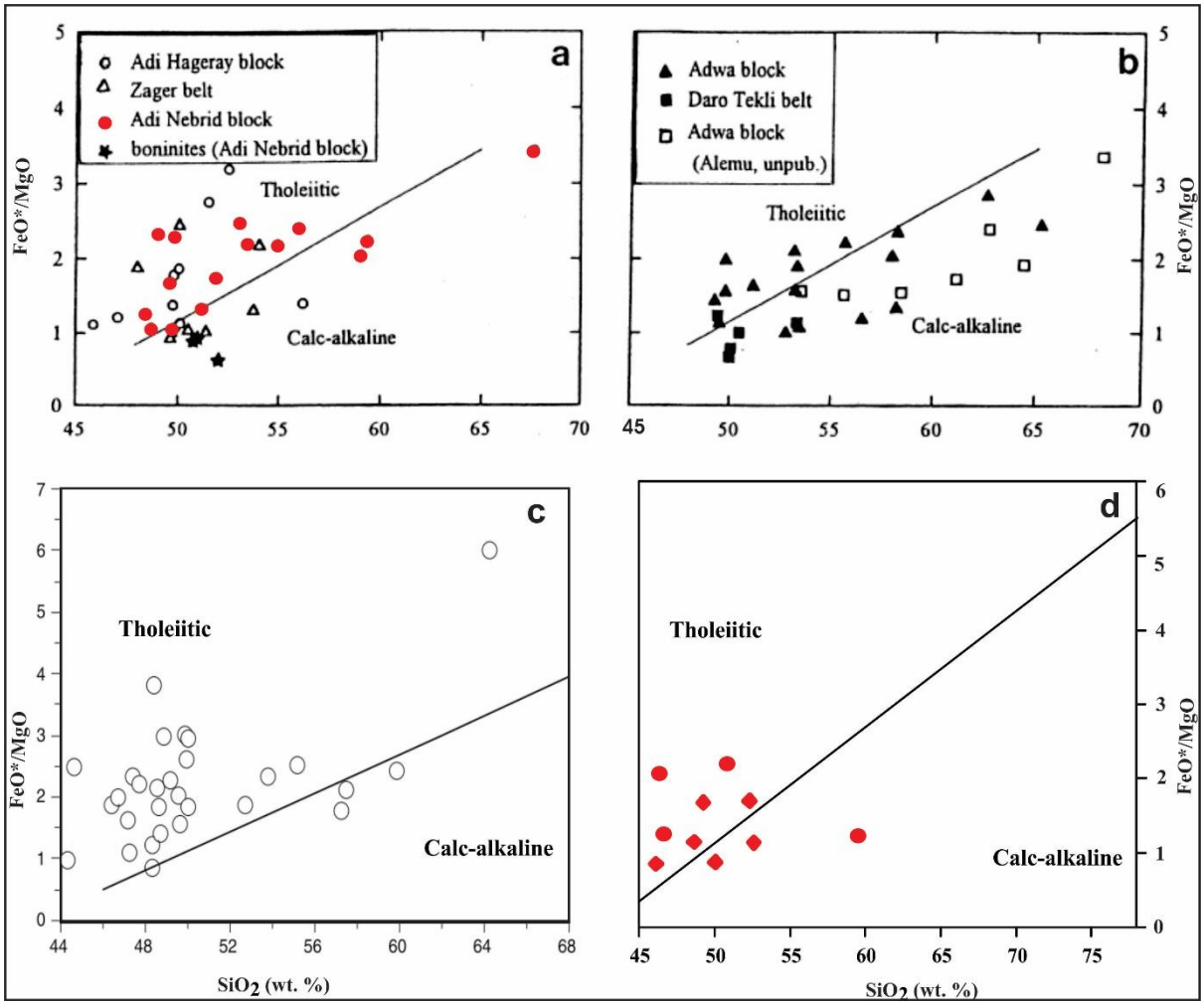

Figure 6.4: Petrological classification comparison diagrams of the metavolcanics on SiO2 versus FeO*/MgO (Miyashiro, 1974) of (a) Adi Nebrie'ed block, (b) Adwa block of Northern Ethiopia (Tadesse et al., 1999), (c) Augaro area, western Eritrea (after Teklay et al., 2003) (Miyashiro and Shido, 1975) area, and (d) the present study area (Miyashiro, 1974).

6.4 Tectonic Setting

In order to determine the tectonic setting of the Adi-Nebri'ed metavolcanic rocks, it is necessary to compare their geochemical character with the nearby zones of Eritrea and Sudan. Based on the lithological associations and chemical affinities, de Souza and Drury (1998) suggested the following tectonic settings: a MORB setting for the Shemegui Terrain and an oceanic Island-arc setting for both the Hager and Nakfa terrains. Geochemical studies carried out by Kröner et al. (1991) indicate that most basaltic rocks from southeast Sudan, adjacent to the Hager Terrain in the northwest Eritrea, have oceanic Island-arc affinities. Moreover, Teklay (1997) suggests that the Nakfa Terrain characterized as an island-arc setting. According to

many scholars, the Tsaliet Group in northern Ethiopia indicates an arc volcanic sequence or subduction-related arc accretion of the ANS (e.g. Tadesse et al., 1999; 2000; Alene et al., 2006; Avigad et al., 2007). The calc-alkaline affinity with arc-related geochemical characteristics is demonstrated by the geochemical data for the metavolcanic rocks of the Northern Ethiopia areas.

The geochemical data for metavolcanic rocks of Adi-Nebri'ed area shows the calc-alkaline affinity with arc-related geochemical signatures. In this study, geochemical results are supportive evidence with petrographic and structural analysis to predict deformation history of Adi-Nebri'ed area and to correlate with the regional works. Therefore, the geochemical results are consistent with the idea that the rocks of the study area are part of the volcanic arc derived Tsaliet Group rocks. The tectonic environment of the rocks in the Adi Nebried area has been defined using less mobile components during hydrothermal alteration and metamorphism. All of the examined samples are located in the volcanic arc tectonic setting (Fig. 5.6) in the Nb/Yb-Th/Yb diagram (Pearce, 2008). Furthermore, based on the TiO_2 vs Zr discrimination diagram (Fig. 6.5) for metavolcanic and/or metavolcaniclastic rocks (Pearce, 1980) suggests that the rocks are produced in an island arc-tectonic setting. In general, the findings from the tectonic discrimination diagrams for the metavolcanics of the study area (Fig. 6.5d) is highly correlated with the Northern Ethiopia's studies made by Bheemalingeswara and Tadesse (2009) in Negash area (Fig. 6.5c), Bheemalingeswara et al. (2012) near Hawzen area, and studies made by Tadesse et al. (1999) particularly within the Adi Nebri'ed (Fig. 6.5a) and Adwa (Fig. 6.5b) blocks on TiO_2 versus Zr (Pearce, 1980), in which all studies suggests an island arc tectonic setting.

In addition, based on the tectonic discrimination diagrams after Pearce and Cann (1973), and Wood (1980), most of the samples are plotted within the volcanic arc basalt field. Such behavior is the characteristic of back-arc basin basalts. According to field data and the geochemistry of metavolcanic rocks of the Adi Hageray block, which is located west of the Adi Nebri'ed block, it is also thought to be a possible back-arc basin setting (Tadesse et al., 1999). This characteristic is also similar with the Teklay's (2003) Augaro basic rocks classification.

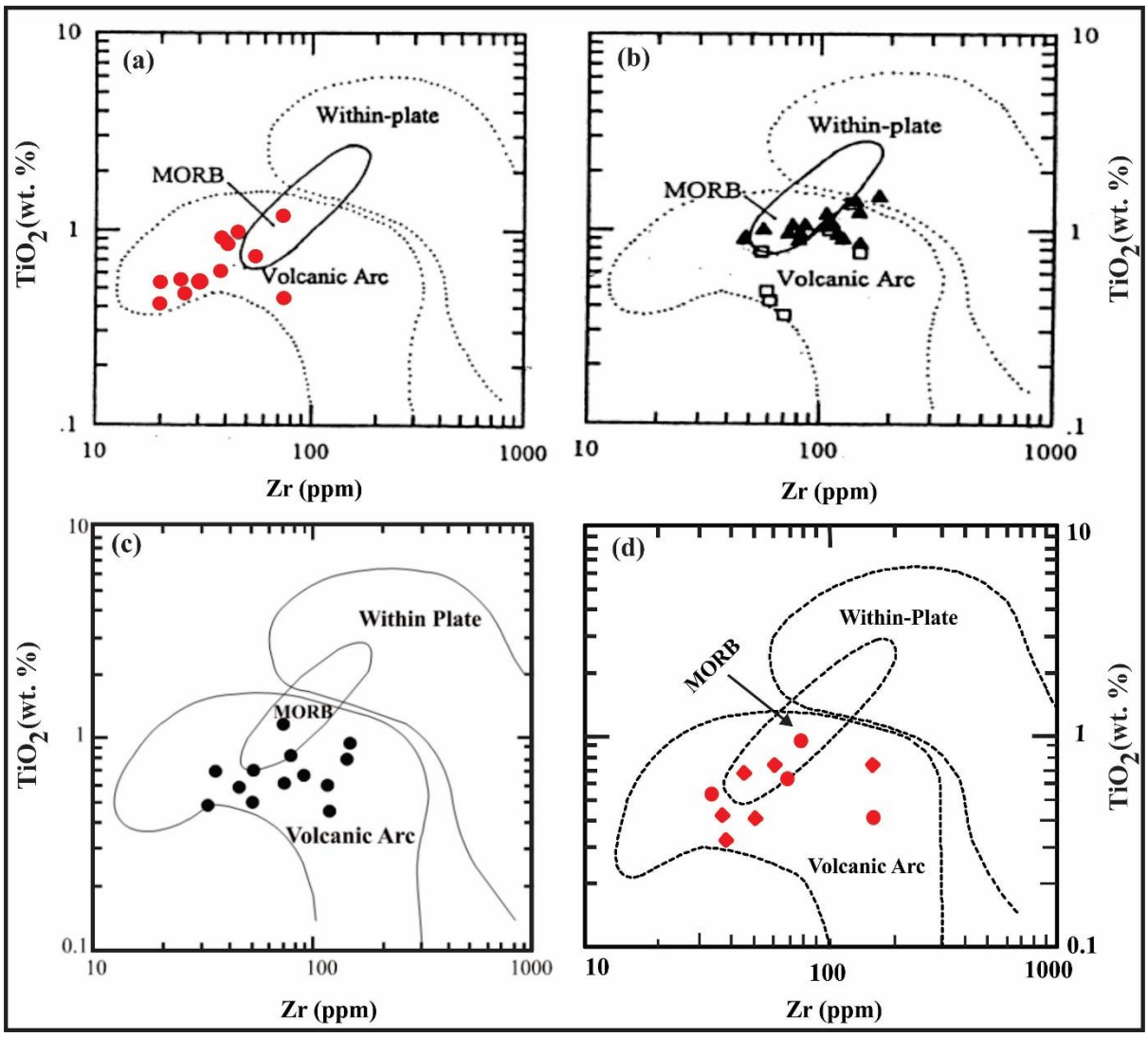

Figure 6.5: Tectonic discrimination comparison diagrams for the metavolcanics of (a) Adi Nebri'ed and (b) Adwa blocks of Northern Ethiopia (Tadesse et al., 1999), (c) Negash area (Bheemalingeswara and Tadesse, 2009), and (d) the current study findings on TiO_2 versus Zr (Pearce, 1980).

The Nb/La ratio < 0.5 (0.42), low (La/Yb) ratio (5.78), low Nb content (0.2-6.8 ppm) and lower overall trace element contents of the studied samples suggest that they are most likely derived from a depleted mantle source (as shown on the results of this study Figure 5.5).

7. CONCLUSION AND RECOMMENDATIONS

7.1. Conclusion

The field observations, petrographic and geochemical data collected for the study area lead to the following conclusions:

This study is conducted in the Adi Nebri'ed block, which is the southern extension of the Asmara-Nakfa Belt and/or Nakfa Terrain. The geologic mapping of the study area indicates that both foliated and non-foliated rocks are prevalent. These include phyllitic and graphitic rock, micaceous slate, ferruginous sandstone, metalimestone, metavolcaniclastic and metavolcanic rocks with varying textures. However, micaceous and graphitic slates cover the majority of the area. The mafic and ultramafic rocks from Adi Nebri'ed block stretch northeast, cross the Mereb River, and connect to the Asmara-Nakfa Belt.

The lithologic units of the study area undergone very low to low-grade metamorphism and belongs to the lower to middle green schist facies because of the presence of relict igneous textures (porphyritic), preserved primary structures (bedding), and particular low-grade mineral assemblages like chlorite, epidote, muscovite, biotite, sericite, and albite. Furthermore, the development of foliation and crenulations in phyllite and moderately developed schistosity along the intrusive contacts and shear zones is also an evidence for grade of metamorphism of the area.

A structural assessment of the study area indicates that the preexisting structural framework has been reoriented and affected because of numerous deformation events. The diverse structures' locations on the maps show that the rocks have experienced varying degrees of deformation, leading to the complete destruction or reorientation of the pre-existing structural framework.

The study area's lithologic units have undergone at least three distinct phases/stages of deformation episodes: The first deformation phase (D1) produced tight minor folds and extensive regional foliation, while the second deformation phase (D2) produced crenulation cleavage and brittle shear fractures such as faults and minor joints. At least two stages of ductile deformation (D1 and D2) impact the metavolcanic and metasedimentary rocks. In addition to ENE trending folds, the D2 deformation produced NE directed sinistral shear zones and

foliations. Locally, NNE-oriented shear zones and folds developed because of D2 deformation. This study be able to connect the deformational imprints left by a variety of structures, such as crenulation and upright harmonic folds, to the local geology. It is believed that the Pan-African orogeny that affected the basement complex is responsible for other characteristics such dykes, joints, and quartz veins.

According to current field and thin section studies of structures, deformation, and microstructural analysis, the study area have been experienced at least three phases of deformations (D1, D2, and D3)

In the study area, widely spaced and NE-SW striking shear zones are commonly found on the contacts of granites associated with green color malachite, sericite, quartz veins, moderately developed schistosity and elongated clasts

A combined structural analysis of vein, foliation, and joint statistics was conducted. Plotting a rose diagram with this data showed that the veins and foliations were running NE-SW. It is evident that the local streams are subject to structural control because they displayed similar patterns.

According to the various tectonic discrimination diagrams done for the metavolcanic rocks in the study area, they are synchronous in their trend and genesis to many studies conducted in northern Ethiopia, Eritrea, and to a lesser extent in easternmost Sudan, which are located in an island arc tectonic setting.

7.2. Recommendations

As per observation and analytical works on Adi Nebri'ed basement rocks the following recommendations are forwarded for future works:

- Geophysical investigation is highly recommended to verify the sub-surface stratigraphy and structures of the area.
- The natives are familiar with gold panning. Copper and malachite stains are also common within the study area. Therefore, it is recommended to investigate the origins of the base metals for economic reasons. Furthermore, given the abundance of quartz veins and mineralization of the rocks, it is recommended that the economic minerals in the study area be examined.
- Based on the structural, petrographic, and geochemical findings of this study conducted in the Adi Nebri'ed area, the following recommendations are proposed:
- The identification of multiple deformation phases (D1, D2, and D3), including foliations, crenulation cleavage, and shear zones, indicates a complex tectonic history related to the Pan-African Orogeny. Therefore, further detailed structural mapping combined with kinematic analysis is recommended to better constrain the timing, sense of movement, and evolution of these deformation phases.
- To better establish the timing of deformation, magmatism, and metamorphism, radiometric dating techniques (e.g., U–Pb zircon, Ar–Ar methods) should be applied. This would help correlate the local geology more precisely with regional tectonic events in northern Ethiopia and Eritrea.
- Although major and trace element data indicate calc-alkaline affinity and island arc signatures, further isotopic studies (e.g., Sr–Nd–Pb isotopes) are recommended to better constrain magma sources and tectonic setting, particularly to distinguish between volcanic arc and back-arc basin environments.
- The presence of hydrothermal alteration indicators such as quartz veins, and sericitization within shear zones suggests potential for mineralization. Therefore, detailed geochemical sampling and mineral exploration surveys are recommended, particularly targeting structurally controlled zones.
- Future studies should integrate geological data from both Ethiopian and Eritrean researchers, as the study area is part of a continuous Neoproterozoic belt.

References

Abdelsalam, M. G., & Stern, R. J. (1996). Sutures and shear zones in the Arabian-Nubian Shield. *Journal of African Earth Sciences*, *23*(3), 289-310. https://doi.org/10.1016/S0899-5362(97)00003-1.

Alene, M., Ruffini, R., & Sacchi, R. (2000). Geochemistry and geotectonic setting of Neoproterozoic rocks from northern Ethiopia (Arabian-Nubian Shield). *Gondwana Research*, *3*(3), 333-347. https://doi.org/10.1016/S1342-937X(05)70292-6.

Alene, M., Jenkin, G. R., Leng, M. J., & Darbyshire, D. F. (2006). The Tambien Group, Ethiopia: an early Cryogenian (ca. 800–735 Ma) neoproterozoic sequence in the Arabian-Nubian shield. *Precambrian Research*, *147*(1-2), 79-99. https://doi.org/10.1016/j.precamres.2006.02.002.

Almond, D. C., Kheir, O. M., & Poole, S. (1984). Alkaline basalt volcanism in northeastern Sudan: a comparison of the Bayuda and Gedaref areas. *Journal of African Earth Sciences, 2(3), 233–245.* https://doi.org/10.1016/s0731-7247(84)80018-x.

Andersson, U. B., Ghebreab, W., & Teklay, M. (2006). Crustal evolution and metamorphism in east-central Eritrea, south-east Arabian-Nubian Shield. *Journal of African Earth Sciences*, *44*(1), 45-65.

Anonymous (1981). Geological Map of the Sudan, 1:2,000,000. Geological and Mineral Resources Department (G. M. R. D. Khartoum), R. S. C. Jeddah, B. R. G. M. Orleans.

Asrat, A., Barbey, P., & Gleizes, G. (2001). The Precambrian geology of Ethiopia: a review. *Africa Geoscience Review*, *8*(3/4), 271-288.

Asrat, A., Gleizes, G., Barbey, P., & Ayalew, D. (2003). Magma emplacement and mafic–felsic magma hybridization: structural evidence from the Pan-African Negash pluton, Northern Ethiopia. *Journal of Structural Geology*, *25*(9), 1451-1469. https://doi.org/10.1016/S0191-8141(02)00182-7.

Asrat, A., Barbey, P., Ludden, J. N., Reisberg, L., Gleizes, G., & Ayalew, D. (2004). Petrology and isotope geochemistry of the Pan-African Negash Pluton, Northern Ethiopia: Mafic–Felsic magma interactions during the construction of shallow-level calc-alkaline

plutons. *Journal of Petrology*, *45*(6), 1147-1179. https://doi.org/10.1093/petrology/egh009.

Avigad, D., Stern, R. J., Beyth, M., Miller, N., & McWilliams, M. O. (2007). Detrital zircon U–Pb geochronology of Cryogenian diamictites and Lower Paleozoic sandstone in Ethiopia (Tigrai): age constraints on Neoproterozoic glaciation and crustal evolution of the southern Arabian–Nubian Shield. *Precambrian Research*, *154*(1-2), 88-106. https://doi.org/10.1016/j.precamres.2006.12.004.

Ayele, B., & Gangadharan, R. (2016). Study on geological and structural characterization around Mai Kenetal, Central Tigray in Northern Ethiopia. *International Journal of Engineering and Applied Sciences*, *3*(11), 257-562.

Barrett, T. J., & MacLean, W. H. (1994). Mass changes in hydrothermal alteration zones associated with VMS deposits of the Noranda area. *Exploration and Mining Geology*, *3*(2), 131-160.

Beyth, M., (1971). A suggestion for interpretation of the stratigraphy of northern Ethiopia according to the model of plate tectonics. Geology 1, 81–82.

Beyth, M. (1972). Paleozoic-Mesozoic sedimentary basin of Mekele outlier, northern Ethiopia. *AAPG Bulletin*, *56*(12), 2426-2439.

Beyth, M. (1978). A comparative study of the sedimentary fills of the Danakil Depression (Ethiopia) and Dead-Sea Rift (Israel). *Tectonophysics*, *46*(3-4), 357-367. https://doi.org/10.1016/0040-1951(78)90213-5.

Beyth, M., Stern, R. J., & Matthews, A. (1997). Significance of high-grade metasediments from the Neoproterozoic basement of Eritrea. *Precambrian Research*, *86*(1-2), 45-58.

Beyth, M., Avigad, D., Wetzel, H. U., Matthews, A., & Berhe, S. M. (2003). Crustal exhumation and indications for Snowball Earth in the East African Orogen: north Ethiopia and east Eritrea. *Precambrian Research*, *123*(2-4), 187-201. https://doi.org/10.1016/S0301-9268(03)00067-6.

Bheemalingeswara, K., & Tadesse, N. (2009). Petrographic and geochemical study of low-grade metamorphic rocks around Negash with reference to base metal mineralization and groundwater quality, Tigray, northern Ethiopia. *Momona Ethiopian Journal of*

Science, *1*(2).

Billi, P. (Ed.). (2015). Landscapes and landforms of Ethiopia. Springer.

Bosworth, W. (2015). Geological evolution of the Red Sea: historical background, review, and synthesis. *The Red Sea: The formation, morphology, oceanography and environment of a young ocean basin*, 45-78.

Collins, A. S., & Pisarevsky, S. A. (2005). Amalgamating eastern Gondwana: the evolution of the Circum-Indian Orogens. *Earth-Science Reviews*, *71*(3-4), 229-270.

Coney, P. J., Jones, D. L., & Monger, J. W. (1980). Cordilleran suspect terranes. Nature, *288*(5789), 329-333.

Dalziel, I. W. (1991). Pacific margins of Laurentia and East Antarctica-Australia as a conjugate rift pair: evidence and implications for an Eocambrian supercontinent. *Geology*, *19*(6), 598-601.

De Souza Filho, C.R. (1995). Remote sensing and the tectonic evolution of Northern Eritrea (Doctoral dissertation, The Open University).

De Souza Filho, C. R., & Drury, S. A. (1998). A Neoproterozoic supra-subduction terrane in northern Eritrea, NE Africa. *Journal of the Geological Society, 155(3), 551–566. doi:10.1144/gsjgs.155.3.0551*.

De Wit, M. J., & Chewaka, S. (1981). Plate tectonic evolution of Ethiopia and the origin of its mineral deposits: an overview. *Plate tectonics and metallogenesis: some guidelines to Ethiopian mineral deposits. Abbis Ababa, Ethiopian Institute of Geological Survey*, 115-129.

Dow, D. B., Beyth, M., & Hailu, T. (1971). Palaeozoic glacial rocks recently discovered in northern Ethiopia. *Geological Magazine*, *108*(1), 53-60.

Drury, S. A., & Berhe, S. M. (1993). Accretion tectonics in northern Eritrea revealed by remotely sensed imagery. *Geological Magazine*, *130*(2), 177-190.

Drury, L. C., Aharonian, F. A., & Völk, H. J. (1994). The gamma-ray visibility of supernova remnants. A test of cosmic ray origin. Astronomy and Astrophysics, Vol. 287, p. 959-971 (1994), 287, 959-971.

Drury, S. A., & De Souza Filho, C. R. (1998). Neoproterozoic terrane assemblages in Eritrea: review and prospects. Journal of African Earth Sciences, 27(3-4), 331-348.

Fazzini, M., Bisci, C., Billi, P. (2015). The Climate of Ethiopia. In: Billi, P. (eds) Landscapes and Landforms of Ethiopia. World Geomorphological Landscapes. Springer, Dordrecht.

Filjak, R., Glumicic, N., & Zagorak, Z. (1959). Oil possibilities of the Red Sea region in Ethiopia. *Naftaplin, Zagreb, 104pp*.

Fritz, H., Abdelsalam, M., Ali, K. A., Bingen, B., Collins, A. S., Fowler, A. R., Ghebreab, W., Hauzenberger, C. A., Johnson, P. R., Kusky, T. M., Macey, P., Muhongo, S., Stern, R. J., & Viola, G. (2013). Orogen styles in the East African Orogen: A review of the Neoproterozoic to Cambrian tectonic evolution. *Journal of African Earth Sciences, 86*, 65–106. https://doi.org/10.1016/j.jafrearsci.2013.06.004.

Garland, C.R., (1980). Geology of the Adigrat Area. Geological Survey of Ethiopia, Memoir1, 51 p.

Gebremariam, S. (2009). Nature and characteristics of metasedimentary rock hosted gold and base metal mineralization in the Workamba area, central Tigray, northern Ethiopia (Doctoral dissertation, Ludwig Maximilians, Munich University, Germany), 148P.

Ghebreab, W., & Talbot, C. J. (2000). Red Sea extension influenced by Pan-African tectonic grain in eastern Eritrea. Journal of Structural Geology, 22(7), 931-946.

Ghebreab, W., Talbot, C. J., & Page, L. (2005). Time constraints on exhumation of the East African Orogen from field observations and 40Ar/39Ar cooling ages of low-angle mylonites in Eritrea, NE Africa. *Precambrian Research, 139*(1-2), 20-41.

Ghebreab, W., Greiling, R. O., & Solomon, S. (2009). Structural setting of Neoproterozoic mineralization, Asmara district, Eritrea. *Journal of African Earth Sciences, 55(5), 219–235.* doi:10.1016/j.jafrearsci.2009.05.

Gray, D. R., Foster, D. A., Meert, J. G., Goscombe, B. D., Armstrong, R., Trouw, R. A. J., & Passchier, C. W. (2008). A Damara orogen perspective on the assembly of southwestern Gondwana. *Geological Society, London, Special Publications*, *294*(1), 257-278.

Hamimi, Z., Fowler, A. R., Liégeois, J. P., Collins, A., Abdelsalam, M. G., & Abd El-Wahed, M. (Eds.). (2021). *The geology of the Arabian-Nubian shield*. Springer. doi:10.1007/978-3-030-72995-0.

Hofmann, A. W. (1997). Mantle geochemistry: the message from oceanic volcanism. *Nature*, *385*(6613), 219-229.

Holmes, A. (1951). The sequence of Precambrian orogenic belts in south and central Africa. *Proceed. 18th Internat. Geol. Congr. London 1948*, *14*, 254-269.

Johnson, P. R., Kattan, F. H., & Al-Saleh, A. M. (2004). Neoproterozoic ophiolites in the Arabian Shield: Field relations and structure. *Developments in Precambrian Geology*, *13*, 129-162. https://doi.org/10.1016/S0166-2635 (04)13004-1.

Johnson, P. R. (2021). The Arabian–Nubian Shield, an introduction: historic overview, concepts, interpretations, and future issues. *The Geology of the Arabian-Nubian Shield*, 1-38.

Kazmin, V. (1971). Precambrian of Ethiopia. *Nature Physical Science*, *230*(16), 176-177.

Kazmin, V. (1975). The Precambrian of Ethiopia and some aspects of the geology of the Mozambique Belt. *Geophysical Observatory Bulletin*, *1*, 14.

Kazmin, V., Shifferaw, A., & Balcha, T. (1978). The Ethiopian basement: stratigraphy and possible manner of evolution. *Geologische Rundschau*, *67(2)*, 531-546. https://doi.org/10.1007/BF01802803.

Kröner, A., Linnebacher, P., Stern, R. J., Reischmann, T., Manton, W., & Hussein, I. M. (1991). Evolution of Pan-African island arc assemblages in the southern Red Sea Hills, Sudan, and in southwestern Arabia as exemplified by geochemistry and geochronology. *Precambrian Research*, *53*(1-2), 99-118.

Kroner, A., & Stern, R.J., (2005). Pan-African Orogeny, Vol.1, Amsterdam: Elsevier. Sudan, Geologische Rundschau. 87: 150–160.

Li, Zheng-Xiang, SVb Bogdanova, A. S. Collins, Anthony Davidson, Bert De Waele, R. E. Ernst, I. C. W. Fitzsimons et al. "Assembly, configuration, and break-up history of Rodinia: a synthesis." *Precambrian research* 160, no. 1-2 (2008): 179-210.

Meert, J. G., & Lieberman, B. S. (2008). The Neoproterozoic assembly of Gondwana and its relationship to the Ediacaran–Cambrian radiation. *Gondwana research*, *14*(1-2), 5-21.

Middlemost, E. A. K. (1985). Naming materials in the magma/igneous rock system. *Earth Sciences Reviews,* 37: 215–224.

Middlemost, E. A. (1994). Naming materials in the magma/igneous rock system. *Earth-science reviews*, *37*(3-4), 215-224.

Miller, N. R., Alene, M., Sacchi, R., Stern, R. J., Conti, A., Kröner, A., & Zuppi, G. (2003). Significance of the Tambien Group (Tigray, Northern Ethiopia) for snowball Earth events in the Arabian–Nubian shield. *Precambrian Research*, *121*(3-4), 263-283. https://doi.org/10.1016/S0301-9268 (03)00014-7.

Miller, N. R., Stern, R. J., Avigad, D., Beyth, M., & Schilman, B. (2009). Cryogenian slate-carbonate sequences of the Tambien Group, Northern Ethiopia (I): Pre-"Sturtian" chemostratigraphy and regional correlations. *Precambrian Research*, *170*(3-4), 129-156.

Miller, N. R., Avigad, D., Stern, R. J., & Beyth, M. (2011). Chapter 21 the Tambien group, Northern Ethiopia (Tigray). *Geological Society, London, Memoirs*, *36*(1), 263-276.

Nance, R. D., Murphy, J. B., & Santosh, M. (2014). The supercontinent cycle: a retrospective essay. *Gondwana Research*, *25*(1), 4-29.

National Meteorological Agency of Tigray region (2019). Daily and monthly data recorded station.

Pearce, J. A., & Cann, J. R. (1973). Tectonic setting of basic volcanic rocks determined using trace element analyses. *Earth and planetary science letters*, *19*(2), 290-300.

Ramsay, J. G., & Huber, M. I. (1987). Modern structural geology. *Folds and Fractures*, *2*, 309-700.

Rollinson, H. (1993). Using geochemical data: Evaluation, presentation, interpretation. Longman Scientific & Technical.

Rollinson, H. R. (2014). Using geochemical data: evaluation, presentation, interpretation. Routledge. Longman Group UK Ltd., 352 p.

Shelly, D. (1993). Igneous and metamorphic rocks under the microscope. Classification,

Textures, Microstructures and Minerals preferred orientation. London (Chapman and Hall), 445p.

Stern, R. J. (1994). Arc assembly and continental collision in the Neoproterozoic African Orogen: implications for the consolidation of Gondwanaland. *Annual Review of Earth and Planetary Sciences, Volume 22, pp. 319-351.*, *22*, 319-351. https://doi.org/10.1146/annurev.ea.22.050194.001535.

Stern, R. J. (2002). Crustal evolution in the East African Orogen: a neodymium isotopic perspective. *Journal of African Earth Sciences*, *34*(3-4), 109-117. https://doi.org/10.1016/S0899-5362(02)00012-X.

Stern, R. J., Johnson, P. R., Kröner, A., & Yibas, B. (2004). Neoproterozoic ophiolites of the Arabian-Nubian shield. *Developments in Precambrian Geology*, *13*, 95-128. https://doi.org/10.1016/S0166-2635(04)13003-X.

Stern, R.J., Kroner, A., (2005). Pan-African Orogen.Encyclopedia of Geology, v. 1. Elsevier, Amsterdam.

Stern, R. J. (2008). Neoproterozoic crustal growth: the solid Earth system during a critical episode of Earth history. *Gondwana research*, *14*(1-2), 33-50. https://doi.org/10.1016/j.gr.2007.08.006.

Stern, R. J., & Johnson, P. (2010). Continental lithosphere of the Arabian Plate: a geologic, petrologic, and geophysical synthesis. *Earth-Science Reviews*, *101*(1-2), 29-67.

Sun, S. S., & McDonough, W. F. (1989). Chemical and isotopic systematics of oceanic basalts: implications for mantle composition and processes. *Geological Society, London, Special Publications*, *42*(1), 313-345. https://doi.org/10.1144/GSL.SP.1989.042.01.19.

Tadesse, G., & Allen, A. (2005). Geology and geochemistry of the Neoproterozoic Tuludimtu Ophiolite suite, western Ethiopia. *Journal of African Earth Sciences*, *41*(3), 192-211.

Tadesse, T. (1996). Structure across a possible intra-oceanic suture zone in the low-grade Pan-African rocks of northern Ethiopia. *Journal of African Earth Sciences*, *23*(3), 375-381. https://doi.org/10.1016/S0899-5362(97)00008-0.

Tadesse, T. (1997). The geology of Axum area. *Addis Ababa: Ethiopian Institute of Geological*

Survey. Memoir, (9), 184.

Tadesse, T., Suzuki, K., & Hoshino, M. (1997). Chemical Th–U total Pb Isochron age of zircon from the Mareb Granite in northern Ethiopia. *J. Earth Planet. Sci. Negoya Uni*, *44*, 21-27.

Tadesse A. (1998). Geochemistry of Neoproterozoic granitoids from the Axum area, northern Ethiopia. *Journal of African Earth Sciences*, *27*(3-4), 437-460.

Tadesse, T., Hoshino, M., & Sawada, Y. (1999). Geochemistry of low-grade metavolcanic rocks from the Pan-African of the Axum area, northern Ethiopia. *Precambrian Research*, *96*(1-2), 101-124. https://doi.org/10.1016/S0301-9268(99)00008-X.

Tadesse, T., Hoshino, M., Suzuki, K., & Iizumi, S. (2000). Sm-Nd, Rb-Sr and Th-UPb zircon ages of syn-and post-tectonic granitoids from the Axum area of northern Ethiopia. *Journal of African Earth Sciences*, *30*(2), 313-327. https://doi.org/10.1016/S0899-5362(00)00022-1.

Teklay, M. (1997). Petrology, geochemistry and geochronology of Neoproterozoic magmatic arc rocks from Eritrea: implications for crustal evolution in the southern Nubian Shield. Department of Mines-Ministry of Energy Mines and Water Resources-State of Eritrea.

Teklay, M., Kröner, A., Mezger, K., & Oberhänsli, R. (1998). Geochemistry, Pb-Pb single zircon ages and Nd-Sr isotope composition of Precambrian rocks from southern and eastern Ethiopia: implications for crustal evolution in East Africa. *Journal of African Earth Sciences*, *26*(2), 207-227. https://doi.org/10.1016/S0899-5362(98)00006-2.

Teklay, M., Kröner, A., & Mezger, K. (2001). Geochemistry, geochronology and isotope geology of Nakfa intrusive rocks, northern Eritrea: products of a tectonically thickened Neoproterozoic arc crust. *Journal of African Earth Sciences*, *33*(2), 283-301. https://doi.org/10.1016/S0899-5362(01)80064-6.

Teklay, M., Haile, T., Kröner, A., Asmerom, Y., & Watson, J. (2003). A back-arc palaeotectonic setting for the Augaro Neoproterozoic magmatic rocks of western Eritrea. *Gondwana Research*, *6*(4), 629-640.

Wilson, M. (1989). Review of igneous petrogenesis: aglobal tectonic approach. *Terra Nova*, *1*(2), 218-222.

Woldehaimanot, B. (2000). Tectonic setting and geochemical characterisation of Neoproterozoic volcanics and granitoids from the Adobha Belt, northern Eritrea. *Journal of African Earth Sciences*, *30*(4), 817-831.

Wood, D. A. (1980). The application of a Th-Hf-Ta diagram to problems of tectonomagmatic classification and to establishing the nature of crustal contamination of basaltic lavas of the British Tertiary Volcanic Province. *Earth and planetary science letters*, *50*(1), 11-30. https://doi.org/10.1016/0012-821X(80)90116-8.

Woodhead, J., Eggins, S., & Gamble, J. (1993). High field strength and transition element systematics in island arc and back-arc basin basalts: evidence for multi-phase melt extraction and a depleted mantle wedge. *Earth and Planetary Science Letters*, *114*(4), 491-504. https://doi.org/10.1016/0012-821X(93)90078-N.

Yibas, B., Reimold, W. U., Anhaeusser, C. R., & Koeberl, C. (2003). Geochemistry of the mafic rocks of the ophiolitic fold and thrust belts of southern Ethiopia: constraints on the tectonic regime during the Neoproterozoic (900–700 Ma). *Precambrian Research*, *121*(3-4), 157-183. https://doi.org/10.1016/S0301-9268(02)00197-3.

Yihunie, T., & Hailu, F. (2007). Possible eastward tectonic transport and northward gravitational tectonic collapse in the Arabian–Nubian shield of western Ethiopia. *Journal of African Earth Sciences*, *49*(1-2), 1-11. https://doi.org/10.1016/j.jafrearsci.2007.04.006.

APPENDICES

Table-1: Rock Sample Location

S/No	Sample ID	Location		Rock Sample Name
		x	y	
1	RS-3	409714	1601204	Metavolcaniclast
2	RS-14	408299	1598508	Metavolcaniclast
3	RS-15	413366	1600010	Metavolcaniclast
4	RS-17	409340	1596073	Metavolcaniclast
5	RS-21	417678	1601164	Metavolcaniclast
6	RS-32	413888	1596620	Metavolcaniclast
7	RS-2	410595	1590171	Metavolcanic
8	RS-6	411363	1594516	Metavolcanic
9	RS-10	409387	1592984	Metavolcanic
10	RS-12	411007	1599764	Micaceous Slate
11	RS-37	416017	1593154	Slate - Phyllite
12	RS-16	418393	1598580	Phyllite
13	RS-25	421147	1596294	Phyllite
14	RS-8	416180	1601764	Graphitic Schist

Table-2: Foliation Measurements

S/No	Easting	Northing	Strike	Dip/Dip direction	Measured Rock
1	413345	1591234	$N5^0E$	65^0SE	Metavolcanic
2	413564	1591543	$N15^0E$	60^0SE	Metavolcanic
3	413986	1591765	$N10^0E$	50^0SE	Metavolcanic
4	414003	1591875	$N60^0E$	55^0SE	Metavolcanic
5	414543	1591897	$N20^0E$	40^0SE	Metavolcanic
6	415123	1592076	$N25^0E$	43^0SE	Metavolcanic
7	415234	1592342	$N10^0E$	45^0SE	Metavolcaniclast
8	415563	1592765	$N15^0E$	55^0SE	Metavolcaniclast
9	415876	1591543	$N5^0E$	55^0SE	Metavolcaniclast
10	414509	1592345	$N10^0E$	45^0SE	Metavolcaniclast
11	416707	1592347	$N60^0W$	55^0SW	Metavolcaniclast
12	416067	1592987	$N70^0W$	38^0SW	Metavolcaniclast
13	412045	1590034	$N50^0W$	55^0SW	Metavolcaniclast
14	411876	1590543	$N70^0W$	53^0SW	Metavolcaniclast
15	410876	1590324	$N15^0E$	65^0SE	Metavolcaniclast
16	407650	1590564	$N30^0E$	45^0SE	Metavolcaniclast

17	406545	1590645	N80^{0}E	65^{0}SE	Metasediment
18	410453	1501023	N25^{0}E	55^{0}SE	Metasediment
19	408345	1591564	N10^{0}E	57^{0}SE	Metasediment
20	409123	1591745	N20^{0}E	65^{0}SE	Metasediment
21	411876	1592543	N50^{0}W	70^{0}SW	Metasediment
22	412342	1592879	N5^{0}E	50^{0}SE	Metasediment
23	412002	1595023	N85^{0}E	60^{0}SE	Metavolcanic
24	423456	1595346	N80^{0}W	40^{0}SW	Metavolcanic
25	414254	1598034	N60^{0}W	65^{0}SW	Metavolcanic
26	412654	1597654	N50^{0}W	65^{0}SW	Metavolcanic
27	416021	1595673	N20^{0}E	45^{0}SE	Metavolcanic
28	413467	1598564	N35^{0}E	52.5^{0}SE	Metavolcanic
29	413657	1597986	N65^{0}W	65^{0}SW	Metavolcanic
30	413980	1598076	N78^{0}E	50^{0}SE	Metavolcanic
31	415345	1591234	N15^{0}E	55^{0}SE	Metavolcanic
32	416564	1591543	N25^{0}E	65^{0}SE	Metavolcaniclast
33	415986	1591765	N20^{0}E	35^{0}SE	Metavolcaniclast
34	414303	1591875	N45^{0}E	60^{0}SE	Metavolcaniclast
35	414543	1591897	N55^{0}W	45^{0}SW	Metavolcaniclast
36	411123	1592076	N25^{0}E	50^{0}SE	Metavolcaniclast
38	415563	1592765	N25^{0}E	65^{0}SE	Metavolcaniclast
39	415876	1591543	N85^{0}W	60^{0}SW	Metasediment
40	414509	1592345	N45^{0}W	60^{0}SW	Metasediment
41	416707	1592347	N60^{0}W	42^{0}SW	Metasediment
42	416067	1592987	N70^{0}W	53^{0}NE	Metasediment
43	415045	1590034	N50^{0}W	60^{0}SW	Metasediment
44	411876	1590543	N30^{0}E	58^{0}SE	Metasediment
45	411676	1590324	N15^{0}E	65^{0}SE	Metasediment
46	417653	1590564	N20^{0}E	62^{0}NW	Metasediment
47	417545	1590645	N5^{0}E	60^{0}SE	Metasediment
48	416453	1501023	N25^{0}E	57^{0}SE	Metasediment
49	417345	1591564	N10^{0}E	65^{0}SE	Metasediment
50	417123	1591764	N50^{0}W	80^{0}SW	Metasediment
51	418876	1592543	N70^{0}W	42^{0}SW	Metasediment
52	412342	1592879	N7^{0}E	62.5^{0}SE	Metavolcaniclast
53	416002	1595023	N65^{0}W	65^{0}SW	Metavolcaniclast
54	423456	1595346	N12^{0}E	50^{0}SE	Metavolcaniclast
55	414254	1598034	N18^{0}E	65^{0}SE	Metavolcanic
56	417654	1597654	N75^{0}W	45^{0}SW	Metavolcanic
57	416021	1595673	N60^{0}W	42.5^{0}SW	Metasediment

58	416467	1598564	N20^{0}E	40^{0}SE	Metasediment
59	416657	1597986	N15^{0}E	65^{0}SE	Metasediment

Table-3: Vein Measurements

S/No	Easting	Northing	Strike	Thickness (cm)	Veined rock
1	416840	1591744	N15^{0}E	90	Metavolcanic
2	411123	1592076	N30^{0}E	57	Metavolcanic
3	409034	1600753	N45^{0}E	30	Metavolcanic
4	411405	1597281	N60^{0}E	100	Metavolcaniclast
5	414326	1602361	N30^{0}W	54	Metavolcaniclast
6	417120	1599673	N48^{0}E	123.5	Metavolcaniclast
7	416872	1590429	N35^{0}E	131	Metavolcanic
8	420312	1591064	N38^{0}E	70	Metasediment
9	422070	1590560	N42^{0}E	117.5	Metasediment
10	418891	1599024	N65^{0}W	87	Metasediment
11	422072	1590565	N55^{0}E	12.5	Granite intrusion
12	421100	1590447	N35^{0}W	5	Granite intrusion
13	422715	1590424	N87^{0}E	17	Granite intrusion
14	422793	1601798	N65^{0}W	30	Granite intrusion

Table-4: Fault Measurements

S/No	Easting	Northing	Strike	Dip/Dip direction	Measures Rock
1	420173	1596215	N85^{0}E	45^{0}SE	Metavolcaniclast
2	416157	1598164	N45^{0}E	38^{0}SE	Metavolcaniclast
3	414390	1596320	N42^{0}E	52^{0}SE	Metavolcaniclast
4	414512	1598132	N25^{0}E	35^{0}SE	Metavolcaniclast
5	414182	1599132	N22^{0}E	48^{0}SE	Metavolcaniclast
6	412200	1597101	N45^{0}E	58.5^{0}SE	Metavolcanic
7	410100	1610053	N48^{0}E	60^{0}SE	Metavolcanic
8	411423	1594525	N30^{0}W	43^{0}SW	Metavolcanic
9	408000	1598030	N85^{0}E	62.5^{0}SE	Metavolcanic
10	412274	1592905	N70^{0}E	42^{0}SE	Metavolcanic
11	411562	1593519	N25^{0}E	60^{0}SE	Metavolcanic
12	414104	1595272	N32^{0}E	68^{0}SE	Metasediment
13	415015	1593823	N78^{0}E	45^{0}SE	Metasediment
14	413135	1589726	N80^{0}E	57^{0}SE	Metasediment
15	410900	1594981	N88^{0}W	45^{0}SW	Metasediment
16	421686	1600617	N45^{0}W	52^{0}SW	Granite intrusion

17	420686	1599967	N50^{0}W	48^{0}SW	Granite intrusion
18	422070	1590560	N48^{0}E	60^{0}SE	Granite intrusion

Table-5: Joint Measurements

S/No	Easting	Northing	No of Joint sets	Strike	Dip/Dip direction	Measured rock
1	416067	1591897	JS-1	N45^{0}E	48^{0}SE	Metavolcanic
			JS-2	N70^{0}W	65^{0}SW	
			JS-3	N10^{0}E	60^{0}SE	
2	413564	1592543	JS-1	N15^{0}E	50^{0}SE	Metavolcanic
			JS-2	N60^{0}W	55^{0}SW	
			JS-3	N85^{0}E	80^{0}NE	
3	421986	1591765	JS-1	N60^{0}W	80^{0}SW	Metavolcanic
			JS-2	N12^{0}E	45^{0}SE	
4	414003	1591875	JS-1	N75^{0}E	85^{0}SE	Metavolcanic
			JS-2	N85^{0}W	55NE	
			JS-3	N7^{0}E	80^{0}SE	
5	413543	1591234	JS-1	N60^{0}W	85^{0}SW	Metavolcaniclast
			JS-2	N15^{0}E	70^{0}NW	
			JS-3	N77^{0}E	85^{0}SE	
6	415723	1592076	JS-1	N70^{0}W	45^{0}SW	Metavolcaniclast
			JS-2	N15^{0}E	57^{0}SE	
			JS-3	N60^{0}E	70^{0}SE	
7	415634	1592342	JS-1	N87^{0}E	65^{0}SE	Metavolcaniclast
			JS-2	N35^{0}W	75^{0}SW	
			JS-3	N5^{0}E	65^{0}SE	
8	414508	1593765	JS-1	N15^{0}E	65^{0}NW	Metavolcaniclast
			JS-2	N50^{0}W	70^{0}SW	
			JS-3	N45^{0}E	50^{0}SE	
9	415876	1592543	JS-1	N3^{0}E	60^{0}SE	Metasediment
			JS-2	N80^{0}W	40^{0}SW	
			JS-3	N60^{0}E	85^{0}SE	
10	416809	1592345	JS-1	N50^{0}W	85^{0}SW	Metasediment
			JS-2	N45^{0}E	80^{0}SE	
11	416707	1591347	JS-1	N5^{0}E	80^{0}NW	Metasediment
			JS-2	N55^{0}E	85^{0}SE	
			JS-3	N60^{0}W	80^{0}SW	
12	413345	1592987	JS-1	N15^{0}E	58^{0}SE	Metasediment
			JS-2	N60^{0}W	75^{0}SW	

13	412045	1591034	JS-1	N15^{0}E	60^{0}SE	Metasediment
			JS-2	N25^{0}W	50^{0}SE	
14	411876	1590543	JS-1	N80^{0}W	65^{0}SW	Metasediment
			JS-2	N80^{0}E	40^{0}SE	
15	415576	1591764	JS-1	N30^{0}W	60^{0}SW	Metasediment
			JS-2	N17^{0}E	55^{0}NE	
16	407650	1590564	JS-1	N65^{0}E	45^{0}SE	Metasediment
			JS-2	N55^{0}W	65^{0}NE	
			JS-3	N7^{0}E	70^{0}SE	
17	414545	1590645	JS-1	N45^{0}W	75^{0}SW	Metasediment
			JS-2	N25^{0}E	60^{0}NW	
18	410453	1591023	JS-1	N65^{0}E	65^{0}SE	Metasediment
			JS-2	N50^{0}W	45^{0}SW	
19	408345	1591564	JS-1	N25^{0}E	40^{0}SE	Metasediment
			JS-2	N60^{0}E	65^{0}SE	
20	409323	1590324	JS-1	N80^{0}E	55^{0}SE	Metavolcaniclast
			JS-2	N45^{0}W	65^{0}SW	
			JS-3	N15^{0}E	48^{0}SE	
21	411876	1592543	JS-1	N25^{0}E	45^{0}NW	Metavolcaniclast
			JS-2	N60^{0}W	60^{0}SW	
22	412342	1592879	JS-1	N35^{0}E	50^{0}SE	Metavolcaniclast
			JS-2	N3^{0}E	55^{0}SE	
23	412002	1595023	JS-1	N60^{0}W	60^{0}NE	Metavolcaniclast
			JS-2	N45^{0}E	85^{0}SE	
24	423456	1595346	JS-1	N50^{0}E	85^{0}SE	Metavolcaniclast
			JS-2	N5^{0}E	60^{0}SE	
25	413754	1598034	JS-1	N15^{0}E	60^{0}NW	Metavolcaniclast
			JS-2	N65^{0}E	75^{0}NE	
			JS-3	N40^{0}W	35^{0}SW	
26	420200	1601110	JS-1	N5^{0}E	65^{0}SE	Granite intrusion
			JS-2	N75^{0}E	65^{0}SE	
27	421920	1599205	JS-1	N45^{0}W	60^{0}SW	Granite intrusion
			JS-2	N45^{0}E	35^{0}SE	
			JS-3	N3^{0}E	45^{0}SE	
28	422793	1601798	JS-1	N65^{0}W	45^{0}NE	Granite intrusion
			JS-2	N45^{0}E	85^{0}SE	
29	421100	1590447	JS-1	N10^{0}W	65^{0}SW	Granite intrusion
			JS-2	N40^{0}E	35^{0}SE	
			JS-3	N5^{0}E	80^{0}NW	
30	422714	1590421	JS-1	N65^{0}E	65^{0}SE	Granite intrusion

			JS-2	$N20^0W$	45^0SW	
			JS-3	$N10^0E$	75^0SE	

Table-6: Dyke Measurements

S/No	Easting	Northing	Strike	Dip/Dip direction	Thickness (m)	Intruded country rock
1	412342	1592879	$N55^0W$	40^0SW	1.20	Metavolcanics
2	421996	1591775	$N35^0E$	35^0SE	0.83	Metavolcanics
3	416159	1598134	$N13^0E$	47^0SE	1.65	Metavolcanics
4	414348	1592264	$N25^0W$	45^0SW	2.11	Metavolcaniclast
5	409333	1592324	$N45^0E$	65^0SE	0.37	Metavolcaniclast
6	413572	1591845	$N18^0E$	35^0SE	1.93	Metavolcaniclast
7	407660	1590574	$N40^0E$	35^0SE	1.34	Metavolcaniclast
8	411836	1590523	$N65^0E$	80^0SE	1.05	Metasediment
9	418145	1589736	$N55^0W$	65^0SW	0.57	Metasediment
10	422173	1590540	$N20^0W$	45^0SW	0.91	Metasediment
11	423981	1592765	$N38^0E$	62^0SE	1.74	Metasediment